

Optimisation and Scope of a Palladium-Catalysed Allylic Alkylation Cascade.

By

Matthew Grahame Fisk



School of Chemical and Physical Sciences

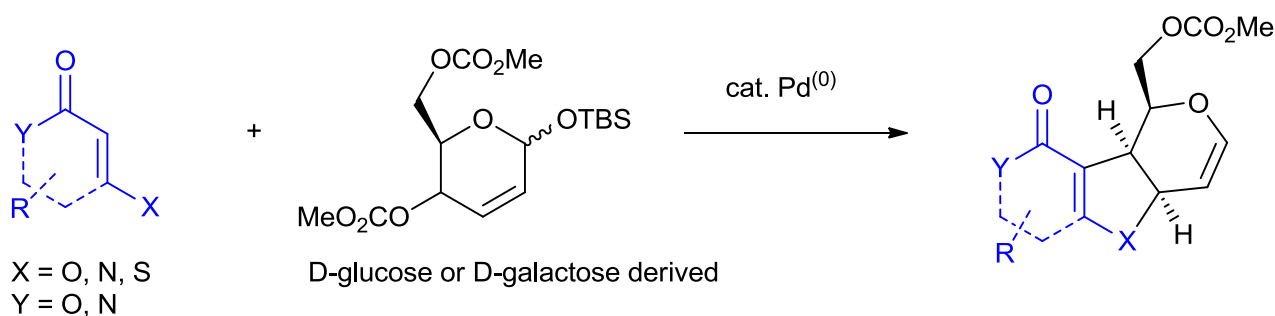
Victoria University of Wellington

A Thesis submitted to Victoria University of Wellington in partial fulfilment of the requirements for the degree of Master of Science in Chemistry

2017

Abstract

The design and development of new chemical reactions is crucial for progress in organic synthesis research. Cascade reactions, involving two or more steps carried out *in situ* in a single pot, provide a step-efficient and atom-economic route to synthesise polycyclic ring systems. The synthesis of new heterocyclic ring systems provides valuable routes towards complex natural products. Previous work in the Harvey group led to the development of a regioselective palladium-catalysed allylic alkylation (Pd-AA) cascade. This research aims to expand the scope and utility of this existing Pd-AA cascade, by optimising the current reaction conditions, and exploring a range of non-symmetric pyran-based bis-electrophiles and nitrogen and sulfur-based β -carbonyl bis-nucleophiles.



Isomeric 2,3-unsaturated silyl glycosides based on D-glucose and D-galactose were successfully synthesised. These substrates were assessed as bis-electrophiles in the Pd-AA cascade. The yield of the cascade was successfully optimised with the glucose-derived substrate 4-hydroxy-6-methylpyran-2-one, using Pd₂(dba)₃ and Xantphos, to 87% from the previously reported 77% yield. However, the galactose-derived silyl glycoside formed an undesired pyranone as the major product. Additionally, a series of β -dicarbonyl compounds (4-hydroxy-6-methylpyran-2-one analogues) were assessed as bis-nucleophiles in the Pd-AA cascade, with all of the analogues forming complex mixtures of side products and a fully unsaturated pyranone as the major isolated product.

Acknowledgements

First and foremost, I would like to thank my supervisor Dr Joanne Harvey. Joanne, you have guided me through the most challenging task I have undertaken so far, and you have managed to keep my love of chemistry alive through it all. I thank you for your guidance, encouragement and support over the last two years.

To my research group, thanks for all the entertaining times in the lab, and also for all the help that each of you have provided.

And to my friends thank you for supporting me and putting up with my high levels of stress for the last two years.

Table of Contents

Abstract.....	iii
Acknowledgements.....	iv
Table of Contents.....	v
List of Figures.....	vii
List of Schemes.....	vii
List of Tables.....	ix
Glossary.....	x
1. Introduction.....	1
1.1. Total Synthesis and Natural Product Analogues in the Drug Discovery Process.....	1
1.1.1. Introduction.....	1
1.1.2. The Pursuit of “Atom Economy” in Total Synthesis.....	3
1.2. Palladium in Organic Synthesis.....	5
1.2.1. Introduction.....	5
1.2.2. The Tsuji-Trost Reaction.....	6
1.2.3. Asymmetric Allylic Alkylation Reactions.....	9
1.3. Allylic Alkylation Cascades.....	11
1.3.1. Cascade Reactions.....	11
1.3.2. Palladium-Catalysed Allylic Alkylation (Pd-AA) Cascades.....	12
1.3.3. A Pd-AA Cascade with Dihydropyrans.....	13
1.4. Bioactivity of Furopyran Compounds.....	18
1.5. Research Objectives.....	20

1.5.1.	Optimisation of the Palladium Allylic Alkylation Cascade.....	20
1.5.2.	Further Development of the Palladium Allylic Alkylation Cascade	21
2.	Results and Discussion	23
2.1.	Synthesis of Bis-electrophiles	23
2.2.	Synthesis of Bis-nucleophiles	27
2.3.	Optimisation of Palladium Cascade	29
2.3.1.	Technical Challenges of Pd-AA Cascades and Initial Exploration	29
2.3.2.	Optimisation of Pd-AA cascade reaction.....	30
2.4.	Pd-AA Cascade with prepared substrates	35
2.4.1.	Pd-AA Cascade with amine bis-nucleophiles and glucosyl bis-electrophile.....	35
2.4.2.	Pd-AA cascade with thiol bis-nucleophile and glucosyl bis-electrophile	40
2.4.3.	Pd-AA cascade with pyridine-2-one bis-nucleophile and glucosyl bis-electrophile	41
2.4.4.	Pd-AA cascade with galactosyl bis-electrophile 48.....	43
3.	Future Work and Conclusion.....	46
3.1.	Future Work on Pd-AA Cascades	47
3.2.	Concluding Remarks	46
4.	Experimental.....	50
4.1.	General Experimental.....	50
4.2.	Experimental Methods and Characterisation	51
4.3.	Palladium-Catalyzed Allylic Alkylation Cascade General Procedures	66
5.	Appendix	69
6.	References	85

List of Figures

Figure 1.1: Therapeutic drugs inspired by natural products	2
Figure 1.2: Structure of Epothilone A (5), and Ixabepilone (6) an Epothilone B analogue	3
Figure 1.3: Structure of Dynemicin (10) and Wender's analogue of Dynemicin (11).....	4
Figure 1.4: Regiochemical possibilities for a Pd-AA cascade.....	13
Figure 1.5: Furopyran compounds tested for bioactivity.....	19
Figure 1.6: Carbohydrate based bis-electrophiles used	21
Figure 1.7: Planned bis-nucleophiles for Pd-AA cascade scope studies	22
Figure 2.1: Spectra showing 282 <i>m/z</i> peak corresponding to dimer 72	29
Figure 2.2: Active Palladium (0) species generated from Pd ₂ (dba) ₃	33
Figure 2.3: Keto-enol and imine-enamine tautomerisation	37
Figure 2.4: Spectroscopic analysis of compound 73	39
Figure 2.5: MS spectra of Pd-AA cascade product 75	42
Figure 2.6: ¹ H NMR spectrum of 75	42
Figure 2.7: Spectroscopic analysis of compound 77	44
Figure 3.1: Different protecting groups for future biological activity testing	49

List of Schemes

Scheme 1.1: Thermal Diels-Alder reaction, with excellent atom economy.....	4
Scheme 1.2: Catalytic hydrogenation of alkenes with palladium catalyst.....	5
Scheme 1.3: Wacker oxidation of ethene.....	5
Scheme 1.4: Reaction of benzyl nitrile palladium(II) chloride with 1,3-butadiene.....	6
Scheme 1.5: Model of the Tsuji–Trost reaction.....	6
Scheme 1.6: Asymmetric induction in Tsuji–Trost reactions with the use of soft and hard nucleophiles	7
Scheme 1.7: Regioselectivity of “symmetric” Pd- π -allyl complexes	8
Scheme 1.8: Regioselectivity of “distorted” Pd- π -allyl complexes	9

Scheme 1.9: Transition metal catalysed asymmetric allylic alkylation reaction.....	10
Scheme 1.10: Enantioselective palladium-catalysed allylic substitution with a stabilised nucleophile.....	10
Scheme 1.11: Robinson's one-pot synthesis of tropinone (25).....	12
Scheme 1.12: General Pd-AA cascade.....	12
Scheme 1.13: Regioselective and stereoconvergent Pd-AA cascade.....	14
Scheme 1.14: Optimised conditions for the Pd-AA cascade with cis-29 and pyrone 31.....	14
Scheme 1.15: Proposed mechanism of Pd-AA cascade with cis-29 and pyrone 31.....	15
Scheme 1.16: Proposed isomerisation of Pd- π -allyl intermediate 36 , allowing a stereoconvergent pathway for the Pd-AA cascade of trans-substituted substrates.....	16
Scheme 1.17: Pd-AA cascade with dihydropyran trans-26 and pyrone 28.....	16
Scheme 1.18: Formation of α,α -disubstituted β -carbonyl side products.....	17
Scheme 1.19: Unsuccessful Pd-AA cascade with tetramic (40) and tetric (41) acids.....	17
Scheme 1.20: Pd-AA cascade using sugar derived bis-electrophile.....	18
Scheme 1.21: Overall reaction for Pd-AA cascade.....	20
Scheme 2.1: Synthesis of D-glucal from D-galactose.....	23
Scheme 2.2: Synthesis of D-galactal from D-galactose.....	24
Scheme 2.3: Synthesis of tri- <i>O</i> -methoxycarbonyl-D-glucal.....	24
Scheme 2.4: Synthesis of tri- <i>O</i> -methoxycarbonyl-D-galactal.....	25
Scheme 2.5: Ferrier-type allylic rearrangement of glucal derivative 62 with water.....	26
Scheme 2.6: Ferrier-type allylic rearrangement of galactal derivative 65 with water.....	26
Scheme 2.7: Silyl protection of hemiacetals 67 with TBSCl.....	26
Scheme 2.8: Silyl protection of hemiacetals 68 with TBSCl.....	27
Scheme 2.9: Method for access to bis-nucleophiles 49 and 50 ⁵¹	27
Scheme 2.10: Attempted synthesis of bis-nucleophile 53	28
Scheme 2.11: Synthesis of bis-nucleophile 53	28
Scheme 2.12: Selected Pd-AA cascade reaction used for initial exploration.....	30
Scheme 2.13: Comparison of reported yields with yields obtained in this work for selected Pd-AA cascades.....	31
Scheme 2.14: Proposed mechanism of <i>C</i> -alkylation step during Pd-AA cascade.....	31
Scheme 2.15: Attempted Pd-AA cascades with new bis-nucleophiles.....	36
Scheme 2.16: Unexpected elimination reaction of lactone 42 under Pd-AA cascade conditions with 49	37
Scheme 2.17: Turner's reaction of bis-electrophile 42 and Meldrum's acid.....	38

Scheme 2.18: Possible mechanism for the formation of 2 <i>H</i> -pyran-2-one 73	39
Scheme 2.19: Unexpected elimination reaction of lactone 42 under Pd-AA cascade conditions with 53	40
Scheme 2.20: Reaction of bis-nucleophile 52 by Pd-AA cascade to potentially afford 75	41
Scheme 2.21: Proposed reaction of galactosyl bis-electrophile 48 in Pd-AA cascade	43
Scheme 2.22: Unexpected elimination reaction of lactone 48 under Pd-AA cascade conditions.....	43
Scheme 2.23: Proposed Pd-mediated mechanism for formation of 77 during Pd-AA cascade	45
Scheme 2.24: Proposed non-Pd-mediated mechanism	45
Scheme 3.1: Future Pd-AA optimisation of amine containing bis-nucleophiles	47
Scheme 3.2: Future Pd-AA optimisation of thiol bis-nucleophiles	47
Scheme 3.3: Future Pd-AA optimisation of galactosyl bis-electrophile.....	48
Scheme 3.4: Optimisation of Pd-AA cascade and purification of 74	48

List of Tables

Table 1.1: Bioactivity of furopyrans compounds measured using IC ₅₀ values.....	19
Table 1.2: List of solvent systems, Pd-based catalysts, and ligands used in the optimisation of the Pd-AA cascade	21
Table 2.1: Probing the effects of external base, and initial solvent effects.....	32
Table 2.2: Optimisation with Pd ₂ (dba) ₃ and selected ligands	34
Table 2.3: Optimisation with Pd(dppf)Cl ₂ and selected ligands	34
Table 2.4: Solvent effects of DCM and Chloroform on the Pd-AA cascade.....	35
Table 2.5: NMR analysis of compound 73	38
Table 2.6: NMR analysis of compound 77	44

Glossary

AAA	asymmetric allylic alkylation
Allyl	$\text{CH}_2=\text{CHCH}_2-$
Anhyd	anhydrous
aq.	aqueous
cat.	catalytic
conc.	concentrated
DCM	dichloromethane
DiPEA	<i>N,N</i> -diisopropylethylamine
DIOP	2,3- <i>O</i> -isopropylidene-2,3-dihydroxy-1,4-bis(diphenylphosphino)butane
DMAP	4-(<i>N,N</i> -dimethylamino)pyridine
DMF	<i>N,N</i> -dimethylformamide
DMSO	dimethylsulfoxide
eq.	equivalent(s)
Et	ethyl
<i>et al.</i>	<i>et alia</i> (and others)
IC ₅₀	half the maximal inhibitory concentration
L	ligand
LG	leaving group
Me	methyl

MeCN	acetonitrile
MS	mass spectrometry
Nu	nucleophile
Pd-AA	palladium-catalysed allylic alkylation
Ph	phenyl
quant.	quantitative
r.t.	room temperature
TEA	triethylamine
TBS	<i>tert</i> -butyldimethylsilyl
THF	tetrahydrofuran
TsCl	<i>p</i> -toluenesulfonyl chloride

1.Introduction

1.1. Total Synthesis and Natural Product Analogues in the Drug Discovery Process

1.1.1. Introduction

Natural products have inspired the development of many effective therapeutics for treating disease.^{1, 2} Ailments such as bacterial infection, inflammatory diseases and cancer can be effectively treated with natural products or natural product derivatives. Key biologically active motifs (pharmacophores) found in nature represent an unparalleled source of inspiration. All these compounds produced by nature are the result of millions of years of evolutionary selection and are therefore biologically prevalidated.³ For example, the natural products paclitaxel (Taxol[®], **1**), and erythromycin (**2**) are currently used to treat cancer and bacterial infections, respectively.⁴ In addition to their direct use, the structures of paclitaxel and erythromycin have been used as templates in the development of superior semisynthetic drugs, docetaxel (Taxotere[®], **3**) and azithromycin (Zithromax[®], **4**).^{5, 6} Figure 1 shows the structural differences between the natural products and the semisynthetic products, made to provide improved medicinal properties. Docetaxel has better aqueous solubility compared to paclitaxel, which confers improved pharmacokinetic properties. The structural modifications present in azithromycin improve bioavailability of the compound and increase potency against Gram-negative bacteria compared to erythromycin. These examples highlight not only the power of natural products, but also the power of chemical synthesis in discovering novel medicinal compounds.

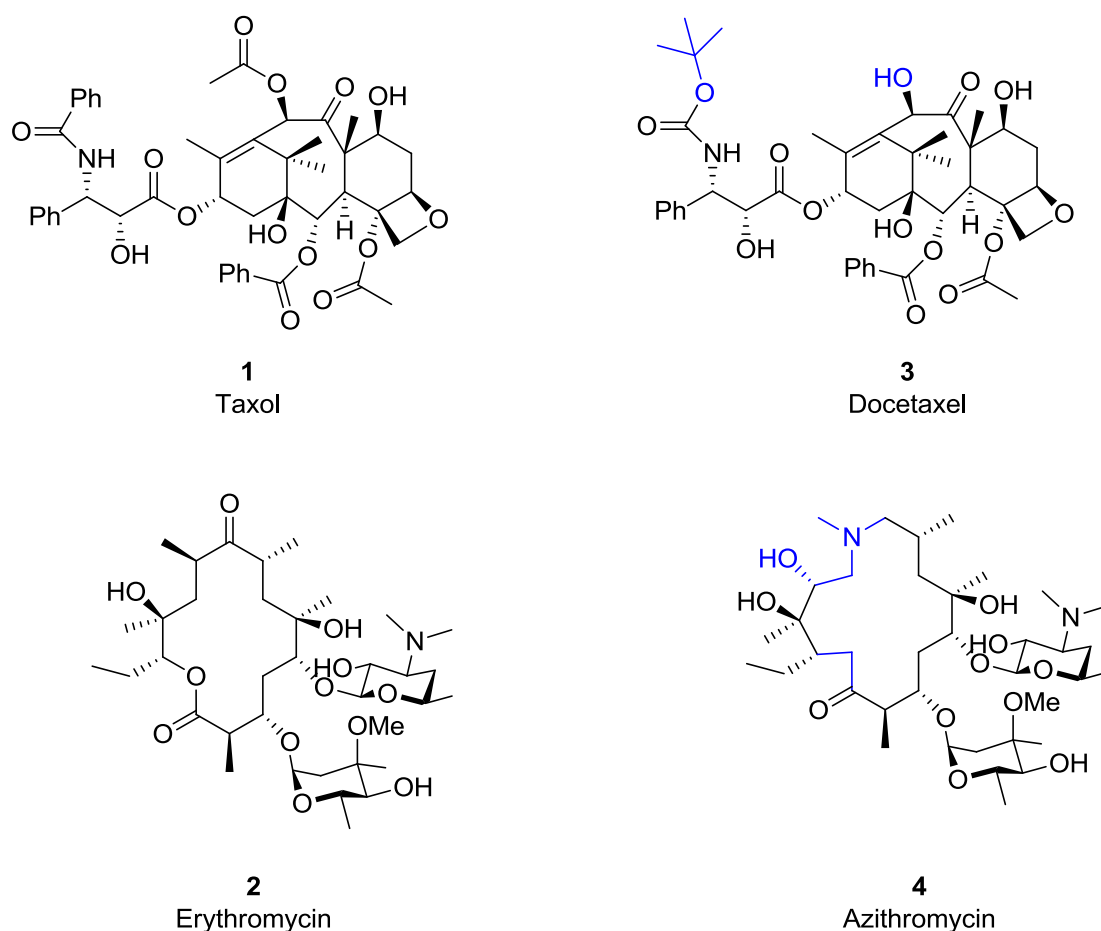


Figure 1.1: Therapeutic drugs inspired by natural products

Total synthesis can provide a means to prepare substantial quantities of scarce, biologically active natural products. These bioactive natural compounds, which are often secondary metabolites, are present in the host organism in minute amounts, making biological evaluation and medical application very difficult when relying on natural sources. The synthetic preparation of natural products allows for further research into their therapeutic properties and is also a useful tool for confirming the structure and absolute stereochemistry of a molecule. Furthermore, a number of structural revisions have been reported as the result of information gained from total synthesis.^{7, 8} Total synthesis provides an excellent platform to investigate the medicinal properties of natural product analogues. Advanced synthetic intermediates provide many opportunities to explore natural product derivatives that are not accessible from the natural product itself. These structural modifications provide insight into structure-activity relationships of specific biological activities.

Epothilone A (**5**) was first isolated from *Sporangium cellulosum*,⁹ and the first total synthesis of epothilone A was reported in 1996.¹⁰ However, despite the promising *in vitro* anticancer

activity of epothilone A, there was significant toxicity even at sub-therapeutic doses.¹¹ Using diverted total synthesis, a number of synthetic intermediates were converted into natural product analogues,¹² some of which have progressed into clinical trials. Including ixabepilone (**6**) a derivative of epothilone B, modified for improved pharmacokinetic profile, as of October 2007, ixabepilone was approved by the FDA for clinical use¹³.

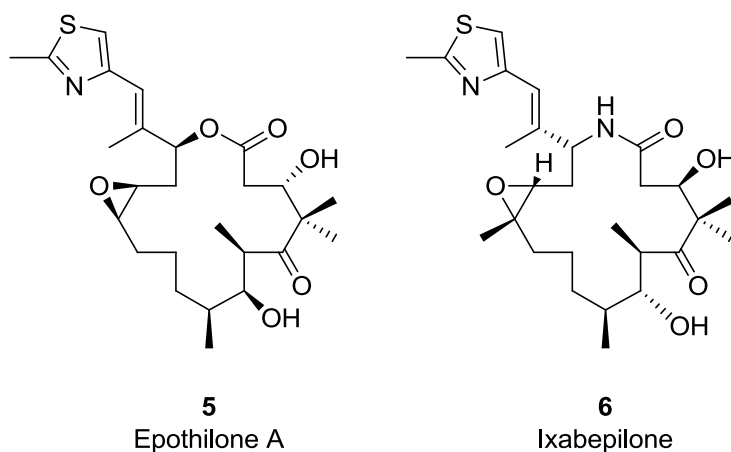


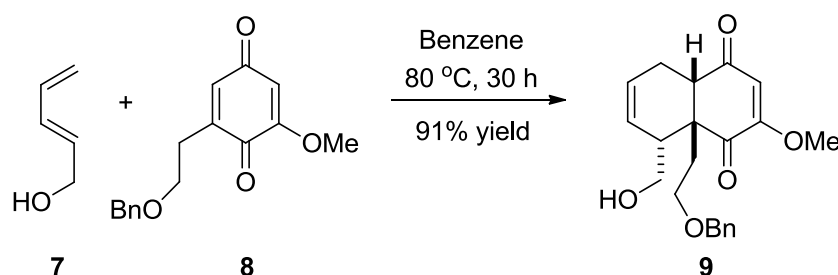
Figure 1.2: Structure of Epothilone A (**5**), and Ixabepilone (**6**) an Epothilone B analogue

1.1.2. The Pursuit of “Atom Economy” in Total Synthesis

Improving the efficiency of chemical synthesis has long been a fundamental goal in the preparation of target compounds. This goal has been pursued primarily through the development of new chemical transformations that generate molecular complexity in a facile and selective manner.¹⁴ The efficiency of a chemical reaction can be measured using a variety of metrics, one of the most useful being “atom economy.”¹⁵ A number of major achievements in atom economy have been the direct result of the development of transition metal-catalysed reactions, such as the Pd-catalysed asymmetric allylic alkylation and the ruthenium-catalysed alkene-alkyne coupling. The application of these methodologies in the synthesis of complex natural products provides a framework for the further refinement of atom economic synthesis.

The goal of atom economy is to maximise the mass efficiency of a reaction, having all or most of the atoms of the starting materials incorporated into the final product, and using all other reagents in a catalytic manner. Atom efficiency is created by the efficient activation of reagents, with control over the selectivity of the bond forming process being very important.

In some instances the adjacent functional groups make bond forming inherently efficient and selective. For example the normal electron demand Diels-Alder reaction, is a particularly atom economic reaction, with all atoms from the reactants incorporated in the product, occurring in a region- an stereoselective manner by heating the appropriate diene **7** and dienophile **8** (Scheme 1.1). The majority of reactions are not this simple and additional atoms are required to activate the reacting centres and control selectivity of the reaction.¹⁶ Maximising atom economy while maintaining high levels of selectivity therefore remains challenging.



Scheme 1.1: Thermal Diels-Alder reaction, with excellent atom economy

Another approach that has successfully addressed some of the current challenges in drug discovery is natural product derived fragments. These fragments often have significantly reduced molecular weights, and decreased structural complexity and require fewer synthetic steps, while retaining key pharmacophores.³ Dynemicin (**10**) was discovered in 1989 and showed potent *in vivo* antitumor activity ($IC_{50} = 7-9 \text{ nmol L}^{-1}$), the first total synthesis was reported by Myers *et al.* in 1995 with a total of 26 steps in 0.3 % yield.^{17, 18} One of the simplest analogues (**11**) was synthesised by Wender in only 7 steps, while retaining similar bioactivity.¹⁹

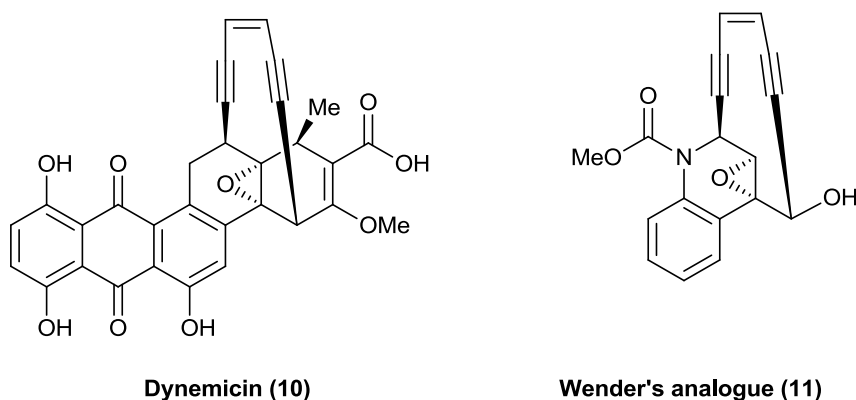


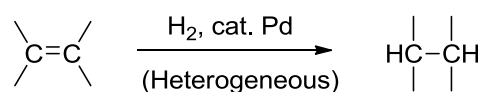
Figure 1.3: Structure of Dynemicin (**10**) and Wender's analogue of Dynemicin (**11**)

1.2. Palladium in Organic Synthesis

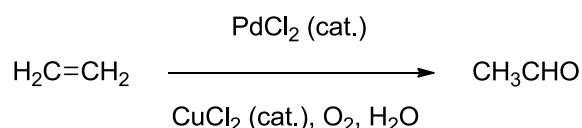
1.2.1. Introduction

Discovered by Wollaston in 1803 and named after the asteroid Pallas, palladium is a remarkable metal and has become one of the most useful catalytic reagents in organic synthesis.²⁰ Since palladium is an expensive noble metal, its derivatives have mainly been employed as catalysts. Discovery of the Wacker process in 1959 and its subsequent industrial development represents one of the most important milestones in the history of organopalladium chemistry.

The catalytic reduction of alkenes (Scheme 1.2) and the Wacker oxidation of ethene (Scheme 1.3) demonstrate that palladium and its compounds can serve as catalysts for both oxidation and reduction.²¹



Scheme 1.2: Catalytic hydrogenation of alkenes with palladium catalyst

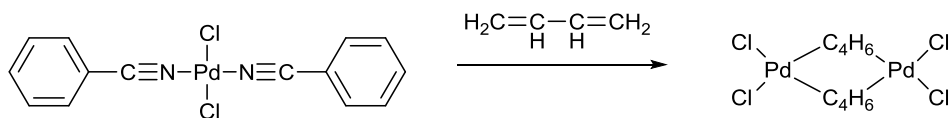


Scheme 1.3: Wacker oxidation of ethene

Palladium has a high affinity for non-polar π -compounds such as alkenes, alkynes and even arenes.²¹ Upon complexation with transition metals, π -compounds are rendered more reactive towards nucleophilic species.

Allyl palladium derivatives readily react with a wide range of nucleophilic reagents to undergo nucleophilic substitution reactions, with palladium serving as a surrogate leaving group. The reaction of buta-1,3-diene with PdCl_2 reported in 1957 most likely represents the

first synthesis of allyl palladium complexes (Scheme 1.4).²² Early investigations of allyl palladium species mainly dealt with structural features and other purely organometallic aspects and it was not until Tsuji's work in 1965 that these compounds became prevalent in organic synthesis.²¹



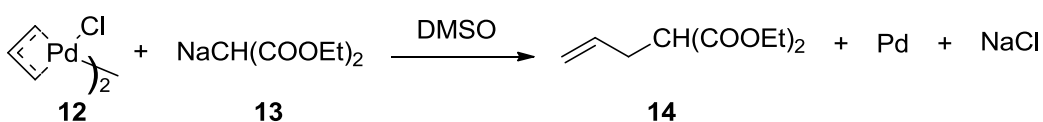
Scheme 1.4: Reaction of benzyl nitrile palladium(II) chloride with 1,3-butadiene

1.2.2. The Tsuji-Trost Reaction

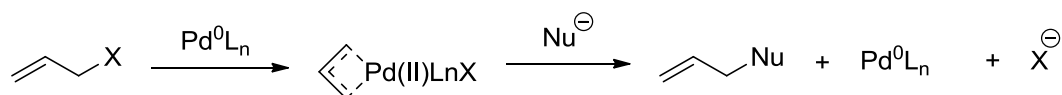
Tsuji's extension of the Wacker process and proposal of its mechanism (nucleophilic attack of H₂O on ethylene complexed with Pd or Pd-complexed ethylene) led to the discovery of carbon-carbon bond formation between π -allylpalladium chloride (**12**) and diethyl sodiomalonate (**13**) to give the allylated malonate (**14**) (Scheme 1.5).²³

This reaction remained stoichiometric with respect to palladium for a few years until a catalytic version was discovered and subsequently extensively developed by Tsuji,²⁴ Trost,²⁵ and many others.

Original Stoichiometric Version



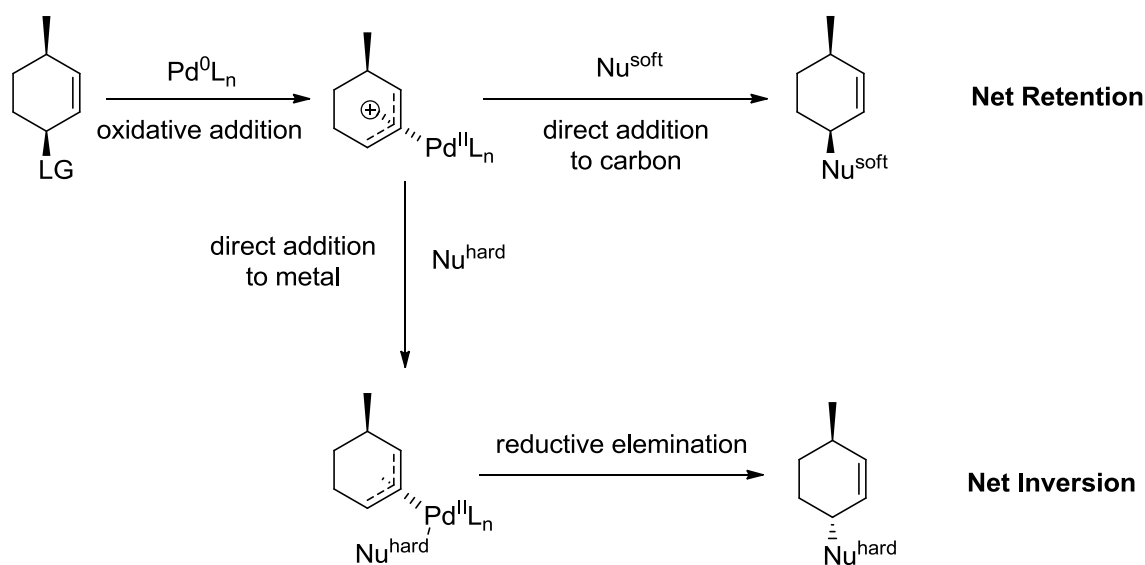
Catalytic Version



Scheme 1.5: Model of the Tsuji–Trost reaction

Oxidative addition of palladium to allyl electrophiles has been shown to proceed with inversion of the electrophilic centre.²⁶ This process was proposed to proceed through π -complexation followed by an intramolecular nucleophilic displacement of a leaving group by palladium with inversion of the electrophilic centre. It is now understood that there are two

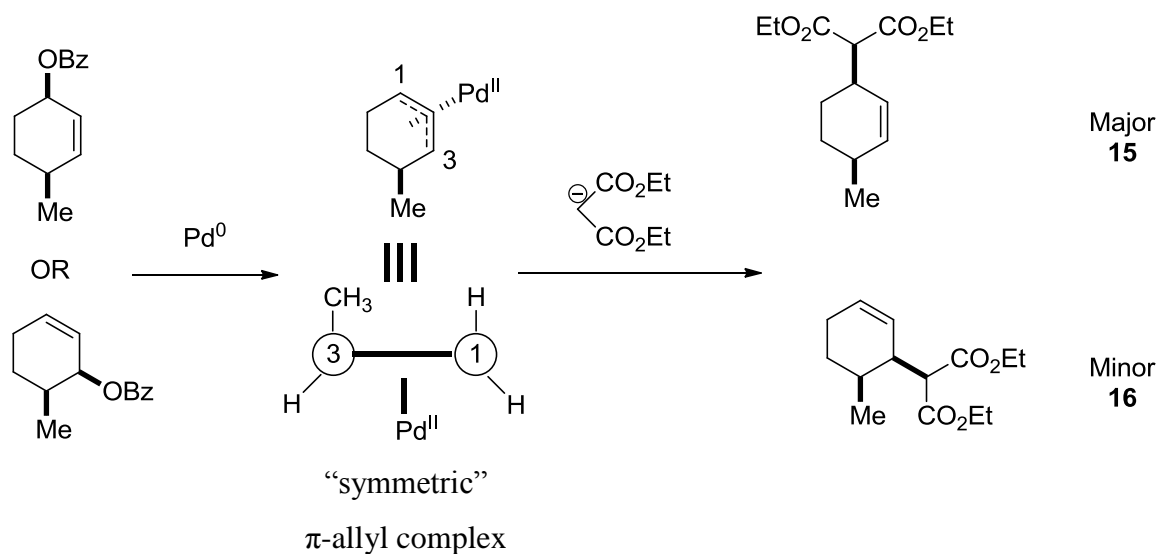
general mechanistic classes that operate for the Tsuji–Trost reaction, which are distinguished by the nature of the nucleophile.²⁷ “Hard” nucleophiles, defined as those derived from conjugate acids with $pK_a > 25$, involve nucleophilic attack at palladium, followed by reductive elimination to provide allylic substitution with overall inversion of stereochemical configuration.²⁸ On the other hand, “soft” nucleophiles, defined as those derived from conjugate acids with $pK_a < 25$, normally attack directly at the π -allyl ligand proceeding via a second inversion at the site of substitution and leading to substitution of allylic electrophiles with retention of overall stereochemistry (Scheme 1.6).²⁶



Scheme 1.6: Asymmetric induction in Tsuji–Trost reactions with the use of soft and hard nucleophiles

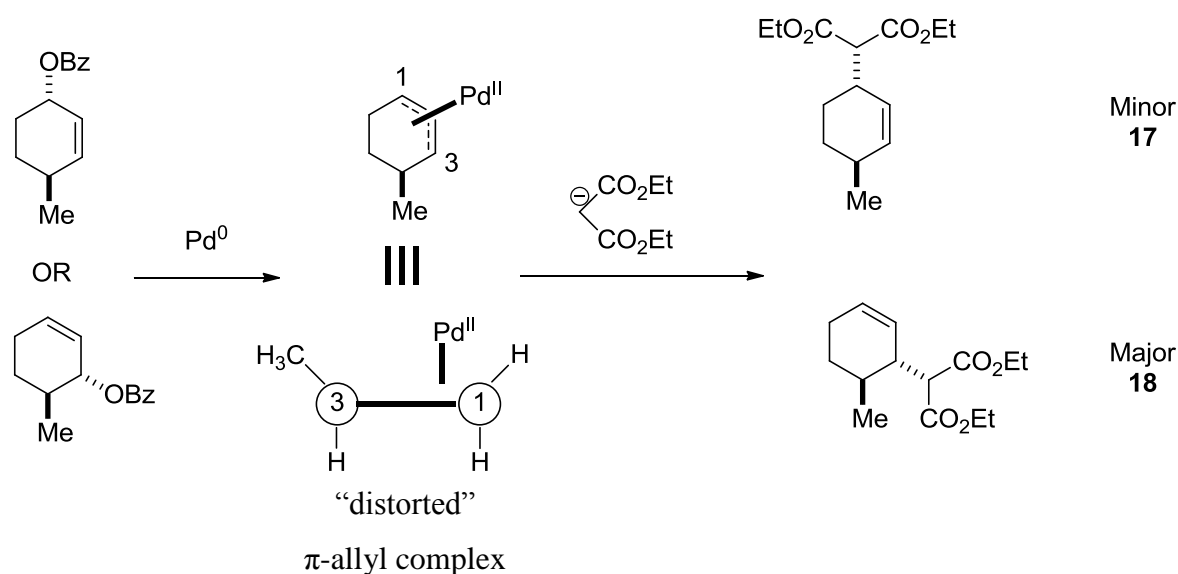
The palladium-catalysed allylic alkylation (Pd-AA) has become a widely studied area of organometallic chemistry,²¹ and it involves a substitution reaction of a substrate containing a leaving group in an allylic position with a nucleophile. The regioselectivity in a Pd-AA reaction is influenced by steric and electronic factors. The analysis of Pd- π -allyl intermediates provides a reliable method for predicting and understanding regiochemical outcomes of Pd-AA reactions.²⁹ In many cases, ionisation of an allylic acetate or benzoate caused by displacement of the leaving group by palladium, provides a “symmetric” η^3 complex, where the metal centre resides “symmetrically” over the π -allyl system (Scheme 1.7). This generally occurs when the Pd-allyl complex rests on the opposite face to any allylic substituents, the η^3 complex is close to symmetrical. This arrangement typically favours the

1,4-substituted regioisomer (**15**) over the 1,2-regioisomer (**16**), as nucleophilic addition to the least hindered carbon is preferred.²⁹



Scheme 1.7: Regioselectivity of “symmetric” Pd- π -allyl complexes

The formation of “distorted” Pd- π -allyl complexes, where ionisation of the allylic acetate or benzoate results in the Pd-allyl complex residing on the same side as any allyl substituents, have been proposed in cases where unfavourable steric interactions between palladium and neighbouring substituents on the same face are possible, leading to very different regiochemical outcomes (Scheme 1.8).²⁹ The “distorted” Pd-allyl complexes have been described as σ - η^2 species that undergo nucleophilic substitution through an S_N2 -like mechanism, giving rise to the 1,2-regioisomer (**18**) as the major product.²⁹



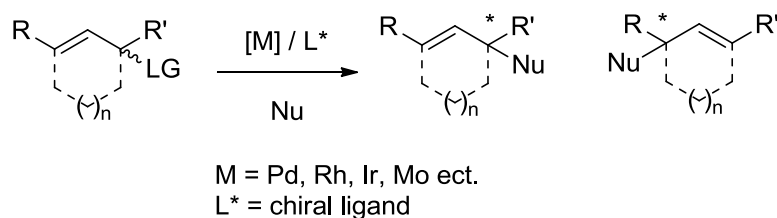
Scheme 1.8: Regioselectivity of “distorted” Pd- π -allyl complexes

Palladium-catalysed AA reactions are extremely versatile and have the ability to form several different kinds of new bonds, using the same catalyst. The synthetic utility arises from the wide range of possible nucleophiles, with H, N, O, S, C being most widely used. This provides access to C-H, C-N, C-O, C-S, and C-C bonds in a selective manner. By changing the metal centre and/or nucleophile, net retention or net inversion of stereochemistry can be achieved. AA reactions are not limited to Pd catalysts, with metals such as Rh, Ru, Ir, Mo, Ni, W, Cu, and Pt all having been used to successfully catalyse AA reactions.³⁰ However these reactions occur through different mechanisms and have alternative stereochemical outcomes.

1.2.3. Asymmetric Allylic Alkylation Reactions

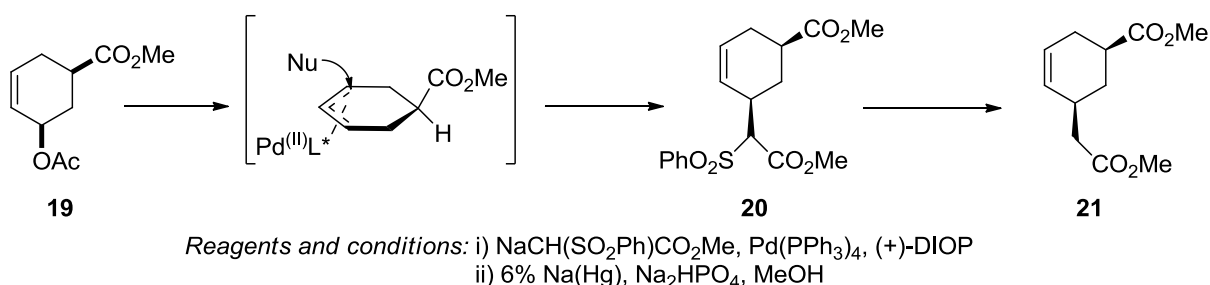
Transition metal-catalysed asymmetric allylic alkylation (AAA) reactions (Scheme 1.9) are enantioselective extensions of the Pd-AA reaction and are unique and versatile for several reasons. The presence of a carbon-carbon double bond in the overall product is very advantageous to total synthesis as it provides great potential for further functionalisation.³⁰ AAA reactions have the ability to convert prochiral or racemic substrates into

enantiomerically pure compounds, typically accomplished using chiral ligands.³⁰ These reactions also have numerous modes of enantiomeric selectivity, compared to most other asymmetric reactions where there is only one. In AAA reactions, both the electrophile and nucleophile may be prochiral, in which case the configurations of the positions resulting from either or both substrates can be controlled. AAA reactions, like palladium-catalysed allylic alkylations, also have the potential to form many different types of bonds, and can be tailored to undergo either net inversion or net retention of stereochemical centres. Pd-AAA reactions involve a net retention of the stereochemistry *via* a double inversion of stereo-centres with “soft” nucleophiles and a net inversion of stereo-centres with “hard” nucleophiles (*vide supra*).



Scheme 1.9: Transition metal catalysed asymmetric allylic alkylation reaction

The first example of enantioselective palladium-catalysed allylic substitution with a stabilised nucleophile was reported in 1977.³¹ When the racemic mixture **19** was treated with the sodium salt of methyl phenylsulfonylacetate in the presence of a palladium catalyst Pd(PPh₃)₄ and a chiral ligand (+)-DIOP, the alkylation product **20** was produced in 77% yield and subsequent desulfonylation of this product afforded **21** with 24% e.e. (Scheme 1.10). Since this achievement, a vast amount of work has been carried out to exploit the asymmetric capability of allylic alkylations and to improve enantioselectivity.^{27, 32}



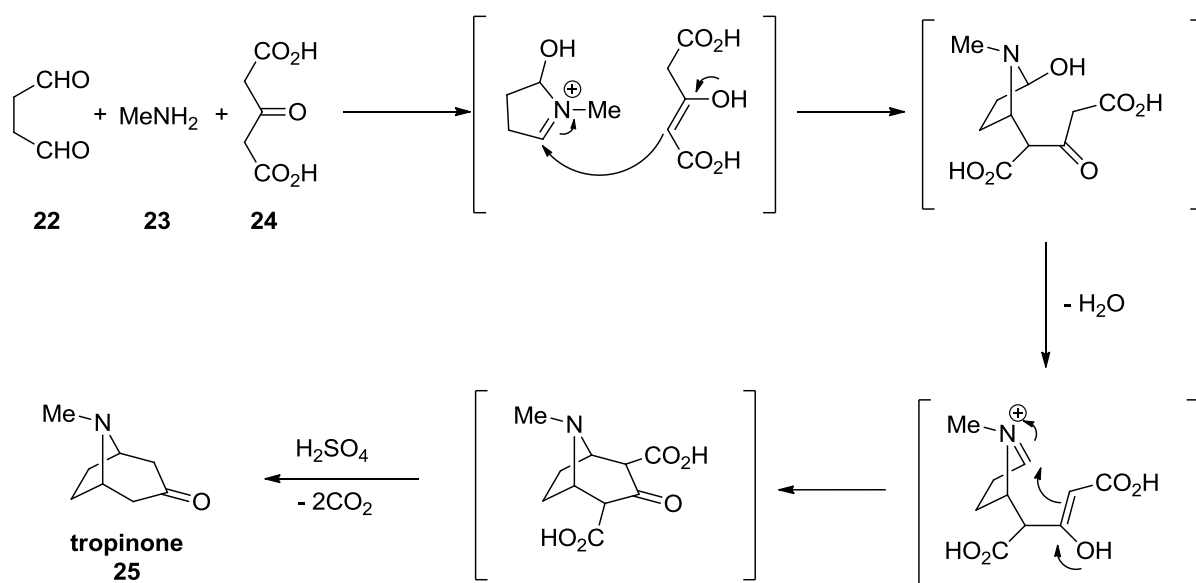
Scheme 1.10: Enantioselective palladium-catalysed allylic substitution with a stabilised nucleophile

1.3. Allylic Alkylation Cascades

1.3.1. Cascade Reactions

Cascade reactions are defined as chemical reactions in which at least two bond-forming transformations take place under the same reaction conditions and where the latter transformations take place at the moieties produced by the former bond-forming processes.³³⁻³⁵ In recent years, examination of biosynthesis as a means to guide synthetic strategies has led to the use of cascade reactions.³⁶ Nature's synthetic transformations typically avoid protecting groups, are generally conducted in aqueous solvent, at ambient temperature and pressure, and many are cascade reaction sequences. The benefits of cascade reactions are undeniable and include atom, time, labour, resource and waste economy.³⁷ Additionally, they are often accompanied by high levels of stereoselectivity.³⁶ Therefore, these impressive reactions can be considered a stepping stone on the path to "green chemistry" because the savings involved when several transformations are carried out in one synthetic step can be significant.³⁸ These can include reducing several individual steps into a single reaction, with only one solvent system, workup and purification step.

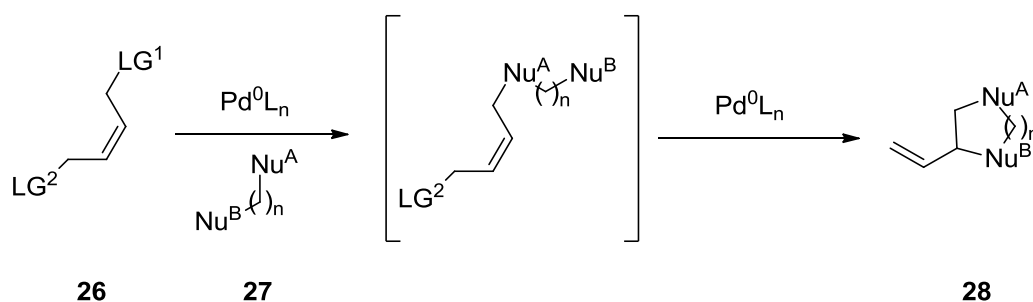
Cascade reactions not only improve the practical efficiency of a synthetic process but also enhance the aesthetic appeal of a proposed synthetic route by enabling the generation of complex molecules in a concise fashion. It is not surprising then that cascade reactions have attracted the attention of organic chemists since the early days of total synthesis. Robinson's 1917 one-pot synthesis of tropinone³⁹ (**25**) set the benchmark for the field of cascade reactions (Scheme 1.11).³⁸ This elegant synthesis constructs tropinone from succindialdehyde (**22**), methylamine (**23**), and either acetone or its dicarboxylic acid derivative (**24**), through the consecutive action of intermolecular and intramolecular Mannich reactions, followed by double decarboxylation.



Scheme 1.11: Robinson's one-pot synthesis of tropinone (25)

1.3.2. Palladium-Catalysed Allylic Alkylation (Pd-AA) Cascades

Palladium catalysts have proven to be reliable tools in a variety of cascade reactions. A generic Pd-AA cascade is one where an allyl bis-electrophile (**26**) is employed alongside a bis-nucleophile (**27**) in the presence of a Pd⁰ catalyst. These annulation reactions can afford an array of vinyl substituted ring systems (**28**) (Scheme 1.12).



Scheme 1.12: General Pd-AA cascade

The problem with these reactions is in differentiating the two nucleophilic and electrophilic centres in order to gain regiochemical control. This results in a large number of possible

regiochemical outcomes (Fig. 1.4). In the first step, ionisation of either leaving group can occur, followed by nucleophilic attack of either nucleophile at either end of the π -allyl intermediate. The number of possibilities may be further compounded by the second addition. This challenge is typically overcome by the use of symmetric bis-electrophiles and/or bis-nucleophiles, which reduces the number of possible regiochemical outcomes.⁴⁰ However, this is not a suitable solution for many synthetic targets, which has limited the use of Pd-AA cascades in total synthesis.

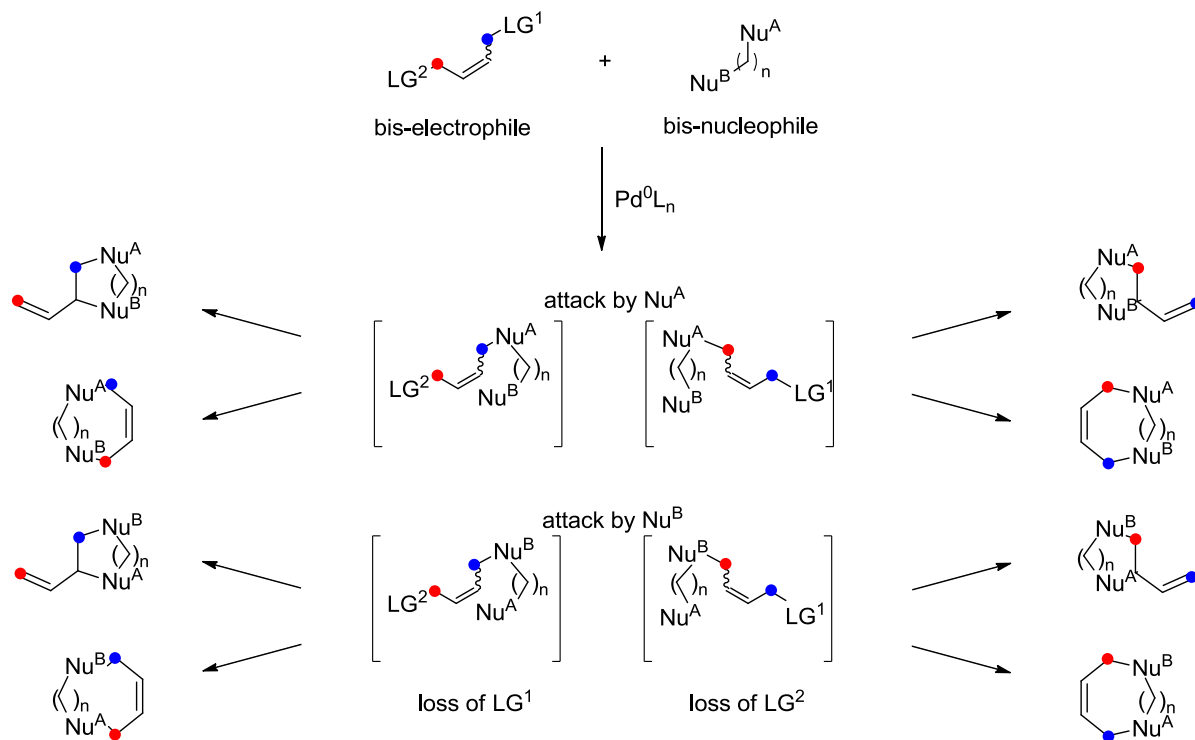
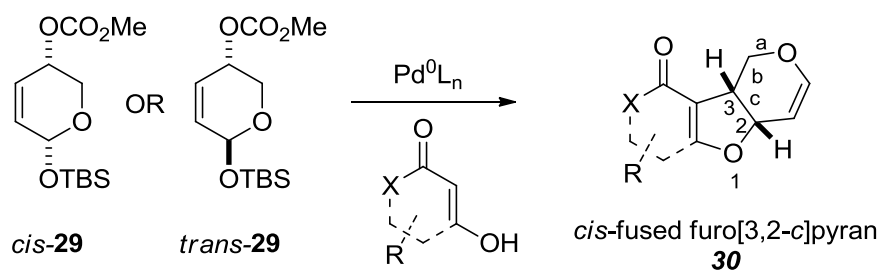


Figure 1.4: Regiochemical possibilities for a Pd-AA cascade

1.3.3. A Pd-AA Cascade with Dihydropyrans

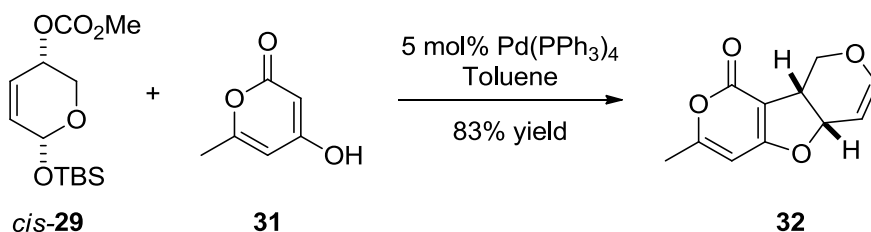
During the course of research by former VUW PhD student Dr Mark Bartlett into the synthesis of pyrone-based natural products, a novel regioselective and stereoconvergent Pd-AA cascade was developed, which was subsequently extended by Masters student Claire Turner and Honours student Stephen Tat.⁴¹⁻⁴⁴ The 3,6-dihydro-2*H*-pyran substrates *cis*- and *trans*-**29** serve as non-symmetric bis-electrophiles for Pd-AA cascades with β -carbonyl compounds (Scheme 1.13). This approach is regioselective and leads to unsaturated furo[3,2-*c*]pyran compounds. The cascade reaction proceeds stereoconvergently, as it was

observed that only the *cis*-fused pyran products were produced, regardless of whether the starting material was *cis*- or *trans*-substituted. Furthermore, computational studies showed that the relative difference in energies between the *cis*- (**30**) and *trans*-fused furopyrans was calculated to be 51 kJmol⁻¹, with the *trans*-furopyran possessing a prohibitively large ring strain energy.⁴²



Scheme 1.13: Regioselective and stereoconvergent Pd-AA cascade

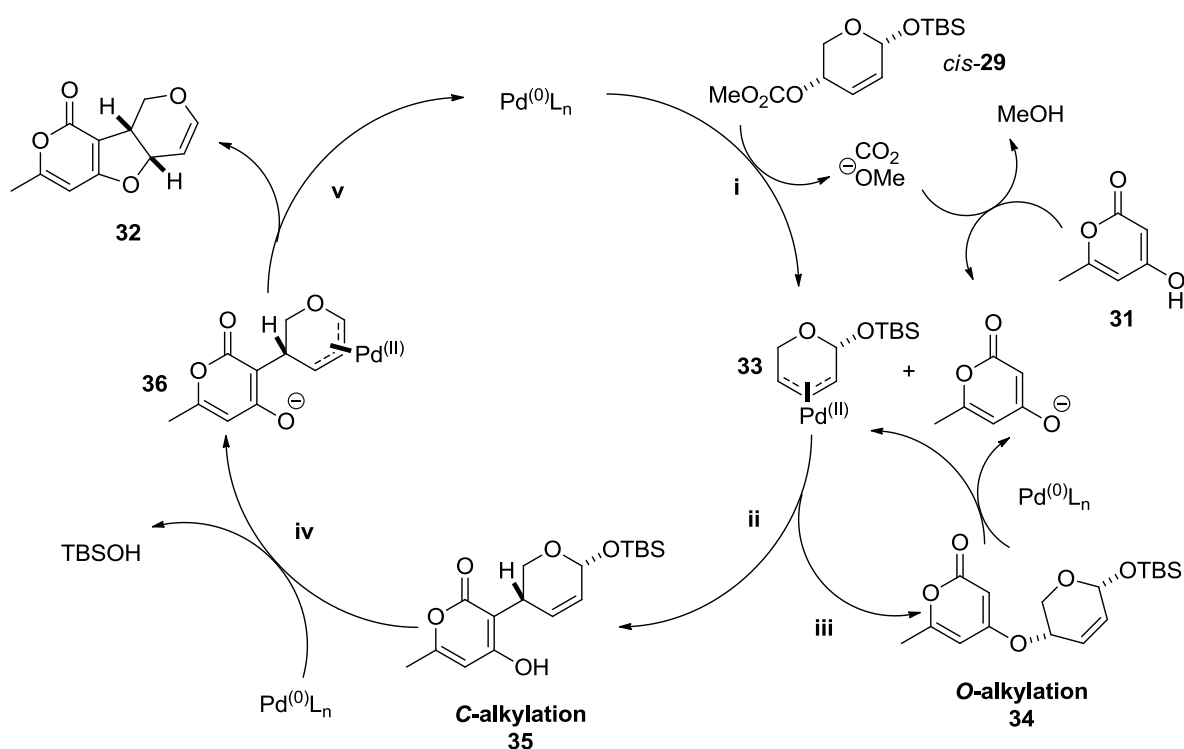
During the course of Bartlett's research, reaction conditions for the Pd-AA cascade were optimised using *cis*-**29** and 4-hydroxy-6-methyl- α -pyrone (**31**) (Scheme 1.14). Toluene was found to be the optimal reaction solvent in conjunction with 5 mol% Pd(PPh₃)₄ and one equivalent of **31**.⁴²



Scheme 1.14: Optimised conditions for the Pd-AA cascade with *cis*-**29** and pyrone **31**

Regiochemical control in this Pd-AA reaction is achieved through the differing relative reactivities of the silyl ether and the methyl carbonate leaving groups at the allylic positions. The anomeric siloxy group has a relatively low reactivity and the steric and electronic demands lead to a preferential ionisation of the allylic carbonate group, causing the formation of the Pd- π -allyl intermediate **33** (Scheme 1.15). The presence of two inductively electron-withdrawing oxygen atoms at C-1 of the dihydropyran reduces the cationic character at the adjacent C-2 position. This has been proposed to also cause an increase in the cationic nature

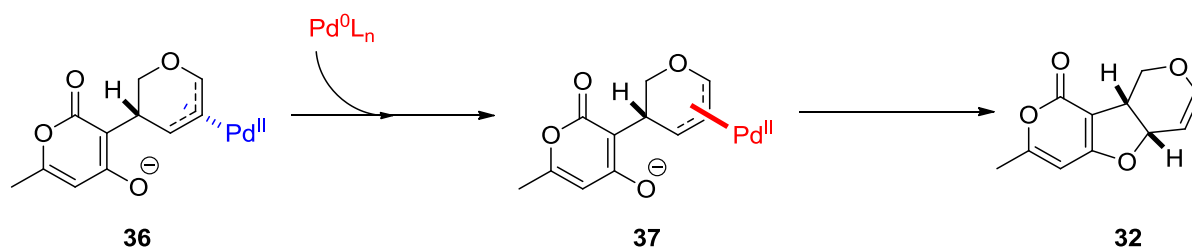
of the C-4 position in the initial Pd- π -allyl intermediate, resulting in preferential alkylation of the C-4 position over the C-2 position.⁴⁵ The methyl carbonate functional group also alleviates the need for an external base, as it readily breaks down, forming methoxide and carbon dioxide (Scheme 1.15, step i).⁴²



Scheme 1.15: Proposed mechanism of Pd-AA cascade with *cis*-**29** and pyrone **31**

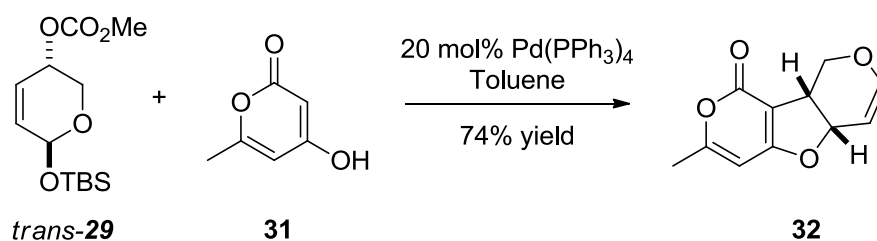
In the proposed mechanism of the reaction between *cis*-**29** and pyrone **31**, ionisation of the allylic carbonate by palladium forms the first Pd- π -allyl intermediate **33**. At this point, nucleophilic attack by either the carbon or oxygen centre can occur, to form either the C-alkylated (**35**) (Scheme 1.15, step ii), or O-alkylated (**34**) adducts (Scheme 1.15, step iii). In the case of *O*-alkylation, it is envisioned that the pyrone would be a suitable leaving group under the reaction conditions due to the similarity of its pK_a to that of acetic acid (a commonly used leaving group in similar chemistry). Therefore in the presence of palladium, ionisation of the pyrone could occur to regenerate the Pd- π -allyl intermediate **33**, followed by carbon attack to afford **36**. Ionisation of the anomeric OTBS group followed by preferential 5-membered ring formation gives the furopyran **32** (Scheme 1.15, steps iv-v).

As mentioned previously, the use of *trans*-**29** in this Pd-AA cascade also produces the *cis*-fused furopyran product, this is proposed to be the result of the large amount of strain energy present in the *trans*-fused furopyrans product. Mechanistically, it was proposed that from the alternative Pd- π -allyl system (**36**) that would be derived from *trans*-**29**, attack by a second palladium species at the π -allyl system, which proceeds with inversion of configuration, forms intermediate **37** (Scheme 1.16). Subsequent annulative oxygen attack then occurs as shown above in scheme 15 to provide the *cis*-fused furopyran **32**.



Scheme 1.16: Proposed isomerisation of Pd- π -allyl intermediate **36**, allowing a stereoconvergent pathway for the Pd-AA cascade of *trans*-substituted substrates

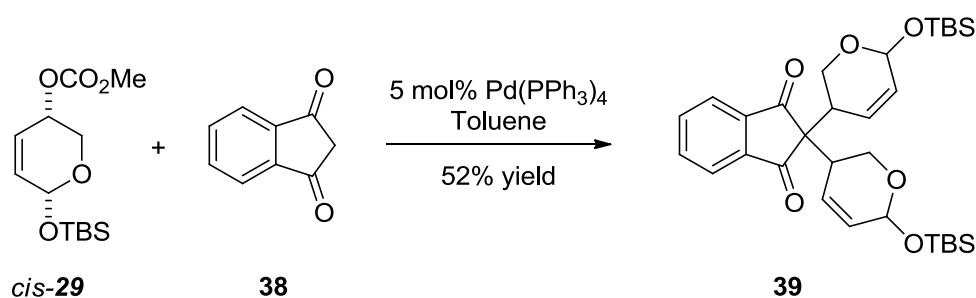
It was shown that in order to achieve stereoconvergence and obtain *cis*-fused furopyrans in good yields from *trans*-**29**, a higher catalyst loading was required. Reaction between *trans*-**29** and pyrone **31** in the presence of 5 mol% Pd(PPh₃)₄ resulted in poor conversion and a low yield (10%) of the desired *cis*-fused furopyran **32**. Increased catalyst loading to 20 mol% increased yield to 74% (Scheme 1.17). The higher catalyst loading required for efficient transformation of *trans*-**29** suggests that the initial *syn*-palladium-allyl complex **36** is isomerised by intermolecular nucleophilic attack of a transient Pd(0) species, supporting the proposed mechanism of Pd- π -allyl isomerisation.



Scheme 1.17: Pd-AA cascade with dihydropyran *trans*-**29** and pyrone **31**

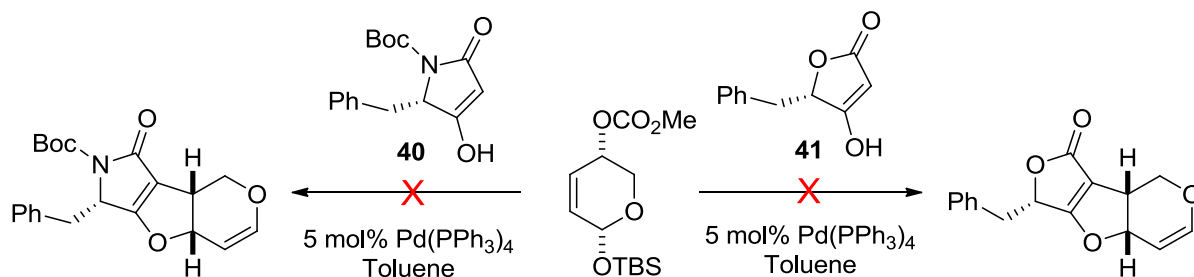
The scope of this Pd-AA cascade was explored using various β -dicarbonyl bis-nucleophiles.^{41, 43, 44} In general, nucleophiles with high enol content such as α -pyrones and

coumarins produced the highest yields. Substrates which favour the β -diketo form, such as dimedone and 1,3-indandione (**38**), were prone to the formation of side products such as α,α -disubstituted β -dicarbonyl **39** (Scheme 1.18). This implied that the β -dicarbonyl species with a propensity to exist in the enol form were better substrates for this chemistry.



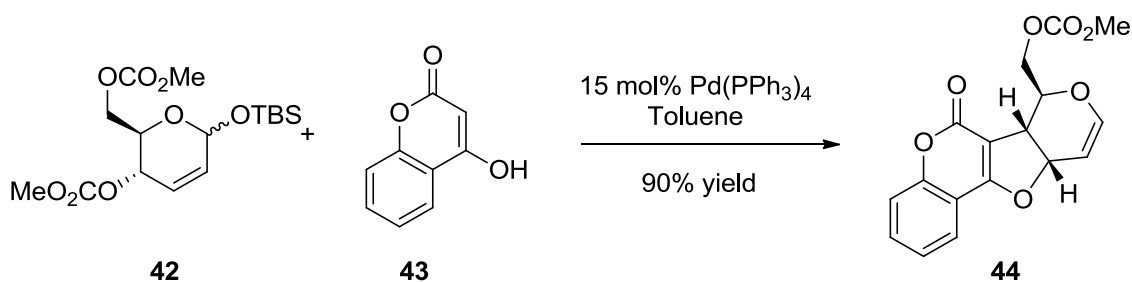
Scheme 1.18: Formation of α,α -disubstituted β -carbonyl side products

High enol content alone did not guarantee formation of the desired products as shown below in Scheme 1.19. Tetramic (**40**) and tetronic acids (**41**), which predominantly exist in the enolic form, did not produce the desired furopyran product.⁴²



Scheme 1.19: Unsuccessful Pd-AA cascade with tetramic (**40**) and tetronic (**41**) acids

The sugar-derived bis-electrophile (**42**) showed similar reactivity to bis-electrophile **29** (Scheme 1.20). The starting material contained a 3:2 mixture of α : β anomers which also yielded *cis*-fused furopyran compounds.⁴³ A higher catalyst loading was required for efficient conversion, with optimal loading found to be 15 mol% Pd(PPh₃)₄.⁴²



Scheme 1.20: Pd-AA cascade using sugar derived bis-electrophile **42**

1.4. Bioactivity of Furopyran Compounds

Application of the Pd-AA cascade methodology has led to the synthesis of multiple furo[3,2-*c*]pyran species, some of which exhibit promising bioactivities. Products shown in Table 1.1 were tested using a previously developed method⁴⁶ employing an MTT assay against HL-60, a human leukemia cell line. IC₅₀ values, half the maximal inhibitory concentration, measures the effectiveness of a compound in inhibiting biological function.⁴⁷ Previous work found that compounds **45** and **32** were virtually inactive, based on the concentration needed for 50% inhibition being greater than the highest measured amount (100 or 250 μM respectively). The dimedone-derived compound **46** exhibited a modest activity with an IC₅₀ value of 29 μM. The introduction of a methyl carbonate substituted branch on the dihydropyran ring of compounds **45** and **32** was shown to provide a marked increase in activity. With the pyrone and coumarin-based compounds **44** and **47** having IC₅₀ values of 21 μM and 25 μM respectively, a large improvement in activity when compared to their unsubstituted analogues **45** and **32**.^{41, 43}

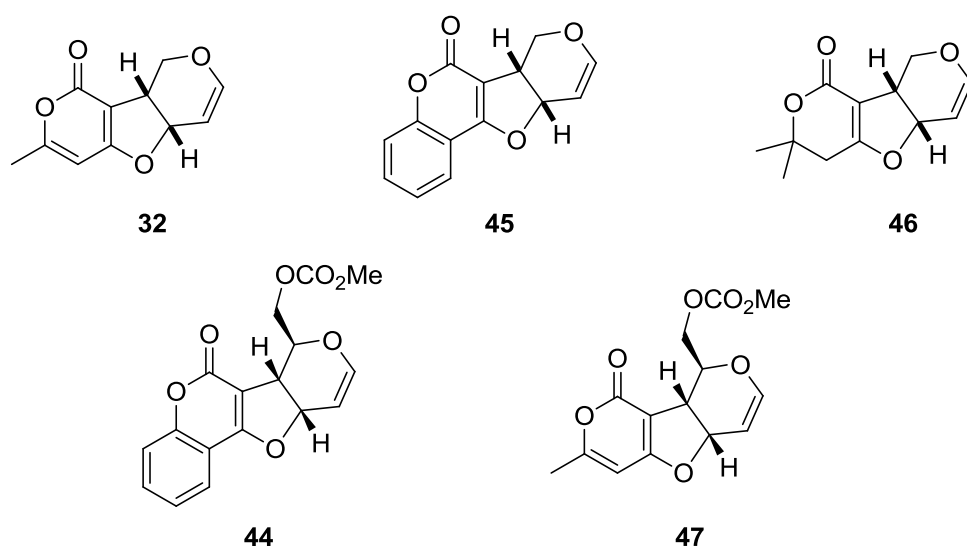


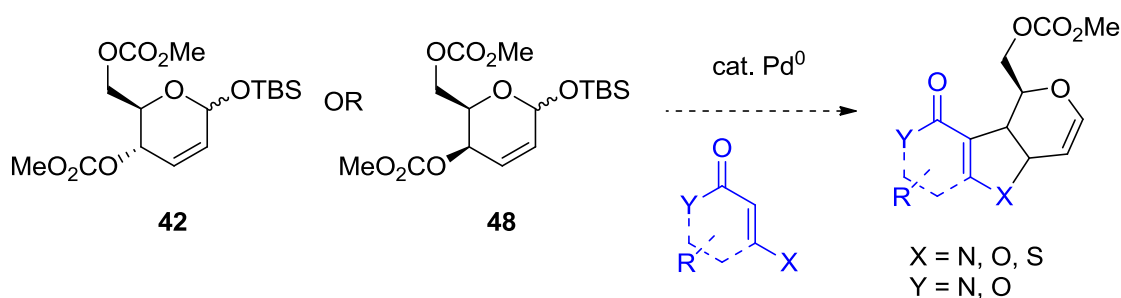
Figure 1.5: Fuopyran compounds tested for bioactivity

Table 1.1: Bioactivity of fuopyrans compounds measured using IC₅₀ values

Compound	HL-60 (IC ₅₀)
32	> 250 μM
45	> 100 μM
46	29 μM
44	21 μM
47	25 M

1.5. Research Objectives

The research objectives of this project were two fold. The first objective was to optimise the current Pd-AA cascade conditions as developed by Bartlett and Harvey,⁴² using a variety of solvent systems, pre-catalysts and ligands. The second objective was to further expand the scope and utility of the Pd-AA cascade methodology through using novel nitrogen, sulfur and oxygen containing bis-nucleophiles as substrates and galactose or glucose derived pyrans as bis-electrophiles (**42**, **48**) to synthesise new furo[3,2-*c*]pyran-based heterocycles (Scheme 1.21).



Scheme 1.21: Overall reaction for Pd-AA cascade

1.5.1. Optimisation of the Palladium Allylic Alkylation Cascade

The Pd-AA cascade reaction was first carried out under the optimised conditions developed at VUW by Bartlett *et al.*⁴² Following the first generation of Pd-AA cascade reactions, optimisation using a variety of solvent systems and catalysts was sought, as detailed below in Table 1.2. Careful choice of ligands can facilitate the reactivity of the catalytic cycle: allyl- π -Pd formation, and attack of nucleophile at the electrophilic centre. Strong σ -donating ligands increase the electron density around the metal centre, accelerating the oxidative addition of the catalyst to the substrate. This is believed to be the rate determining step. Choice of ligand can also determine the mechanism by which oxidative addition occurs.⁴⁸⁻⁵⁰ To fully explore the Pd-AA cascade: a polarity range of solvents, more suitable palladium sources, and ligands

(Figure 1.7) would probe the effect of different heteroatomic substitutions on the reactivity in Pd-AA cascades, and to generate novel and potentially bioactive compounds

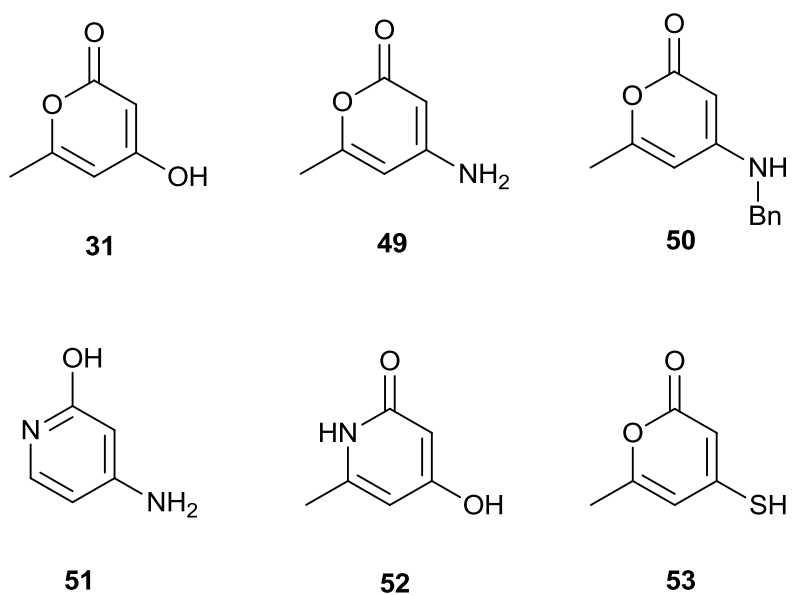
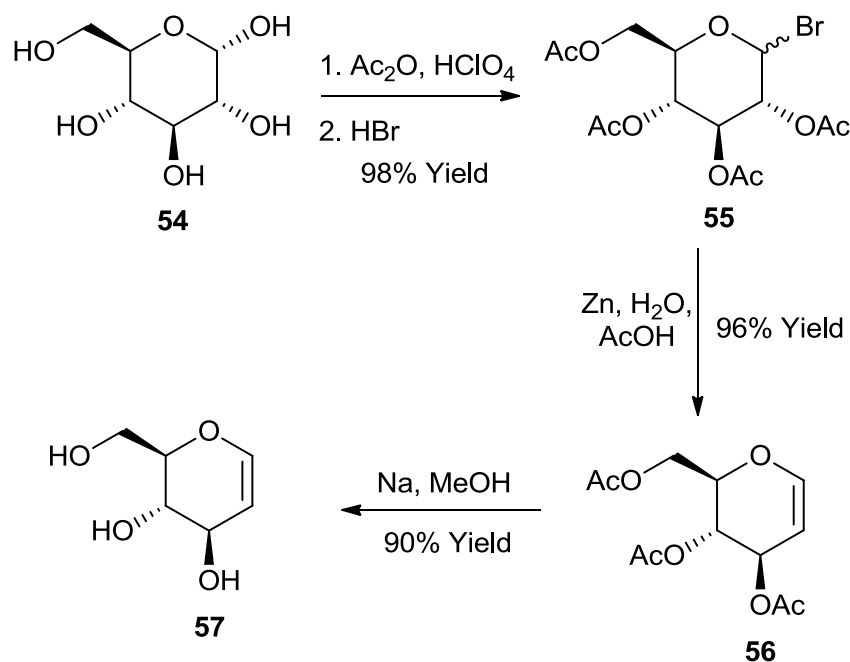


Figure 1.7: Planned bis-nucleophiles for Pd-AA cascade scope studies

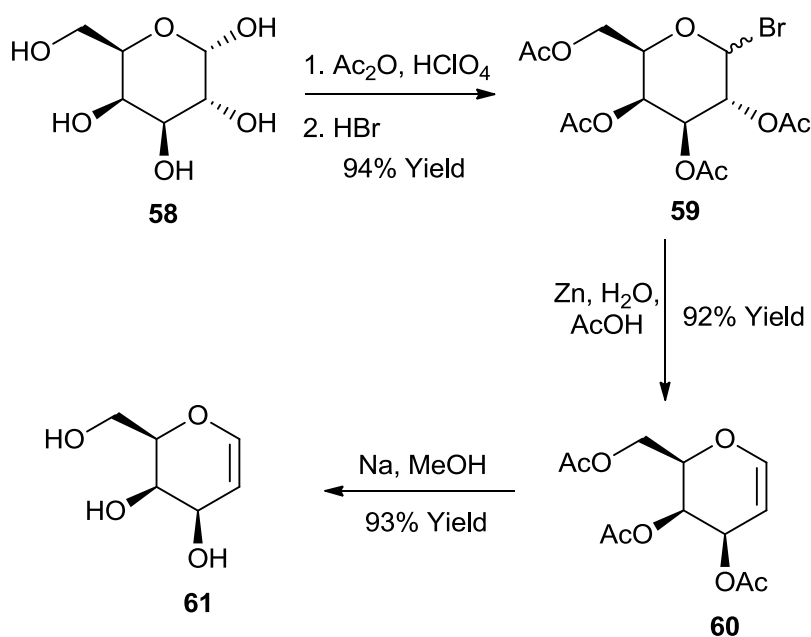
2. Results and Discussion

2.1. Synthesis of Bis-electrophiles

During previous work by Bartlett and Turner, a synthesis of dicarbonate silyl 2,3-unsaturated sugar **42** was developed and this methodology was applied to the synthesis of the target bis-electrophiles. Synthesis of both D-glucal and D-galactal proceeded smoothly at 100 mmol scales with yields of 85% and 80%, respectively, over three steps (Scheme 2.1).

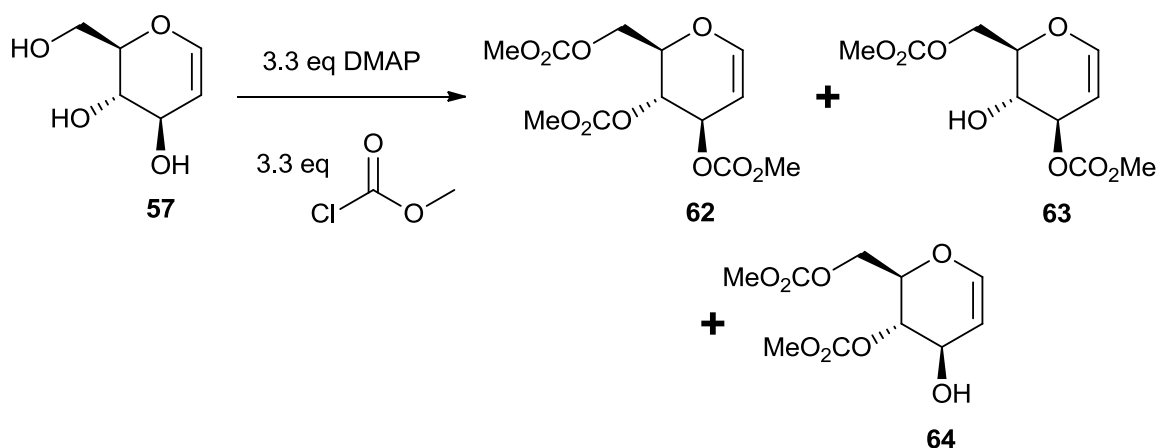


Scheme 2.1: Synthesis of D-glucal from D-galactose



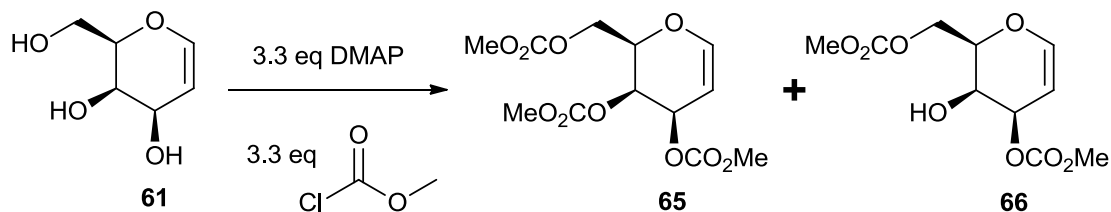
Scheme 2.2: Synthesis of D-galactal from D-galactose

Conversion of **57** and **61** to the tricarbonate species **62** and **65** through reaction with methyl chloroformate and stoichiometric DMAP, serving as both a catalyst and base, was consistently low yielding. The desired tricarbonate glucal product (**52**) was isolated in 50–55% yields from crude reaction mixtures that also contained the 3,6- and 4,6- dicarbonate glucal products (**63**, **64**) in an approximately 20:1:1 ratio (**62**:**63**:**64**).



Scheme 2.3: Synthesis of tri-*O*-methoxycarbonyl-D-glucal

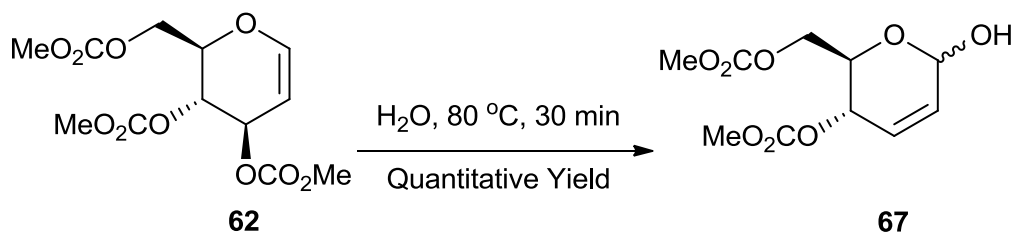
The desired tricarbonate galactal product (**65**) was isolated in 42-45 % yields from crude reaction mixtures that also contained the 3,6- dicarbonate glucal products (**66**) in an approximately 3:1 (**65**:**66**).



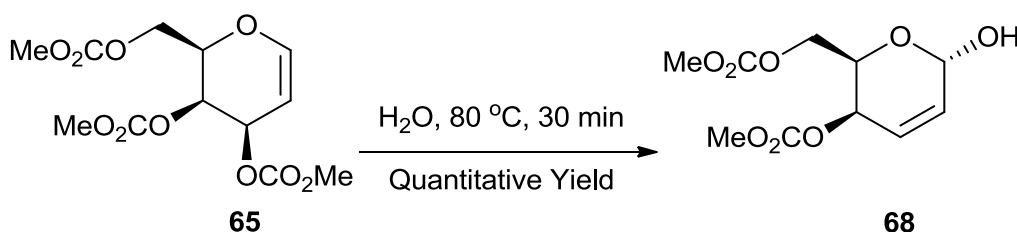
Scheme 2.4: Synthesis of tri-*O*-methoxycarbonyl-D-galactal

After purifying the mixture, the regioisomeric dicarbonate products were combined and resubjected to the reaction conditions produced further **62** and **65**, allowing the recycling of unreacted dicarbonate products. D-Glucal afforded the 3,6-protected product in higher yield than the 4,6-protected product indicating that the issues surrounding this reaction could be due to steric hindrance induced upon dicarbonate formation. This conclusion is supported by D-galactal producing lower yields of the desired tricarbonate **65** (42-45%), and only the 3,6-protected by-product was isolated; presumably, the additional steric strain arising from a 1,3 diaxial interaction of the hydroxyl group at the C-4 position makes this position harder to protect, resulting in lower yields and no observable 4,6-protected by-product forming.

Despite the problems associated with the protection of D-glucal and D-galactal, the synthesis of the carbonate bis-electrophiles was continued with the Ferrier-type allylic rearrangement of glucal **62** and galactal **65** with water as the nucleophile. Following the procedure set by Turner this reaction took only 30 minutes, providing quantitative yields of **67** in a 3:1 ratio of α : β anomers (Scheme 2.5), and **68** as only the α anomer (Scheme 2.6). This is not surprising as the additional steric bulk of the axial C-4 protecting group will further disfavour attack on the top face, leading to facial selectivity for the lower face. This factor in addition to the anomeric effect gives the α anomer as the only detectable product.



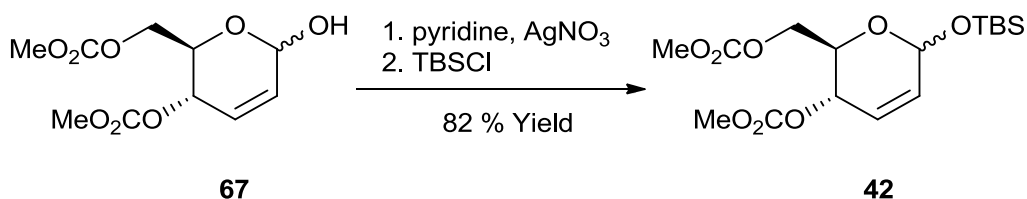
Scheme 2.5: Ferrier-type allylic rearrangement of glucal derivative **62** with water



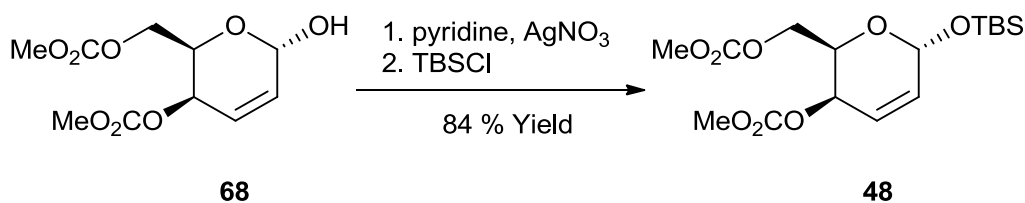
Scheme 2.6: Ferrier-type allylic rearrangement of galactal derivative **65** with water

Due to the only by-products of this reaction being methanol and carbon dioxide formed from the breakdown of the C-3 methylcarbonate leaving group, no work up was required except the removal of water. Furthermore, the yield is quantitative, no organic solvents or metal promoters are used, and there is no need for addition of reagents or catalysts, the reaction is atom economical and requires only short reaction times. Therefore this reaction is a wonderful example of the ideals of green chemistry.

The final synthetic step is silyl protection of the hemiacetals **67** and **68** with TBSCl which proceeded smoothly, providing carbonate bis-electrophiles **42** in 82% yield in a 1:3 ratio of the α : β anomers (Scheme 2.7) and **48** in 84% yield with only the α anomers (scheme 2.8)



Scheme 2.7: Silyl protection of hemiacetals **67** with TBSCl

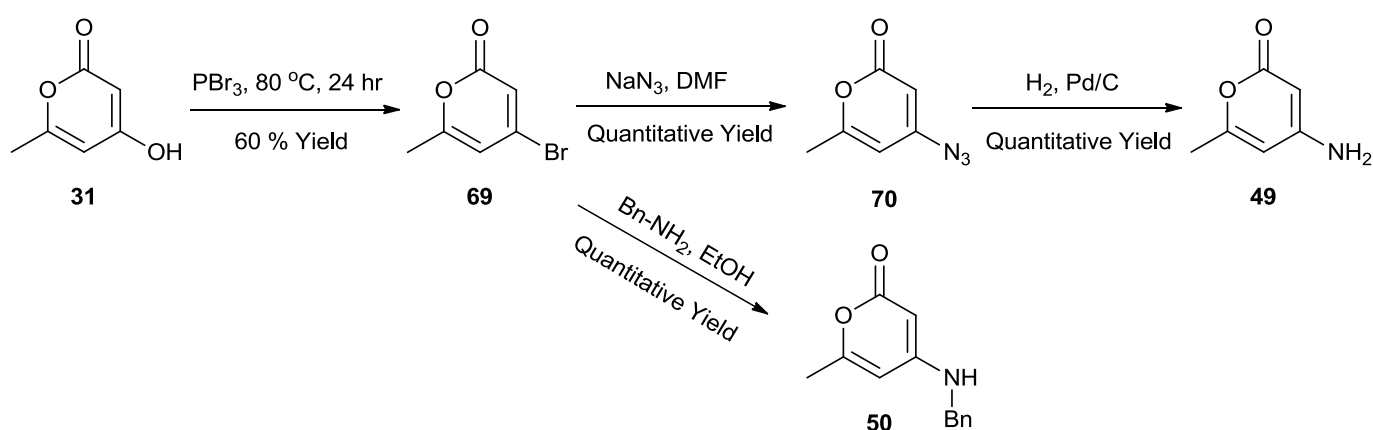


Scheme 2.8: Silyl protection of hemiacetals **68** with TBSCl

2.2. Synthesis of Bis-nucleophiles

During exploration of the scope of the earlier Pd-AA cascade, a variety of cyclic β -dicarbonyl bis-nucleophiles were tested by Bartlett. In general, it was found that nucleophiles with high enol content, such as α -pyrones and coumarins, yielded the best results.

A series of nitrogen and sulfur analogues of β -dicarbonyl bis-nucleophiles were targeted as a means to probe the chemoselective effects of heteroatoms in the cascade. Several nitrogen containing bis-nucleophiles were envisioned for use in the Pd-AA cascade. A synthetic route based on that devised by Cervera *et al.*⁵¹ was used to access the desired nitrogen bis-nucleophiles **49** and **50** from the starting material 4-hydroxy-6-methyl pyran-2-one (**31**) (Scheme 2.9).

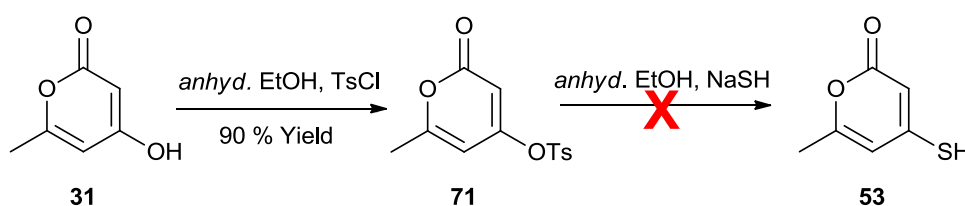


Scheme 2.9: Method for access to bis-nucleophiles **49** and **50**⁵¹

Conversion of **31** to the bromo-species proceeded smoothly with a yield of 60% after purification *via* sublimation. Bromide **69** was then treated with sodium azide in DMF to afford the azide intermediate **70**, or benzyl amine in EtOH to produce benzyl-protected amine

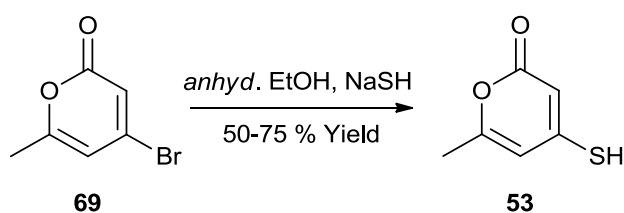
50 in quantitative yields. The azide intermediate was then subjected to hydrogenation to afford the amine bis-nucleophile **49** in quantitative yields.

For the synthesis of the sulfur bis-nucleophile, an attractive two-step literature method for the synthesis of 4-mercapto-6-methyl pyran-2-one (**53**) from 4-hydroxy-6-methyl pyran-2-one (**31**), tosyl chloride, and sodium hydrosulfide was reported by Majumdar *et al.*⁵², and was employed as a starting point for the synthesis of bis-nucleophile **53**. While 6-methyl-4-tosyl pyran-2-one (**71**) was successfully synthesised in 90% yield, the nucleophilic attack by sodium hydrosulfide was unsuccessful (Scheme 2.10).



Scheme 2.10: Attempted synthesis of bis-nucleophile **53**

With the success of the method of Cervera *et al.*⁵¹, used for the nitrogen nucleophiles, the synthesis of 4-mercapto-6-methyl pyran-2-one was envisioned using the same 4-bromo-6-methyl pyran-2-one intermediate, which proceeded smoothly to afford the bis-nucleophile **53** (Scheme 2.11).



Scheme 2.11: Synthesis of bis-nucleophile **53**

The sulfur bis-nucleophile **50** was, however, both light and air sensitive, degrading upon concentration or after long periods of exposure to light. MS analysis showed that the disulfide dimer ($M+H$: 282.278) was the major product of the degradation (Figure 2.1). In order to counteract the degradation it was necessary to store bis-nucleophile **53** as a solution in dry chloroform and under an inert atmosphere of argon, which impeded the ability to get an accurate yield. Through TLC analysis and estimation of spot intensity, it can be estimated that the yield of this reaction is in the range of 50–75 %.

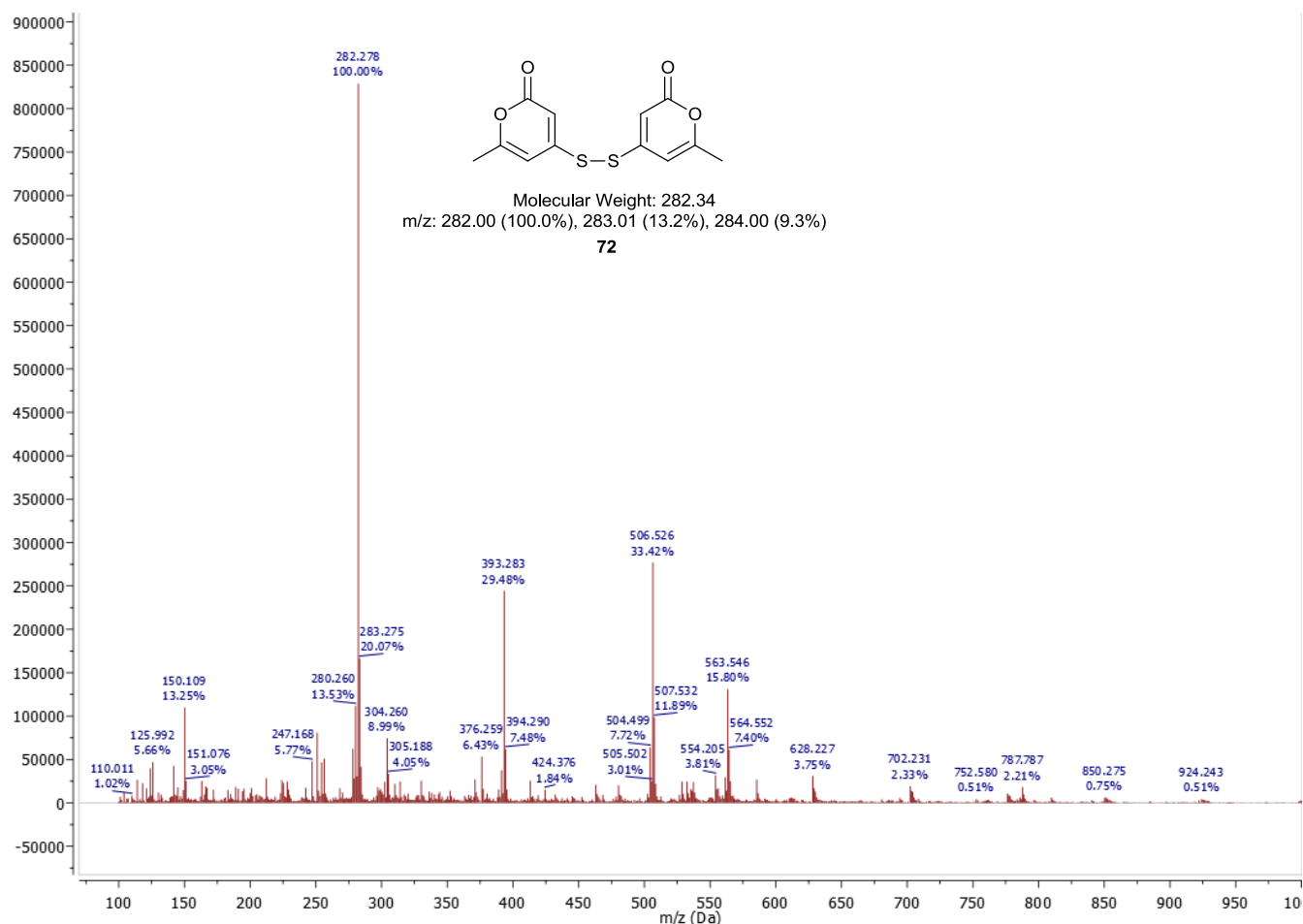


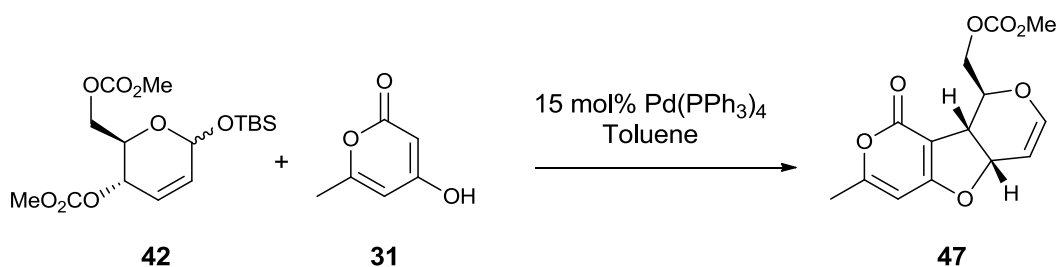
Figure 2.1: Spectra showing 282 m/z peak corresponding to dimer **72**

2.3. Optimisation of Palladium Cascade

2.3.1. Technical Challenges of Pd-AA Cascades and Initial Exploration

Prior to incorporating the prepared substrates, it was necessary to gain competence in carrying out the experimentally challenging Pd-AA cascades by achieving consistency in results of known reactions. Consistent experimental technique was essential in order to maximise the validity of any results gained. This was achieved through repeating Pd-AA cascades on substrates already tested by Bartlett and Turner, and comparing the results with those obtained previously.

An existing Pd-AA cascade was employed as a platform to learn the Pd-AA cascade technique, namely the reaction of pyranone **31** with the glucosyl bis-electrophile **42**.



Scheme 2.12: Selected Pd-AA cascade reaction used for initial exploration

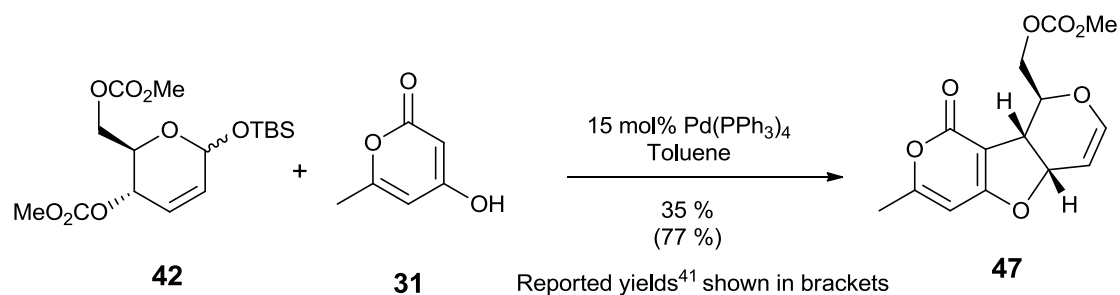
After a few attempts at the synthesis of **47**, it became apparent how sensitive the Pd-AA cascade was to modifications in experiment technique and also to subtle changes in the integrity of solvents or reagents. The initial attempts of the Pd-AA cascade were met with inconsistent results, from low conversion to no reaction at all. In general, this was seen as a direct result of the sensitivity of the Pd(PPh₃)₄ catalyst.

In order to achieve consistent and reliable results, the following techniques were deemed necessary. Firstly, all glassware used in the reactions, or in preparation of the reactions, were thoroughly cleaned and heated to 600 °C with a heat gun under high vacuum and then immediately placed under an inert atmosphere of argon. Secondly, all solvents and liquids were placed over 4 Å molecular sieves, and then degassed using the freeze, pump, thaw method for a minimum of 3 times, and then, when required, transferred into the reaction flask via a cannula that had been dried in an oven overnight and cooled in a desiccator prior to use. The quality of solvent was also found to be a contributing factor in the success of the reactions and freshly distilled solvents were found to produce the best results. Solvents of poorer quality produced lower yields or completely inhibited consumption of the bis-electrophiles. For overnight reactions, new rubber septa with minimal previous use were beneficial to the reaction by eliminating contamination by air and moisture. Furthermore, after all reagents were added a balloon of argon was inserted, and the septa were secured and sealed with parafilm, forming, as much as possible, a closed system.

2.3.2. Optimisation of Pd-AA cascade reaction

Employing the above techniques and Bartlett's methods on the reported cascades eventually led to consistent results; however, in all cases, the yields gained were lower than those

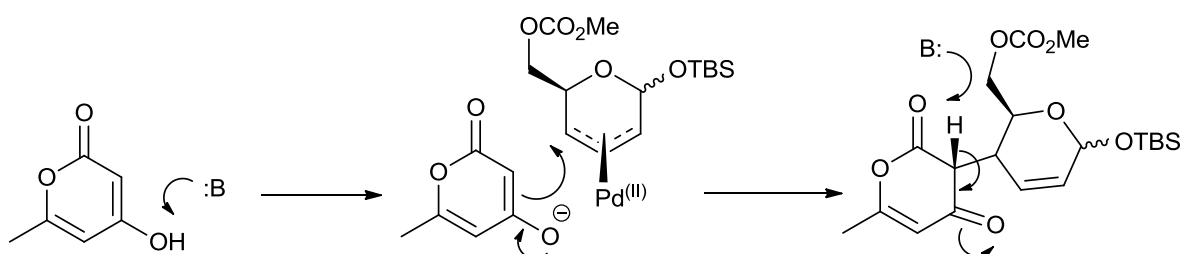
reported by Bartlett (Scheme 2.13). This result emphasises the degree of sensitivity of these reactions where, despite considerable efforts, reproducibility of yields between researchers is limited.



Scheme 2.13: Comparison of reported yields with yields obtained in this work for selected Pd-AA cascades

Using Bartlett's optimised conditions for Pd-AA cascades with the glucosyl bis-electrophile **42** and 6-methyl-4-hydroxypyran-2-one (**31**) as a starting point for the optimisation of the Pd-AA cascade, a study of pre-catalyst, pre-ligand, solvent, and addition of external base was carried out.

Initially the role of an external base in the Pd-AA cascade was investigated. Base, in the form of the methoxide ion liberated from the carbonate leaving group, is generated *in situ*. It is thought to deprotonate the hydroxyl motif which then tautomerises to allow the nucleophilic attack and C-alkylation of the glycal (Scheme 2.14). It was therefore envisioned that addition of external base would increase the rate of reaction as the activation of the nucleophile can occur, simultaneously, alongside the oxidative addition of palladium to the allyl system.



Scheme 2.14: Proposed mechanism of C-alkylation step during Pd-AA cascade

Two solvent systems were used in the first optimisation run, toluene and a 3:1 ratio of toluene and DMF. In all cases the more polar solvent system had worse performance, with little or no reaction occurring (Table 2.1, compare entries 1–5 with entries 6–10). The suspected stabilisation of the both the enolate ion and allyl cation by the polar solvent, increasing the overall activation energy required for the transformation, can explain the observed trend.

Addition of a sub-stoichiometric amount of triethylamine (TEA) increased the yield of the reaction to 52% from 35% (Table 2.1, entry 2) while the addition of the more sterically hindered di-isopropylethylamine (DiPEA) caused a decrease in yield to 22% (Table 2.1, entry 3). The addition of a stoichiometric amount of base had a negative effect on the cascade reaction, decreasing the yield (Table 2.1, entries 4–5 and 9–10).

Table 2.1: Probing the effects of external base, and initial solvent effects.

Entry	Catalyst	Base (eq)	Solvent	Yield
1	Pd(PPh ₃) ₄	-	Toluene	35%
2	Pd(PPh ₃) ₄	0.15 TEA	Toluene	52%
3	Pd(PPh ₃) ₄	0.15 DiPEA	Toluene	22%
4	Pd(PPh ₃) ₄	1 TEA	Toluene	11%
5	Pd(PPh ₃) ₄	1 DiPEA	Toluene	7.5%
6	Pd(PPh ₃) ₄	-	3:1 Toluene:DMF	15%
7	Pd(PPh ₃) ₄	0.15 TEA	3:1 Toluene:DMF	33%
8	Pd(PPh ₃) ₄	0.15 DiPEA	3:1 Toluene:DMF	6%
9	Pd(PPh ₃) ₄	1 TEA	3:1 Toluene:DMF	0%
10	Pd(PPh ₃) ₄	1 DiPEA	3:1 Toluene:DMF	0%

With the exception of some novel air-stable palladium catalysts, organopalladium chemistry typically requires rigorously inert conditions due to the tendency for palladium complexes to decompose upon reaction with oxygen or moisture.⁵³ Pd₂(dba)₃ is a useful source of Pd(0) as, in contrast to Pd(PPh₃)₄, it is insensitive to oxygen and so special care in handling and storage is unnecessary. When Pd₂(dba)₃ is in solution in the presence of phosphine ligands (L) dba dissociates and allows formation of the active species, Pd(dba)L₂, in the reaction mixture (Figure 2.2).^{54, 55} Alternatively palladium (II) pre-catalysts which exhibit increased stability in

atmospheric conditions, can also produce the active Pd⁽⁰⁾ species *in situ*,⁵³ therefore Pd(dppf)Cl₂ was chosen as an alternative pre-catalyst to Pd₂(dba)₃.

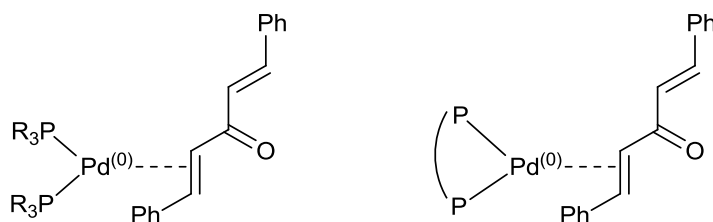


Figure 2.2: Active Palladium (0) species generated from Pd₂(dba)₃

Three mono-dentate phosphorus ligands were assessed for optimisation: bulky P(*o*-tol)₃ and P(*t*Bu)₃.BF₄ with large cone angles of 194° and 182°,⁵⁶ respectively, which promote the reductive elimination step during catalysis, and PPh₃ as a less bulky ligand with a smaller cone angle of 145°.⁵⁶ P(*t*Bu)₃, PPh₃, and P(*o*-tol)₃ are all σ donors of varying strength, with P(*t*Bu)₃ donating the most electron density and P(*o*-tol)₃ donating the least electron density.⁵⁷ Xantphos was chosen as a bi-dentate phosphorus ligand that has a relatively large bite angle of 108°⁵⁸ and has aryl groups also making it a strong σ-donor.⁵⁹

The combination of Pd₂(dba)₃ and PPh₃ (Table 2.2, entries 1,2) produced similar results to the original reaction conditions with Pd(PPh₃)₄ (Table 2.1, entries 1,2); this is not surprising as they both produce the same active species of Pd⁽⁰⁾(PPh₃)₂.⁵³ The catalyst system derived from Pd₂(dba)₃ and P(*o*-tol)₃.BF₄ was unreactive with only starting material recovered (Table 2.2 entries 3,4). P(*o*-tol)₃ has a Tolman-cone angle of 195°; this large steric bulk and the lesser ability of P(*o*-tol)₃ to σ donate when compared to the other mono-dentate phosphorus ligands is most likely responsible for the lack of reaction.⁶⁰ Both the ligands P(*t*Bu)₃ and Xantphos showed improved reactivity when compared to Pd(PPh₃)₄ (Table 2.2, entries 5-8) and catalytic TEA increased the yields in both cases.

Table 2.2: Optimisation with Pd₂(dba)₃ and selected ligands

Entry	Pre-catalyst	Ligand (eq relative to Pd mol amount)	Base (eq)	Solvent	Yield
1	Pd ₂ (dba) ₃	2 eq PPh ₃	-	Toluene	36 %
2	Pd ₂ (dba) ₃	2 eq PPh ₃	0.15 TEA	Toluene	53 %
3	Pd ₂ (dba) ₃	2 eq P(o-tol) ₃	-	Toluene	0 %
4	Pd ₂ (dba) ₃	2 eq P(o-tol) ₃	0.15 TEA	Toluene	0 %
5	Pd ₂ (dba) ₃	2 eq P(^t Bu) ₃ .BF ₄	-	Toluene	46 %
6	Pd ₂ (dba) ₃	2 eq P(^t Bu) ₃ .BF ₄	0.15 TEA	Toluene	67 %
7	Pd ₂ (dba) ₃	1 eq Xantphos	-	Toluene	50 %
8	Pd ₂ (dba) ₃	1 eq Xantphos	0.15 TEA	Toluene	87 %

Pd(dppf)Cl₂ also showed similar yields to the model reaction (Table 2.3, entries 1,2); however Pd(dppf)Cl₂ gave vastly improved yields when PPh₃ was introduced to reduce Pd(II) to Pd(0) *in situ* (Table 2.3, entries 3,4). Xantphos was less effective at reducing Pd(dppf)Cl₂ most likely due to its increased steric bulk. Pd(dppf)Cl₂ did provide one obstacle however: upon chromatographic purification of the completed reaction mixture, the dppf ligand co-eluted with the desired product, which therefore required further purification.

Table 2.3: Optimisation with Pd(dppf)Cl₂ and selected ligands

Entry	Pre-catalyst	Ligand (eq relative to Pd mol amount)	Base (eq)	Solvent	Yield
1	Pd(dppf)Cl ₂	-	-	Toluene	20 %
2	Pd(dppf)Cl ₂	-	0.15 TEA	Toluene	43 %
3	Pd(dppf)Cl ₂	2 eq PPh ₃	-	Toluene	56 %
4	Pd(dppf)Cl ₂	2 eq PPh ₃	0.15 TEA	Toluene	96 %
5	Pd(dppf)Cl ₂	1 eq Xantphos	-	Toluene	16 %
6	Pd(dppf)Cl ₂	1 eq Xantphos	0.15 TEA	Toluene	32 %

It was also noted that Pd(dppf)Cl₂ was only sparingly soluble in toluene, so to address this problem, both DCM and chloroform were trialed as solvent systems. Reactions with the more polar chloroform resulted in lower yields when compared to both DCM and toluene (Table 2.4, compare entries 3 and 4 with entries 1 and 2, and Table 2.3 entry 4, and Table 2.2 entry 8).

Table 2.4: Solvent effects of DCM and Chloroform on the Pd-AA cascade

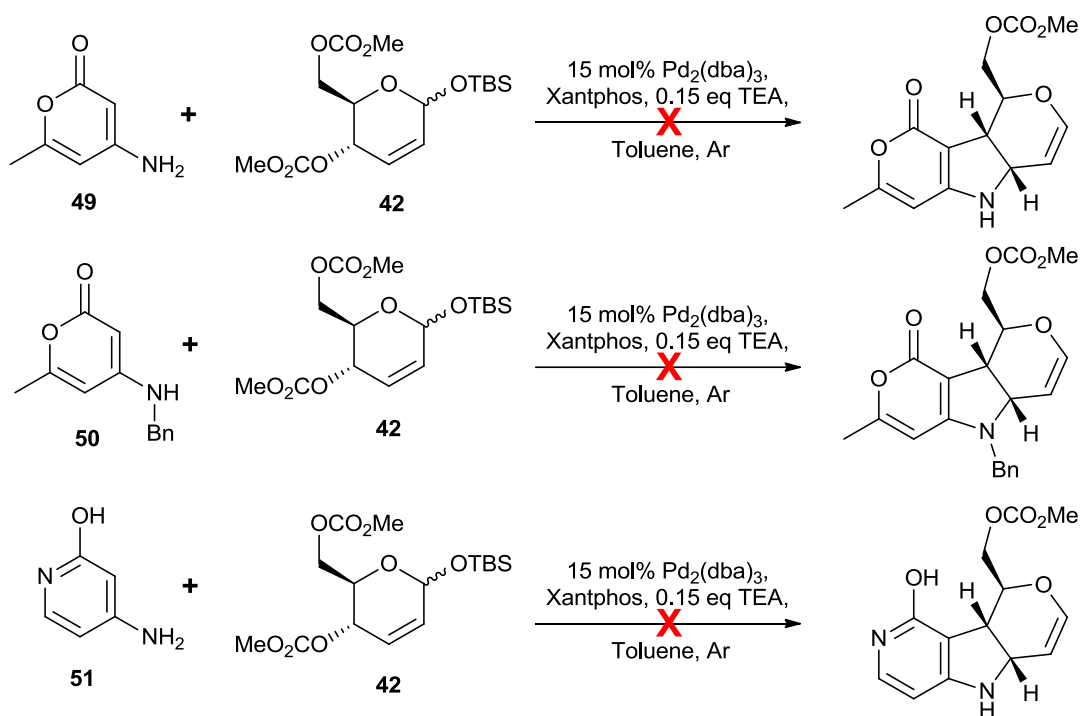
Entry	Pre-catalyst	Ligand (eq relative to Pd mol amount)	Base (eq)	Solvent	Yield
1	Pd ₂ (dba) ₃	1 eq Xantphos	0.15 TEA	DCM	90 %
2	Pd(dppf)Cl ₂	2 eq PPh ₃	0.15 TEA	DCM	76 %
3	Pd(dppf)Cl ₂	2 eq PPh ₃	0.15 TEA	Chloroform	40 %
4	Pd ₂ (dba) ₃	1 eq Xantphos	0.15 TEA	Chloroform	50 %

It was decided that the optimal conditions of the Pd-AA cascade for the reaction of glucosyl bis-electrophile **42** and 6-methyl-4-hydroxypyran-2-one (**31**) were 15 mol% Pd₂(dba)₃, Xantphos, 0.15 eq TEA, in toluene under an inert atmosphere of argon (Table 2.2, entry 8). Even though this wasn't the highest yielding result, the ease of purification and use of a non-halogenated solvent were thought to outweigh the slightly lower yield.

2.4. Pd-AA Cascade with prepared substrates

2.4.1. Pd-AA Cascade with amine bis-nucleophiles and glucosyl bis-electrophile

Initial attempts at the Pd-AA cascade using the newly optimised conditions (Table 2.2, entry 8) with the nitrogen containing bis-nucleophiles **49**, **50**, **51**, and the glucosyl bis-electrophile **42** all resulted in no reaction occurring, with only starting material recovered.



Scheme 2.15: Attempted Pd-AA cascades with new bis-nucleophiles

It was thought that the reduced reactivity could be due to the inductive effect of the nitrogen pulling electron density away from the nucleophilic carbon, either preventing or slowing down the *C*-alkylation that would normally occur. Alternatively, the relative differences between the keto-enol and amine-enamine tautomerism might affect the effectiveness of the nucleophilic carbon. Normally, the keto-enol tautomerism equilibrium is thermodynamically driven, and at room temperature, favours the keto form. However in the amine-enamine tautomerisation the amine form is more stable and therefore favoured. This could also cause the retardation of the *C*-alkylation step as the nitrogen could act as a better nucleophile leading to *N*-alkylation instead. (Figure 2.3)

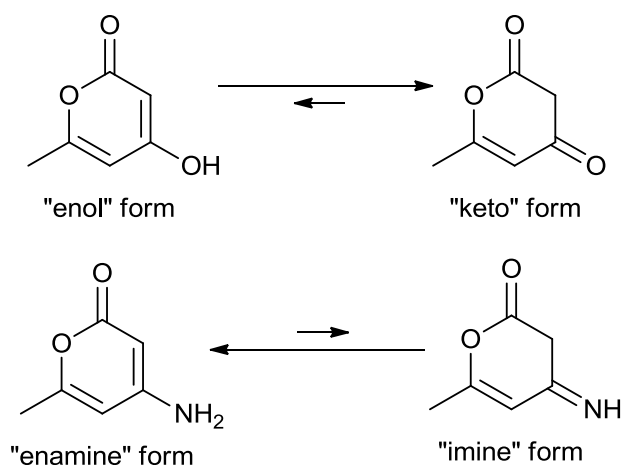
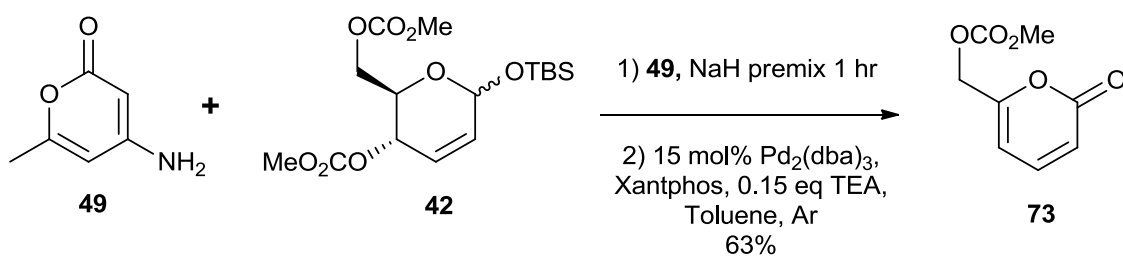


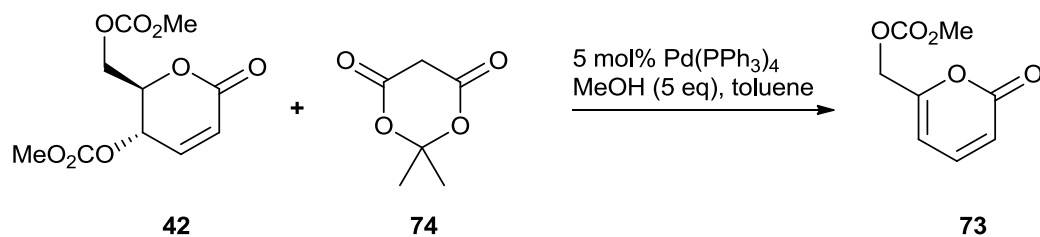
Figure 2.3: Keto-enol and imine-enamine tauomerisation

To probe this hypothesis a strong base was added to bis-nucleophile **49** to try and force the enamine form. NaH was premixed with **49** in toluene before adding the resulting solution to a mixture of **42**, Pd₂(dba)₃ and Xantphos in toluene.



Scheme 2.16: Unexpected elimination of bis-electrophile **42** under Pd-AA cascade conditions with **49**

TLC analysis of this reaction showed complete consumption of **42** and the formation of a new spot with an R_f similar to that of **47**. NMR spectroscopy (Table 2.5), however, showed clearly that **49** had not reacted with **42**. Instead **42** had undergone a transformation in a high yield to one product that, upon isolation, was found to be 2*H*-pyran-2-one **73**. This was previously prepared by Turner, having isolated it when reacting the 2,3-unsaturated lactone **42** and Meldrum's acid (**74**) under the Pd-AA cascade conditions (Scheme).⁴³



Scheme 2.17: Turner's reaction of bis-electrophile **42** and Meldrum's acid

The environments E,F, and G indicate that there was an aromatic impurity (Table 2.5, entries E,F,G) as these peaks sit in the aromatic region in both the ^{13}C NMR and 1H NMR and show no short- or long-range coupling to the rest of the environments present.

Table 2.5: NMR analysis of compound **73**

Comments	Entry	^{13}C NMR	Mult.	1H NMR	Mult.	INT	COSY	HMBC H-C
	A	161.5						
	B	158.6						
	C	155.5						
	D	143.2	CH	7.74	d (15.3)	.68		$C_F, C_G, C_B,$ C_A
				7.33	dd (11,7.8)	1.02	H_J, H_K	
Aromatic impurity	E	130.9		7.40	d (4.4)	0.59		
	F	128.8		7.42	d (4.7)			
	G	125.8		7.63	dd (6.4,3.8)	0.32		C_e
	H	116.3	CH	6.28	d(9.2)	"1.52"	H_E	$C_H, C_I, C_J,$ C_B, C_A
	I	103.3	CH	6.28	d (6.6)	"1.52"		$C_H, C_I, C_J,$ C_B, C_A
	J	65.0	CH ₂	4.94	s	2.01		$C_H, C_I, C_C,$ C_B
	K	55.8	CH ₃	3.8	s	3		C_C

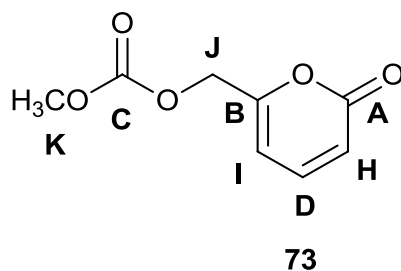
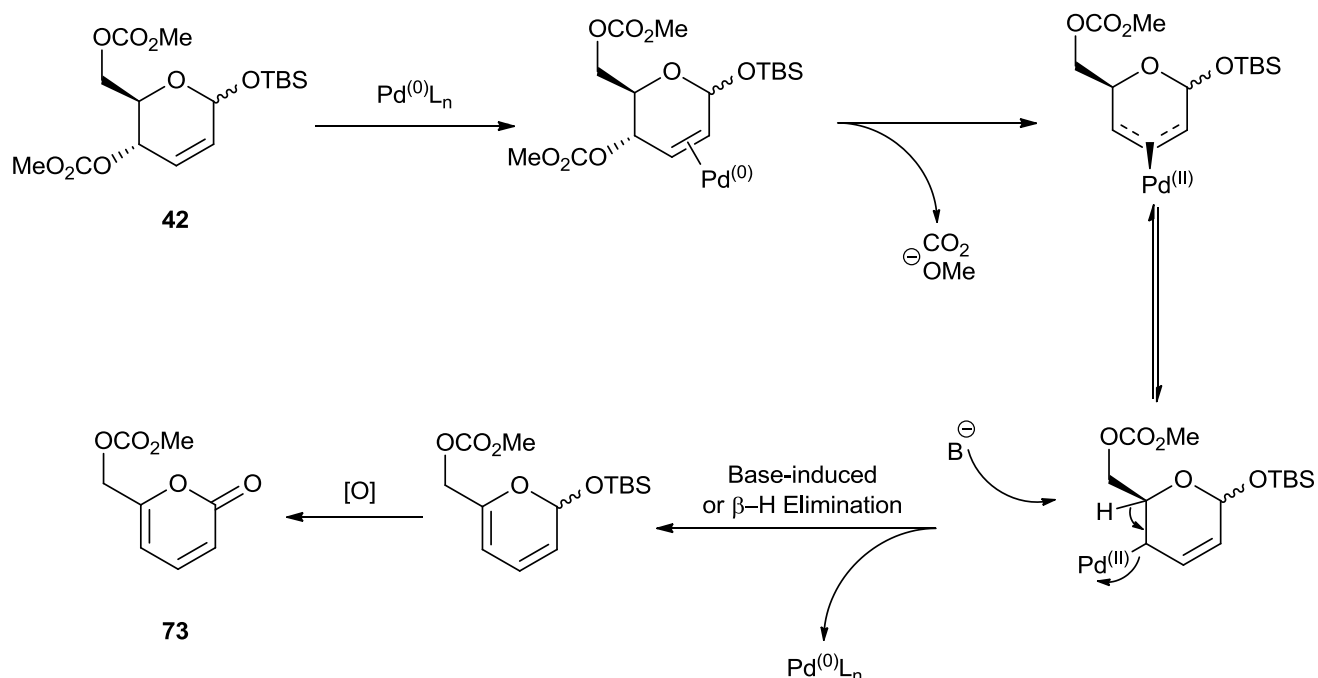


Figure 2.4: Spectroscopic analysis of compound **73**

An intense colour change from purple to red/orange of the reaction mixture that formed **73** was observed. This could indicate that the formation of this compound is a palladium-assisted process. A plausible mechanism could involve the same initial π -allyl formation anticipated for the desired reaction. Instead of *C-4* alkylation by **46**, either β -hydride elimination or base induced elimination of H-5 followed by dissociation of Pd, with the latter being more likely due to the presence of a strong amine base in the form of deprotonated **X**, and subsequent oxidation of C-1 would form the observed pyranone (**73**).

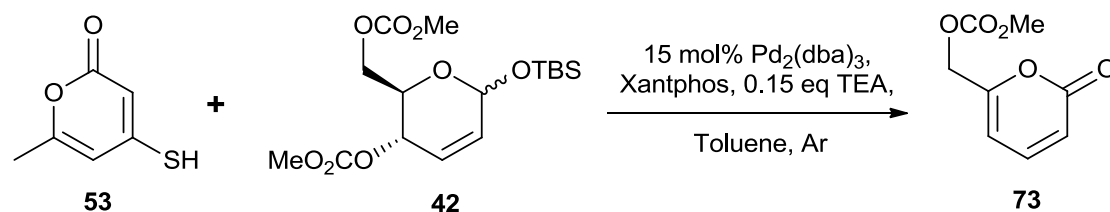


The facile and high yielding synthesis of pyranone **73** could be promoted by the conjugation inherent to the *2H*-pyran-2-one structure. Nature provides further evidence for the favoured

formation of these compounds, as this type of ring system has been found in a plethora of compounds isolated from plants, animals, marine organisms, bacteria, insects and fungi. Some 2*H*-pyran-2-one derivatives have been found to display a wide range of cytotoxic, neurotoxic and phytotoxic properties whilst others have been used as synthetic precursors to pharmacologically active compounds such as HIV protease inhibitors, antifungals, anticonvulsants, antimicrobials, pheromones, natural pigments, antitumour agents, and plant growth regulators.^{61, 62} It should be noted that although this research does provide a new synthetic route to this important class of compounds, the pathway does not hold many advantages over the traditional strategies for the synthesis of 2*H*-pyran-2-ones, and will find limited use due to its atom and step inefficiency.

2.4.2. Pd-AA cascade with thiol bis-nucleophile and glucosyl bis-electrophile

The Pd-AA cascade was also attempted with the sulfur bis-nucleophile **53** (Scheme 2.18).

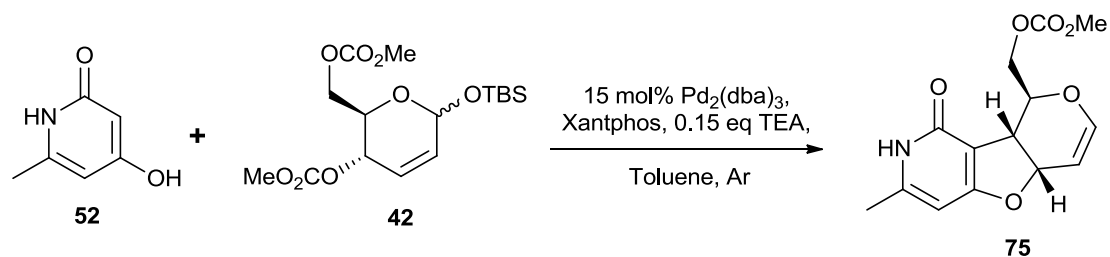


Scheme 2.19: Unexpected elimination reaction of lactone **42** under Pd-AA cascade conditions with **53**

TLC analysis of the reaction of the sulfur bis-nucleophile **53** with bis-electrophile **42** showed the complete consumption of **42** and another product spot with a similar R_f to **47**. Much like the reaction of the deprotonated nitrogen bis-nucleophile (**49**) NMR analysis showed clearly that the reaction had undergone the same transformation as previously mentioned. Yielding that upon isolation is thought to be a mixture of 2*H*-pyran-2-one (**73**) and the sulfur dimer **72**. The formation of the by-product **73** is thought to occur *via* the same process described above (Scheme 2.17).

2.4.3. Pd-AA cascade with pyridine-2-one bis-nucleophile and glucosyl bis-electrophile

The Pd-AA cascade was also attempted with the pyridin-2-one bis-nucleophile **52** and bis-electrophile **42** (Scheme 2.19).



Scheme 2.20: Reaction of bis-nucleophile **52** by Pd-AA cascade to potentially afford **75**

Analysis of the ¹H NMR spectrum of the crude reaction mixture indicated the reaction had proceeded with good conversion in that a distinctive doublet was observed at 6.71 ppm corresponding to the enol ether proton at C-1 of the desired product (**75**), and similar to a previously reported compound (**44**) as well as several other peaks highlighted in figure 2.6. However, even after multiple purification attempts the product was contaminated and it appeared this might be due to rapid degradation, resulting in no usable NMR data and the inability to fully characterise the compound. The suggestion that the desired product was produced in the reaction is further supported by the MS of the isolated fraction: while there are many degradation product peaks, the parent ion peak has a *m/z* of 294.094 which matches (M+H)⁺ of 294.09 the desired product (Figure 2.5). However, the inability to purify the product renders this result highly tentative.

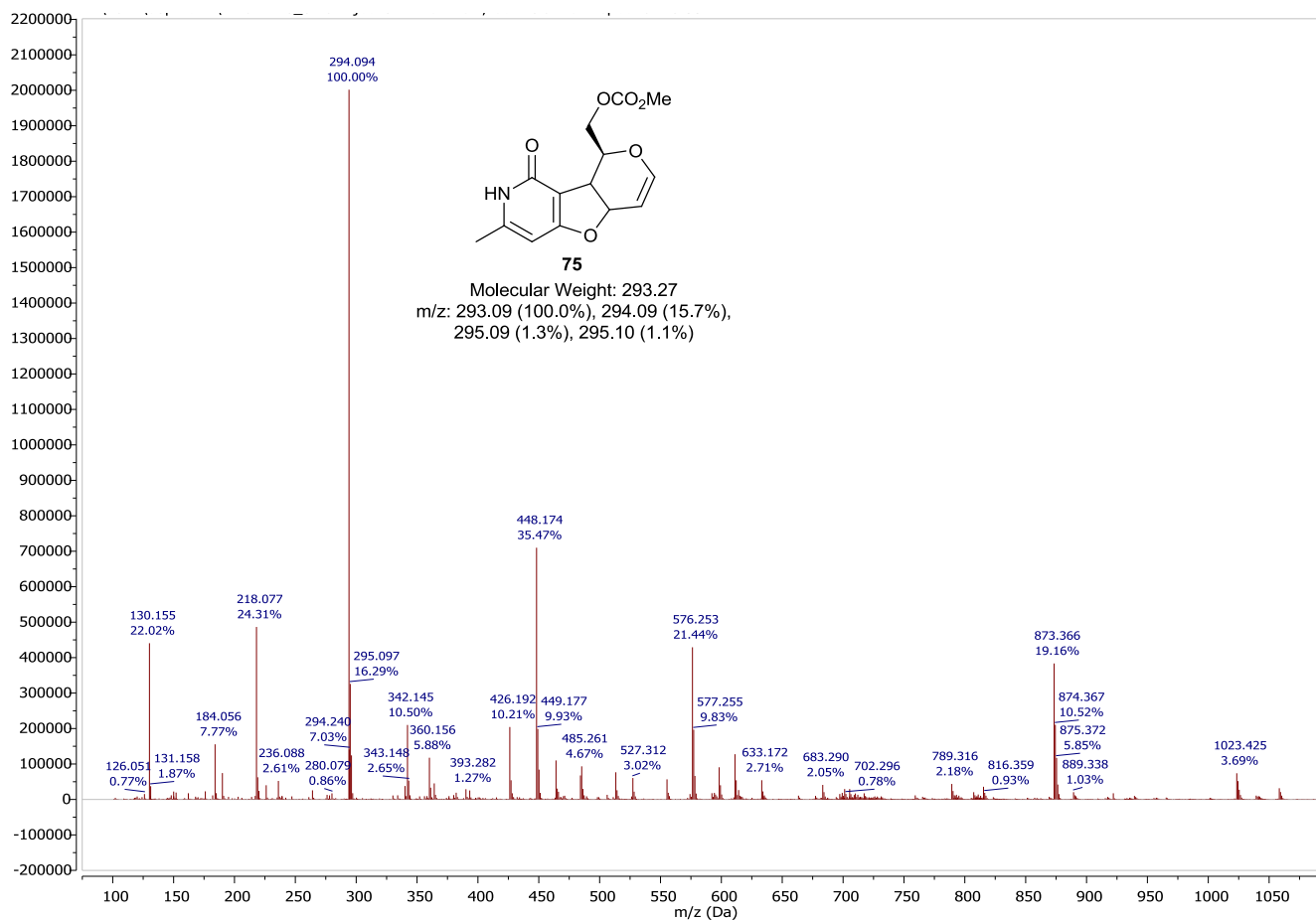


Figure 2.5: MS spectra of Pd-AA cascade product **75**

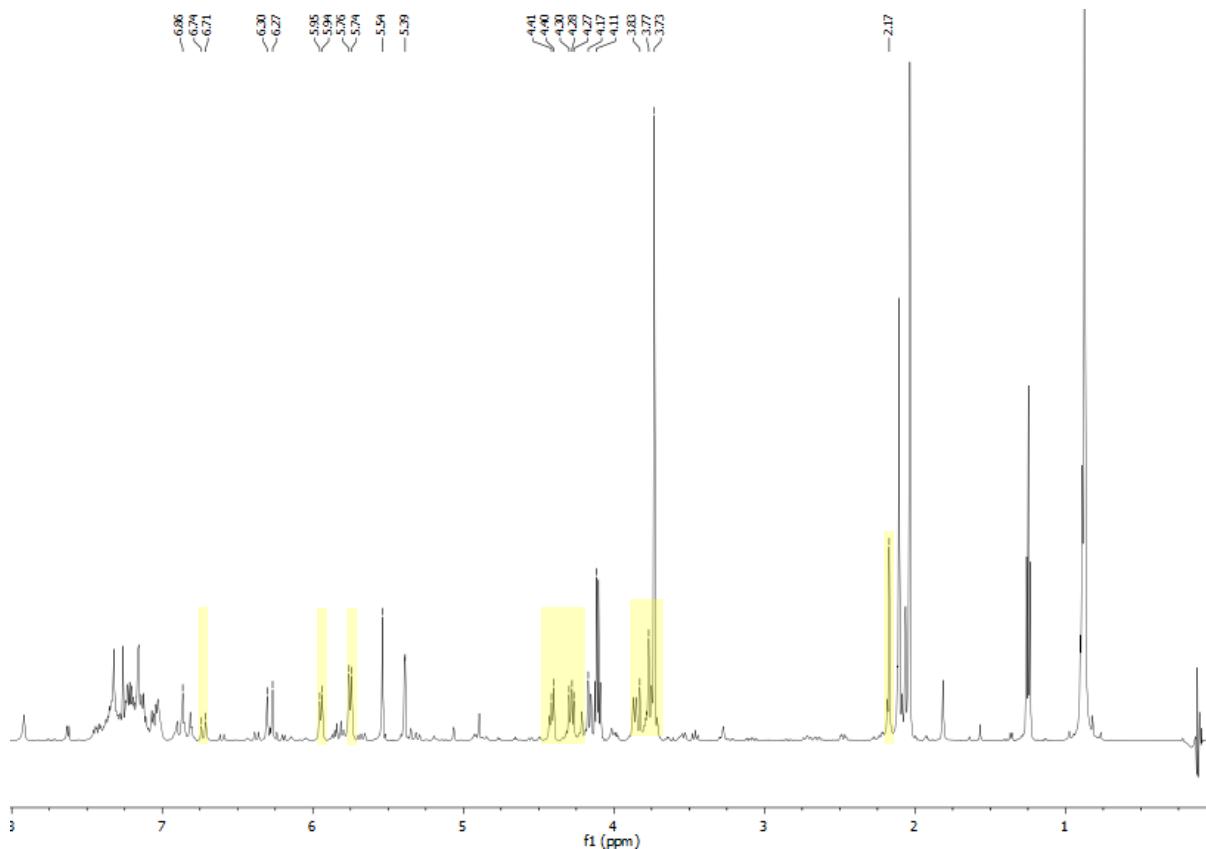
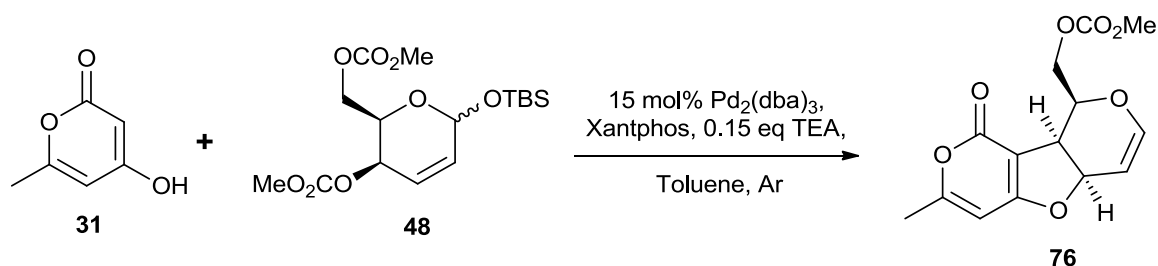


Figure 2.6: ^1H NMR spectrum of **75**

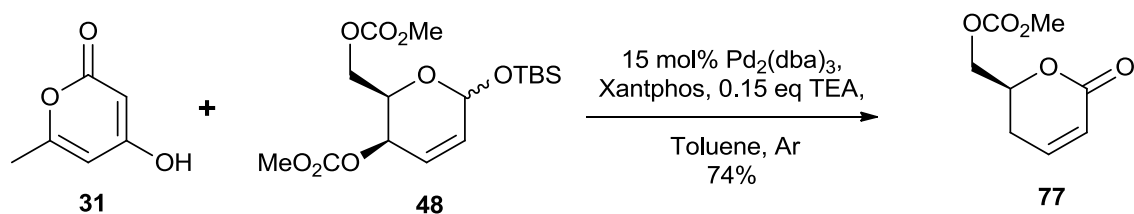
2.4.4. Pd-AA cascade with galactosyl bis-electrophile **48**

To conclude the scope studies of the Pd-AA cascade the galactosyl bis-electrophile **48** was trialled with 4-hydroxy-6-methylpyran-2-one (**31**). Initial reactions under the previously developed optimal conditions resulted in no reaction occurring and recovery of the starting materials (Scheme 2.20).



Scheme 2.21: Proposed reaction of galactosyl bis-electrophile **48** in Pd-AA cascade

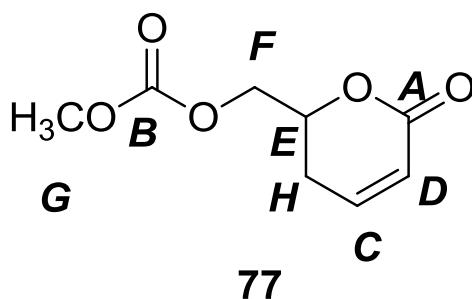
It was hypothesised that a higher loading of catalyst might be needed to overcome the steric constraints of formation of the endo-substituted furofuran ring **76**. TLC analysis of the reaction of **48** and **31** with a 30 mol% catalyst loading showed the complete consumption of **48**. Upon NMR analysis of the purified product it was discovered that instead of the desired reaction, **48** had undergone a transformation in a high yield to one product that upon purification, was found to be 5,6-dihydro-2*H*-pyran-2-one **77** (Scheme 2.21). Lactone **77** had a very similar ¹H NMR profile to the fully unsaturated pyranone **73** however the coupling pattern of signals F, E, and H had changed significantly. The HSQC showed coupling between E (C-5) 74.9 ppm and a proton at 4.71 ppm, showing C-5 was no longer unsaturated. The change in F and H also supported this hypothesis with the multiplicity changing from a singlet to a doublet in both cases, as well as the multiplicity of C changing to a ddd from a dd, indicating 3 proton environments nearby (Table 2.6).



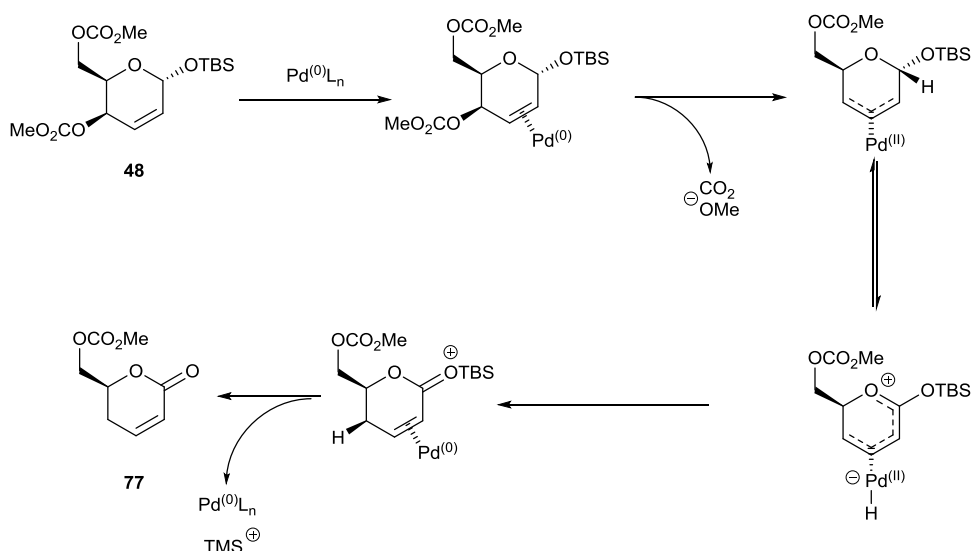
Scheme 2.22: Unexpected elimination reaction of lactone **48** under Pd-AA cascade conditions

Table 2.6: NMR analysis of compound **77**

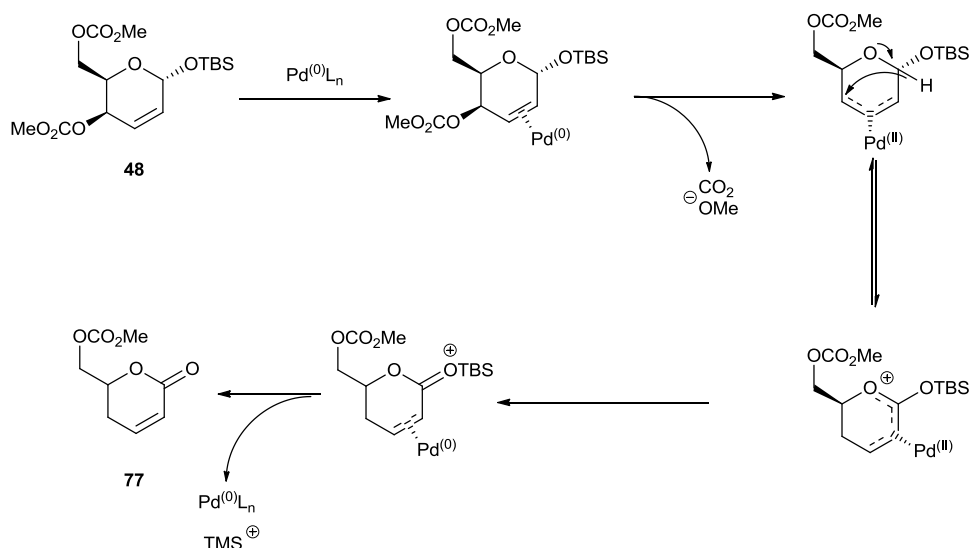
Entry	¹³ C NMR	Mult	¹ H NMR	Mult	INT	COSY	HMBC
A	163.1	C					
B	155.5	C					
C	144.3	CH	6.91	ddd (9.9, 5.9, 2.6)	1.46	H _D , H _H	C _H , C _E , C _A
D	121.5	CH	6.06	ddd (9.8, 2.7, 1.1)	1.23	H _C , H _H	C _H , C _A
E	74.9	CH	4.71	App dq (or ddt)	0.85	H _H H _F	C _C , C _F , C _H
F	67.9	CH ₂	4.36	d (4.77)	3.24	H _E	C _B , C _E , C _H
G	55.3	CH ₃	3.81	s	4.41		C _B
H	25.7	CH ₂	2.53, 2.43	dd		H _C , H _D (weak), H _E	C _D , C _C

**Figure 2.7:** Spectroscopic analysis of compound **77**

An intense colour change from purple to red/orange of the reaction mixture was observed. This could indicate that the formation of this compound is a palladium-assisted process. A plausible mechanism could involve the initial π -allyl formation anticipated for the desired reaction, followed by 1,4-H transfer, that is either Pd mediated or non-Pd mediated (Scheme 2.23). However due to the presence of only the alpha anomer of substrate **48**, and hence Pd occupying the lower face due to displacement of the β -face carbonate at C-4 it is likely that H transfer will occur across the top face in a non-Pd mediated mechanism (Scheme 2.24).



Scheme 2.23: Proposed Pd-mediated mechanism for formation of **77** during Pd-AA cascade



Scheme 2.24: Proposed non-Pd-mediated mechanism for formation of lactone **77**

The proposed mechanism for the formation of **77** is likely somewhat similar to that occurring with the formation of the fully unsaturated pyrone **73**. The different outcomes of these similar mechanistic processes may be due to the presence or lack of a strong base, or because of the stereochemical differences resulting in the Pd being on the same face as the proton at C-1 in the case of bis-electrophile **42** or the opposite face as the proton at C-1 as in the case of bis electrophile **48**. With the above evidence the latter seems more likely.

3. Future Work and Conclusion

3.1. Concluding Remarks

The objectives of this project, *i.e.* to explore both the scope and utility of the Pd-AA cascade, were partially achieved. A series of nitrogen- and sulfur-containing bis-nucleophiles were tested and found to provide poor results in the cascade under the conditions optimised for the *O*-bis-nucleophile. However, further exploration could yield more positive results. The formation of lactone by-products may provide insight into the mechanistic properties of this Pd-AA cascade. Furthermore, bis-nucleophile **52** appeared to successfully react, based on MS and crude NMR analysis, potentially giving the furopyran **77**, but the product was not able to be purified, due to rapid degradation during silica chromatography and so this assignment is tentative.

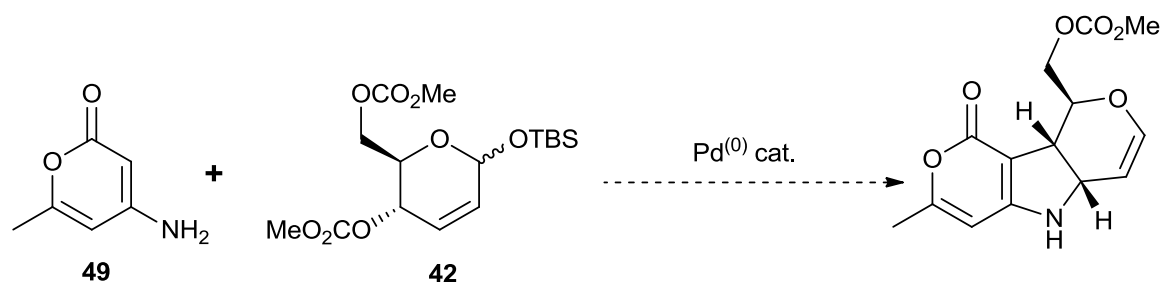
The galactal bis-electrophile **48** was found not to undergo the Pd-AA cascade under the conditions optimised for the glugal bis-electrophile. This was considered to be due to steric interactions with the initial Pd- π -allyl system forming on the bottom face allowing 1,4-hydrogen transfer across the same face, giving more insight into the reaction mechanism.

This project has explored the extension of an efficient Pd-catalysed reaction that forms furopyran products, and has set the platform for future research in a number of areas. Most importantly, this project has investigated the exciting area of chemistry that has opened up upon the development of the Pd-AA cascade. The Pd-AA cascade holds the potential for providing efficient and elegant syntheses of numerous synthetic targets and further research may enable future applications.

Throughout this thesis, there have been indications of further work that could be explored. These aspects are outlined below alongside research that was not able to be carried out due to the time constraints of the project.

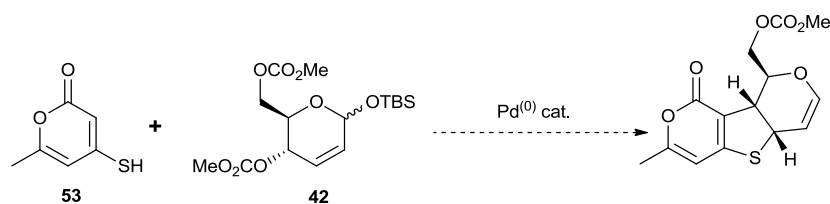
3.2. Future Work on Pd-AA Cascades

The amine containing bis-nucleophiles may be too basic for use in the Pd-AA cascade, favouring base mediated elimination and forming the fully unsaturated pyran-2-one **73**. It would be useful to perform preliminary testing to see if further condition optimisation may render these nucleophiles viable as reactants in the Pd-AA cascade.

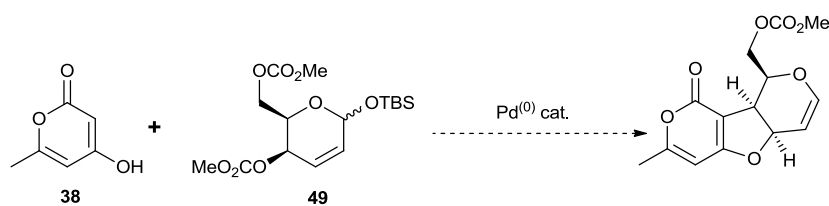


Scheme 3.1: Future Pd-AA optimisation of amine containing bis-nucleophiles

Other avenues for future work inspired by the scope studies of the Pd-AA cascades could be in developing conditions that allow for the thiol bis-nucleophile **53** to successfully undergo a Pd-AA cascade with the bis-electrophile **42**, and for the galactal-derived bis-electrophile **49** with 4-hydroxyl-6-methylpyran-2-one. Therefore, investigating the reactivity of the bis-nucleophile **53** and bis-electrophile **49** (separately) under a variety of Pd-AA cascade conditions might extend the scope of the Pd-AA cascade. If unsuccessful, it would be prudent to abandon the use of these substrates in the Pd-AA cascades.

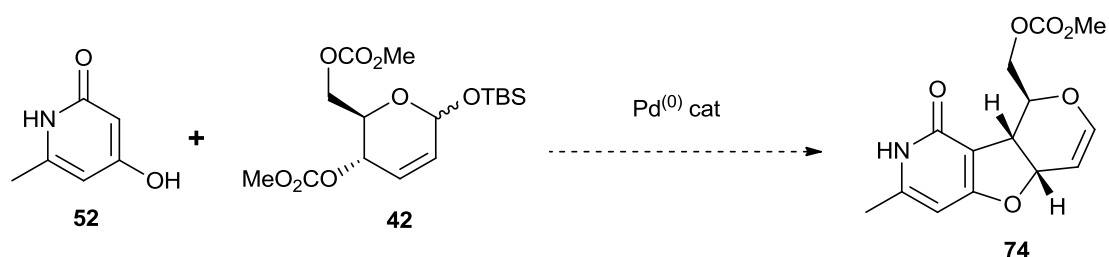


Scheme 3.2: Future Pd-AA optimisation of thiol bis-nucleophiles



Scheme 3.3: Future Pd-AA optimisation of galactosyl bis-electrophile

While it appears likely that the reaction of 4-hydroxy-6-methyl-pyridin-2-one **52** and the 2,3-unsaturated glucosyl bis-electrophile in the Pd-AA cascade successfully occurred, more work on this reaction is needed. In particular, the chromatographic procedure needs to be improved, and future work could involve the use of an alternative solid-phase for chromatography of the cascade products. This would require determination of the current reasons for the degradation occurring during silica gel chromatography. If successful, it would also result in pure product allowing for acquisition of clean spectra as required for full characterisation, and for bioactivity testing.



Scheme 3.4: Optimisation of Pd-AA cascade and purification of **74**

As mentioned in section 1.5 (Table 1.1, compounds **44** and **47**), the presence of a sidechain containing a carbonate substituent was demonstrated to increase the activity of the compounds tested compared to those without the sidechain. It would therefore be expedient to explore the bioactivity of products with different protecting groups on the C-6 hydroxyl group, as well as the free hydroxyl motif.

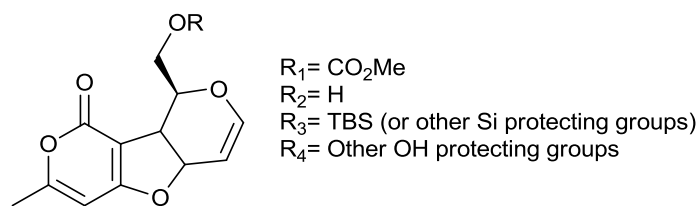


Figure 3.1: Different protecting groups for future biological activity testing

On a different note, testing the bioactivity of the fully unsaturated pyran-2-one **73** and the 2,3-unsaturated pyran-2-one **77** formed by the Pd-AA cascade of both the amine bis-nucleophile **49** and the thiol bis-nucleophile **53** with the glucosyl bis-electrophile **42** and the galactosyl bis-electrophile with 4-hydroxyl-6-methylpyran-2-one, respectively, could be a sensible pursuit. Section 2.4.1 described a number of similar mono-substituted pyranones, which have been found to show bioactivity in a variety of assays.⁵⁸ Therefore, pyran-2-one **73** and **77** have potential to show good bioactivity.

4. Experimental

4.1. General Experimental

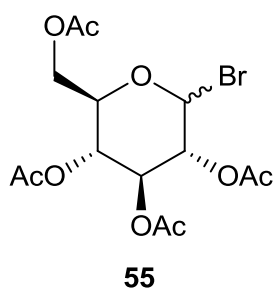
Unless otherwise stated, the following conditions apply. All reactions were performed in oven-dried glassware with magnetic stirring under an atmosphere of argon or nitrogen. Moisture- and oxygen-sensitive liquids and solutions were transferred using a stainless steel cannula. Before use, solvents were refluxed over the appropriate drying agent and distilled under nitrogen: tetrahydrofuran (THF) from sodium benzophenone ketyl radical; dichloromethane (DCM) and trimethylamine (TEA) from calcium hydride or using the Pure Solv™ system to purify solvents. Anhydrous *N,N*-dimethylformamide (DMF) and acetic anhydride were used as purchased without further purification. All other reagents were of commercial quality, purchased from Sigma-Aldrich or AK Scientific, and used as received, without further purification.

Analytical thin layer chromatography (TLC) was performed using plastic-backed pre-coated silica TLC plates (Polygram SilG/UV254). Visualisation was achieved by UV irradiation (254 nm), Iodine staining, or by heating after treatment with a *p*-anisaldehyde dip (0.7 mL *p*-anisaldehyde, 9.54 mL conc. H₂SO₄, 2.7 mL acetic acid, and 250 mL of EtOH). The purification of products by flash column chromatography was conducted using silica gel 60 (220-240 mesh) with the solvent system indicated. ¹H NMR spectra were recorded by a Varian Unity Inova 500 spectrometer at 500 MHz, a Varian DirectDrive 600 spectrometer at 600 MHz or a Varian Inova 300 at 300 MHz. Data are listed as follows: chemical shift in ppm using, as internal standard, chloroform (7.26 ppm) or water (4.79 ppm) or dimethylsulfoxide (DMSO) (2.50 ppm), multiplicity [s = singlet, d = doublet, t = triplet, q = quartet, quint = quintet, m = multiplet or overlap of non-equivalent resonances, br = broad, apt. = apparent, obs. = (partially) obscured], integration, peak assignment. ¹³C NMR spectra were recorded on a Varian Unity Inova 500 spectrometer at 125 MHz or a Varian DirectDrive 600 spectrometer at 150 MHz and the data listed as follows: Chemical shift in ppm using chloroform as internal standard (77.0 ppm) or..., multiplicity, peak assignment.

The assignments of signals are exclusively based on atom connectivity and spatial relationships are derived from 2D NMR correlations (NOESY, $^1\text{H}/^1\text{H}$ -COSY, $^1\text{H}/^{13}\text{C}$ -HMBC, and $^1\text{H}/^{13}\text{C}$ -HSQC). IR bands were measured as a thin film on a (insert make here). High-resolution mass spectrometry (HRMS) was performed on an Agilent 6530 Accurate-Mass Q-TOF LC/MS mass spectrometer with Agilent Jet Stream ESI source. Melting points were measured on a (insert here) with samples in a melting tube and are uncorrected. Optical rotations were measured on an (insert here). The structure of each compound is presented with the corresponding method of preparation and spectroscopic data.

4.2. Experimental Methods and Characterisation

Tetra-*O*-acetyl- α -D-glucopyranosyl bromide (**55**)

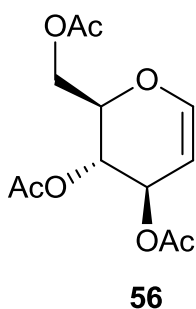


Using a modification of Kozikowski's procedure,⁶³ a magnetically stirred solution of D-glucose (132 mg, 0.7 mmol) in acetic anhydride (76 mL, 804 mmol) was treated dropwise with 70 % (w/w) Perchloric acid (0.45 mL, 6.9 mmol). Additional d-glucose (19.71 g, 109 mmol) was added slowly over one hour, at a rate that maintained a temperature of 40 – 50 °C. Upon complete addition of D-glucose, the solution was allowed to cool to room temperature, and then was treated with a 33% (w/w) solution of hydrobromic acid in acetic acid (78 mL, 430 mmol). After 90 minutes, the solution was diluted with dichloromethane (180 mL) and washed with ice cold water (2 × 50 mL), then cold sat. sodium bicarbonate solution (6 × 50 mL). The organic phase was dried with anhydrous magnesium sulfate, filtered and concentrated to afford crude tetra-*O*-acetyl- α -D-glucopyranosyl bromide as a white solid (45.23 g, 108 mmol, 98%) that was used without further purification. Spectral data matched those which have been previously reported.⁶⁴

^1H -NMR: (500 MHz, CDCl_3) δ_{H} 6.47 (d, $J = 6.0$ Hz, 1H, H-1), 5.35 (t, $J=6.6$ Hz, 1H, H-3), 5.14 (t, $J = 6.6$ Hz, 1H, H-4), 4.85 (dd, $J = 5.0, 3.5$ Hz, 1H, H-2), 4.41 (dd, $J = 12.3, 5.6$ Hz,

1H, H-6a), 4.31 (dd, J = 15.8, 3.2 Hz, 2H, H-5), 4.23 (dd, J = 22.6, 9.9 Hz, 1H, H-6b), 2.100 (s, 3H, CH₃CO), 2.096 (s, 3H, CH₃CO), 2.05 (s, 3H, CH₃CO), 2.03 (s, 3H, CH₃CO), ¹³C-NMR: (126 MHz, CDCl₃) δ_c 170.6 (C, CH₃C=O), 169.6 (C, CH₃C=O), 169.4 (C, CH₃C=O), 168.7 (C, CH₃C=O), 91.7 (CH, C-1), 89.0 (CH, C-5), 69.80 (CH, C-2), 69.16 (CH, C-3), 67.8 (CH, C-4), 61.4 (CH₂, C-6), 20.8 (CH₃, CH₃CO), 20.7 (CH₃, CH₃CO), 20.6 (CH₃, CH₃CO), 20.5 (CH₃, CH₃CO).

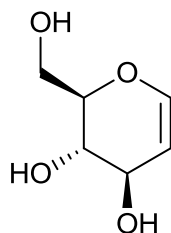
Tri-*O*-acetyl-D-glucal (**56**)



A magnetically stirred dispersion of zinc dust (47.92 g, 733.1 mmol) in water (150 mL) was cooled to 0 °C, diluted with acetic acid (150 mL), then treated dropwise with a solution of glucopyranosyl bromide **55** in diethyl ether (150 mL) over one hour. The reaction was allowed to warm to room temperature and left to proceed overnight. The solution was filtered, and then diluted with dichloromethane (200 mL). The solution was washed successively with water (3 × 60 mL), sat. sodium bicarbonate (4 × 50 mL), then brine (60 mL). The organic phase was dried with anhydrous magnesium sulfate, filtered and concentrated to provide **56** as a white solid (27.7 g, 101.9 mmol, 96%). Spectral data matched those which have been previously reported.⁶⁵

¹H-NMR: (500 MHz, CDCl₃) δ_H 6.46 (d, J = 6.1 Hz, 1H, H-1), 5.33 (m, 1H, H-3), 5.22 (dd, J = 7.6, 5.7 Hz, 1H, H-4), 4.84 (dd, J = 6.1, 3.2 Hz, 1H, H-2), 4.39 (dd, J = 12.1, 5.8 Hz, 1H, H-6a), 4.25 (m, 1H, H-5), 4.19 (dd, J = 12.1, 3.0 Hz, 1H, H-6b), 2.09 (s, 3H, CH₃CO), 2.07 (s, 3H, CH₃CO), 2.04 (s, 3H, CH₃CO); ¹³C-NMR: (126 MHz, CDCl₃) δ_c 170.6 (C, CH₃C=O), 170.4 (C, CH₃C=O), 169.6 (C, CH₃C=O), 145.6 (CH, C-1), 99.0 (CH, C-2), 73.9 (CH, C-5), 67.3 (CH, C-3), 67.2 (CH, C-4), 61.4 (CH, C-6), 21.0 (CH₃, CH₃CO), 20.8 (CH₃, CH₃CO), 20.7 (CH₃, CH₃CO)

D-Glucal (**57**)



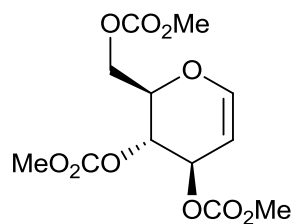
57

Sodium (231 mg, 10 mmol) was added to methanol (180 mL) and allowed to react. This was followed by addition of the protected glucal **56** (8.07 g, 30 mmol). The reaction was stirred at room temperature for 15 minutes and then the solution was concentrated to provide crude D-glucal **57**. The crude product was treated with methanol (6 mL), then successively diluted with acetone (30 mL) and diethyl ether (60 mL), which lead to the precipitation of impurities. The solution was filtered and concentrated to afford **57** (3.95 g, 27 mmol, 90%) as a very viscous orange oil. Spectral data matched those which have been previously reported.⁴³

¹H-NMR: (500 MHz; D₂O) δ_{H} 6.36 (dd, $J = 6.0, 1.5$ Hz, 1H, H-1), 4.74 (dd, $J = 6.0, 2.0$ Hz, 1H, H-2), 4.17 (dt, $J = 7.0, 2.0$ Hz, 1H, H-3), 3.82 (complex m, 3H, H-5, 6-a, 6-b), 3.62 (dd, $J = 9.0, 7.0$ Hz, 1H, H-4); **¹³C-NMR:** (125 MHz; D₂O) δ_{C} 143.7 (CH, C-1), 102.8 (CH, C-2), 78.1 (CH, C-5), 68.7 (CH, C-4), 68.3 (CH, C-3), 60.0 (CH₂, C-6).

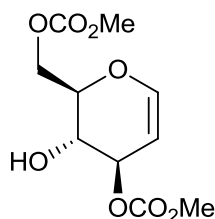
3,4,6-Tri-*O*-methoxycarbonyl-D-glucal (62**), and 3,6-di-*O*-methoxycarbonyl-D-glucal (**63**), and 4,6-di-*O*-methoxycarbonyl-D-glucal (**64**)**

To a solution of D-glucal (6.03 g, 41.3 mmol) in THF (300 mL) at 0 °C was added DMAP (15.92g, 124 mmol), followed by methyl chloroformate (9.6 mL, 124 mmol). The reaction was allowed to warm to room temperature and left to proceed overnight. The solution was filtered through CeliteTM, washed with DMC (50 mL), and concentrated to give the crude products **62:63:64** as an off white solid in a 20:1:1 ratio. Chromatography of the solid (30% EtOAc / pet. ether) afforded **62** (7.2 g, 22.3 mmol, 54%) as a white solid, **63** (2 g, 6.2 mmol, 15%) as a colourless oil and **64** (1.2 g, 3.7 mmol, 9%) as a colourless oil in a combined yield of 78%. Spectral data matched those which have been previously reported.⁴³



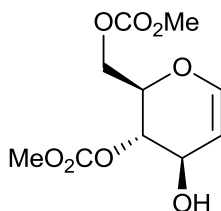
62

R_f : 0.45 (30% EtoAc/ pet. Ether); **¹H-NMR**: (500 MHz; CDCl₃) δ_H 6.49 (d, *J* = 6.0 Hz, 1H, H-1), 5.22 (t, *J* = 4.0 Hz, 1H, H-3), 5.09 (t, *J* = 6.5 Hz, 1H, H-4), 4.94 (dd, *J* = 6.0, 3.5 Hz, 1H, H-2), 4.47 (dd, *J* = 12.0, 6.0 Hz, 1H, H-6a), 4.36 (complex m, 1H, H-5), 4.32 (dd, *J* = 12.0, 4.0 Hz, 1H, H-6b), 3.82 (s, 3H, CH₃OCO), 3.80 (s, 3H, CH₃OCO), 3.79 (s, 3H, CH₃OCO); **¹³C-NMR**: (125 MHz; CDCl₃) δ_C 155.5 (C, CH₃OCO), 154.5 (C, CH₃OCO), 154.6 (C, CH₃OCO), 146.1 (CH, C-1), 98.1 (CH, C-2), 73.5 (CH, C-5), 70.8 (CH, C-4), 70.3 (CH, C-3), 64.8 (CH₂, C-6), 55.6 (CH₃, CH₃OCO), 55.3 (CH₃, CH₃OCO), 55.2 (CH₃, CH₃OCO)



63

R_f : 0.28 (30% EtoAc/ pet. Ether); **¹H-NMR**: (500 MHz; CDCl₃) δ_H 6.30 (d, *J* = 6.5 Hz, 1H, H-1), 5.06 (d, *J* = 6.5 Hz, 1H, H-3), 4.69 (dd, *J* = 6.0, 2.5 Hz, 1H, H-2), 4.37 (dd, *J* = 12.0, 4.0 Hz, 1H, H-6a), 3.99 (mult, 2H, H-6), 3.86 (mult, 2H, H-5, 4), 3.68 (s, 6H, CH₃OCO); **¹³C-NMR**: (125 MHz; CDCl₃) δ_C 171.4 (C, CH₃OCO), 155.8 (C, CH₃OCO), 146.0 (CH, C-1), 98.8 (CH, C-2), 75.7 (CH, C-5), 66.2 (CH, C-3), 65.7 (CH, C-4), 60.3 (CH₂, C-6), 55.0 (CH₃, CH₃OCO), 54.9 (CH₃, CH₃OCO)

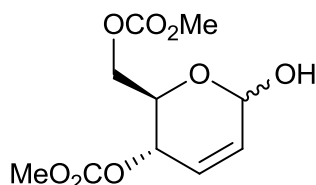


64

R_f : 0.14 (30% EtoAc/ pet. Ether); **¹H-NMR**: (500 MHz, CDCl₃) δ_H 6.40 (d, *J* = 5.5 Hz, 1H, H-1), 4.51 (obs. m, 2H, H-2,4), 4.44-4.39 (m, 3H, H-3,6a,6b), 4.19 (ddd, *J* = 8.5, 5.5, 3.0 Hz, 1H, H-5), 3.84 (s, 3H, CH₃OCO), 3.80 (s, 3H, CH₃OCO), 2.44 (d, *J* = 5.5 Hz, 1H, OH); **¹³C-NMR**: (125 MHz; CDCl₃) δ_C 155.6 (C, CH₃OCO), 155.5 (C, CH₃OCO), 144.1 (CH, C-1),

102.5(CH, C-2), 74.9 (CH, C-4), 73.4 (CH, C-5), 66.8 (CH, C-3), 65.3 (CH₂, C-6), 55.5(CH₃, CH₃OCO), 55.1 (CH₃, CH₃OCO)

4,6-Di-O-(methoxycarbonyl)-2,3-dideoxy-D-erythro-hex-2-eno-pyranose (67)

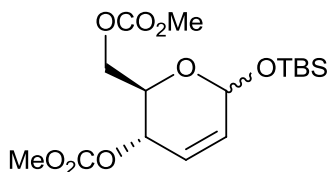


67

A solution of the tricarfonate **62** (4.86 g, 15.1 mmol) in H₂O was stirred at 80 °C for 30 minutes. The solution was then cooled to room temperature and concentrated to afford a 3:1 α : β anomeric mixture of **67** (3.99 g, 15.1 mmol, quantitative yield) as a colourless oil. Spectral data matched those which have been previously reported.⁴³

R_f : 0.43 (50% EtoAc/ pet. Ether); **¹H-NMR**: (500 MHz, CDCl₃) δ _H **Major Anomer (α)**: 6.02 - 5.89 (obs. m, 2H, H-2,3), 5.46 (br s, 1H, H-1), 5.17 (d, J = 10.0 Hz, 1H, H-4), 4.38 (dd, J = 12.0, 2.0 Hz, 1H, H-6a), 4.29 (dd, J = 12.0, 5.0 Hz, 1H, H-6b), 4.25-4.22 (obs. m, 1H, H-5), 3.82 (s, 3H, CH₃OCO), 3.80 (s, 3H, CH₃OCO), 2.99 (d, J = 5.0 Hz, 1H, OH); **Minor Anomer (β)**: 6.02 - 5.89 (obs. m, 2H, H-2,3), 5.46 (br s, 1H, H-1), 5.13 (d, J = 6.5 Hz, 1H, H-4), 4.35 (obs. m, 1H, H-6a), 4.25-4.22 (obs. m, 1H, H-6b), 4.05 (dt, J = 10.0, 5.0 Hz, 1H, H-5), 3.81 (s, 3H, CH₃OCO), 3.80 (s, 3H, CH₃OCO), 3.10 (d, J = 8.0 Hz, 1H, OH); **¹³C-NMR**: (125 MHz; CDCl₃) δ _C **Major Anomer (α)**: 155.6 (C, CH₃OCO), 155.03 (C, CH₃OCO), 128.7 (CH, C-3), 128.6 (CH, C-2), 88.8 (CH, C-1), 68.6 (CH, C-4), 66.5 (CH, C-5), 66.3 (CH₂, C-6), 55.21 (CH₃, CH₃OCO), 55.00 (CH₃, CH₃OCO); **Minor Anomer (β)**: 155.5 (C, CH₃OCO), 154.99 (C, CH₃OCO), 131.6 (CH, C-2), 126.9 (CH, C-3), 90.9 (CH, C-1), 72.8 (CH, C-5), 67.9 (CH, C-4), 66.6 (CH₂, C-6), 55.17 (CH₃, CH₃OCO), 55.04 (CH₃, CH₃OCO)

4,6-Di-O-(methoxycarbonyl)-1-O-(tert-butyldimethylsilyl)-2,3-dideoxy-D-erythro-hex-2-eno-pyranoside (42)

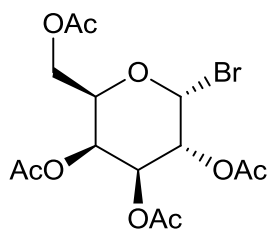


42

A solution of **67** (3.99 g, 15.1 mmol) in DCM (150 mL) and pyridine (1.2 mL, 16.6 mmol) was cooled to 0 °C. Silver nitrate (2.67 g, 16.6 mmol) was added and after all solid was dissolved TBSCl (2.78 g, 16.6 mmol) was added and the reaction was allowed to warm to room temperature and left to proceed overnight. The solution was filtered through Celite™, washed with DCM (50 mL) and concentrated to give the crude product and pyridine as the white semi-crystalline solid. Chromatography of the solid (10% EtOAc / pet. Ether) afforded a 3:2 α : β anomeric mixture of **42** (5.72 g, 15.1 mmol, quantitative yield) as a colourless oil. Spectral data matched those which have been previously reported.⁴³

R_f : 0.9 (30% EtOAc/ pet. Ether); **¹H-NMR**: (500 MHz, CDCl₃) δ _H **Major Anomer (α)**: 5.90 (mult, 2H, H-2, 3), 5.35 (d, J = 1.8 Hz, 1H, H-1), 5.16 (dd, J = 9.6, 0.6 Hz, 1H, H-4), 4.36 - 4.26 (obs. m, 2H, H-6), 4.19 (ddd, J = 9.6, 4.8, 3.0 Hz, 1H, H-5), 3.80 (s, 3H, CH₃OCO), 3.79 (s, 3H, CH₃OCO), 0.91 (s, 9H, OSiC(CH₃)₃), 0.13 (s, 3H, OSiCH₃), 0.10 (s, 3H, OSiCH₃); **Minor Anomer (β)**: 5.93 (mult, 2H, H-2,3), 5.40 (d, J = 1.2 Hz, 1H, H-1), 5.10 (dd, J = 6.6, 1.2 Hz, 1H, H-4), 4.36 - 4.26 (obs. m, 2H, H-6), 4.11 (apt. q, J = 5.7 Hz, 1H, H-5), 3.80 (s, 3H, CH₃OCO), 3.79 (s, 3H, CH₃OCO), 0.89 (s, 9H, OSiC(CH₃)₃), 0.13 (s, 3H, OSiCH₃), 0.10 (s, 3H, OSiCH₃) **¹³C-NMR**: (125 MHz; CDCl₃) δ _C **Major Anomer (α)**: 155.7 (C, CH₃OCO), 155.3 (C, CH₃OCO), 155.1 (CH, C-2), 145.8 (CH, C-3), 90.1 (CH, C-1), 67.8 (CH, C-4), 67.6 (CH, C-5), 65.2 (CH₂, C-6), 55.5 (CH₃, CH₃OCO), 55.3 (CH₃, CH₃OCO), 21.2 (CH₃, OSiC(CH₃)₃), 14.3 (C, OSi(CH₃)₃), -4.5 (CH₃, OSiCH₃), -5.4 (CH₃, OSiCH₃); **Minor Anomer (β)**: 155.5 (C, CH₃OCO), 155.06 (C, CH₃OCO), 133.5 (CH, C-2), 124.7 (CH, C-3), 91.0 (CH, C-1), 72.6 (CH, C-5), 68.2 (CH, C-4), 66.6 (CH₂, C-6), 55.07 (CH₃, CH₃OCO), 54.94 (CH₃, CH₃OCO), 25.7 (CH₃, OSiC(CH₃)₃), 17.98 (C, OSi(CH₃)₃), -4.1 (CH₃, OSiCH₃), -5.1 (CH₃, OSiCH₃)

Tetra-*O*-acetyl- α -D-galactopyranosyl bromide (59)

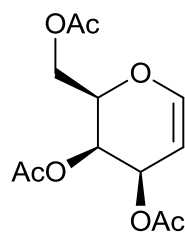


59

Using a modification of Kozikowski's procedure,⁶³ a magnetically stirred solution of D-galactose (132 mg, 0.7 mmol) in acetic anhydride (76 mL, 804 mmol) was treated dropwise with conc. Perchloric acid (0.45 mL, 6.9 mmol). Additional D-galactose (19.71 g, 109 mmol) was added slowly over one hour, at a rate that maintained a temperature of 40 – 50 °C. Upon complete addition of D-galactose, the solution was allowed to cool to room temperature, and then was treated with a 33% (w/w) solution of hydrobromic acid in acetic acid (78 mL, 430 mmol). After 90 minutes, the solution was diluted with dichloromethane (180 mL) and washed with ice cold water (2 × 50 mL), then cold sat. sodium bicarbonate solution (6 × 50 mL). The organic phase was dried with anhydrous magnesium sulfate, filtered and concentrated to afford crude tetra-*O*-acetyl- α -D-galactopyranosyl bromide as a white solid (42.46 g, 102 mmol, 92%) that was used without further purification.

¹H-NMR: (500 MHz, CDCl₃) δ_{H} 6.47 (d, J = 6.0 Hz, 1H, H-1), 5.44 (t, J=6.6 Hz, 1H, H-3), 5.30 (t, J = 6.6 Hz, 1H, H-4), 4.74 (dd, J = 5.0, 3.5 Hz, 1H, H-2), 4.31 (dd, J = 12.3, 5.6 Hz, 1H, H-6a), 4.27 (dd, J = 15.8, 3.2 Hz, 2H, H-5) 4.23 (dd, J = 22.6, 9.9 Hz, 1H, H-6b), 2.13 (s, 3H, CH₃CO) 2.12 (s, 3H, CH₃CO) 2.09 (s, 3H, CH₃CO) 2.03 (s, 3H, CH₃CO) **¹³C-NMR:** (126 MHz, CDCl₃) δ_{C} 170.6 (C, CH₃CCO), 169.6 (C, CH₃CCO), 169.4 (C, CH₃CCO), 168.7 (C, CH₃CCO), 91.7 (CH, C-1), 89.0 (CH, C-5), 69.80 (CH, C-2), 69.16 (CH, C-3), 67.8 (CH, C-4), 61.4 (CH₂, C-6), 20.8 (CH₃, CH₃CO), 20.7 (CH₃, CH₃CO), 20.6 (CH₃, CH₃CO), 20.5 (CH₃, CH₃CO).

Tri-*O*-acetyl-D-galactal (**60**)

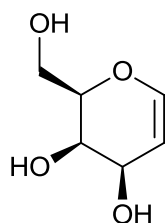


60

A magnetically stirred dispersion of zinc dust (47.92 g, 733.1 mmol) in water (150 mL) was cooled to 0 °C, diluted with acetic acid (150 mL), then treated dropwise with a solution of galactopyranosyl bromide **59** in diethyl ether (150 mL) over one hour. The reaction was allowed to warm to room temperature and left to proceed overnight. The solution was filtered, and then diluted with dichloromethane (200 mL). The solution was washed successively with water (3 × 60 mL), sat. sodium bicarbonate (4 × 50 mL), then brine (60 mL). The organic phase was dried with anhydrous magnesium sulfate, filtered and concentrated to provide **60** as a white solid (26.5 g, 98 mmol, 92%).

¹H-NMR: (500 MHz, CDCl₃) δ_H 6.46 (d, J = 6.1 Hz, 1H, H-1), 5.44 (m, 1H, H-3), 5.33 (dd, J = 7.6, 5.7 Hz, 1H, H-4), 4.74 (dd, J = 6.1, 3.2 Hz, 1H, H-2), 4.39 (dd, J = 12.1, 5.8 Hz, 1H, H-6a), 4.25 (m, 1H, H-5), 4.19 (dd, J = 12.1, 3.0 Hz, 1H, H-6b), 2.09 (s, 3H, CH₃CO), 2.07 (s, 3H, CH₃CO), 2.04 (s, 3H, CH₃CO); **¹³C-NMR:** (126 MHz, CDCl₃) δ_C 170.6 (C, CH₃C=O), 170.4 (C, CH₃C=O), 169.6 (C, CH₃C=O), 145.6 (CH, C-1), 99.0 (CH, C-2), 73.9 (CH, C-5), 67.3 (CH, C-3), 67.2 (CH, C-4), 61.4 (CH, C-6), 21.0 (CH₃, CH₃CO), 20.8 (CH₃, CH₃CO), 20.7 (CH₃, CH₃CO)

D-Galactal (**61**)



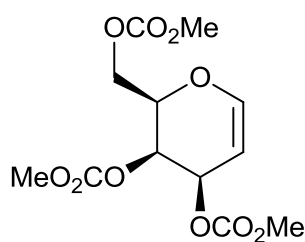
61

Sodium (664 mg, 29 mmol) was added to methanol (180 mL) and allowed to react. This was followed by addition of the protected galactal **60** (23.60 g, 86.7 mmol). The reaction was stirred at room temperature for 15 minutes and then the solution was concentrated to provide crude D-galactal **61**. The crude product was treated with methanol (12 mL), then successively diluted with acetone (60 mL) and diethyl ether (120 mL), which lead to the precipitation of impurities. The solution was filtered and concentrated to afford **61** (11.8 g, 80.6 mmol, 93%) as a very viscous orange oil.

¹H-NMR: (500 MHz; D₂O) δ_{H} 6.36 (dd, $J = 6.0, 1.5$ Hz, 1H, H-1), 4.74 (dd, $J = 6.0, 2.0$ Hz, 1H, H-2), 4.27 (dt, $J = 7.0, 2.0$ Hz, 1H, H-3), 3.82 (complex m, 3H, H-5, 6-a, 6-b), 3.62 (dd, $J = 9.0, 7.0$ Hz, 1H, H-4); **¹³C-NMR:** (125 MHz; D₂O) δ_{C} 143.7 (CH, C-1), 102.8 (CH, C-2), 78.1 (CH, C-5), 68.7 (CH, C-4), 68.3 (CH, C-3), 60.0 (CH₂, C-6).

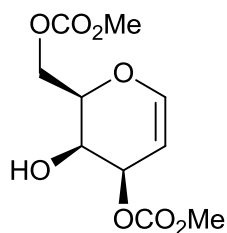
3,4,6-Tri-*O*-methoxycarbonyl-D-galactal (**65**), and 3,6-di-*O*-methoxycarbonyl-D-galactal (**66**)

To a solution of D-galactal (12.67 g, 86.7 mmol) in THF (500 mL) at 0 °C was added DMAP (34.95 g, 286.1 mmol), followed by methyl chloroformate (22.1 mL, 286.1 mmol). The reaction was allowed to warm to room temperature and left to proceed overnight. The solution was filtered through CeliteTM, washed with DMC (50 mL), and concentrated to give the crude products **65:66** as an off white solid in a 3:1 ratio. Chromatography of the solid (30% EtOAc / pet. ether) afforded **62** (12.6 g, 39 mmol, 45%) as a white solid, **63** (4.2 g, 13.0 mmol, 15%) as a colourless oil in a combined yield of 60%.



65

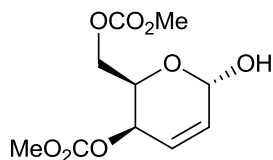
R_f : 0.46 (30% EtoAc/ pet. Ether); **¹H-NMR:** (500 MHz; CDCl₃) δ_{H} 6.46 (d, $J = 6.0$ Hz, 1H, H-1), 5.43 (t, $J = 4.0$ Hz, 1H, H-3), 5.32 (t, $J = 6.5$ Hz, 1H, H-4), 4.83 (dd, $J = 6.0, 3.5$ Hz, 1H, H-2), 4.46 (dd, $J = 12.0, 6.0$ Hz, 1H, H-6a), 4.39 (complex m, 1H, H-5), 4.32 (dd, $J = 12.0, 4.0$ Hz, 1H, H-6b), 3.82 (s, 3H, CH₃OCO), 3.80 (s, 3H, CH₃OCO), 3.79 (s, 3H, CH₃OCO).



66

R_f : 0.25 (30% EtoAc/ pet. Ether); **¹H-NMR**: (500MHz; CDCl₃) δ_H 6.44 (d, *J* = 6.5 Hz, 1H, H-1), 5.20 (d, *J* = 6.5 Hz, 1H, H-3), 4.79 (dd, *J* = 6.0, 2.5 Hz, 1H, H-2), 4.56 (dd, *J* = 12.0, 4.0 Hz, 1H, H-6a), 4.48 (dd, *J* = 12.0, 2.0 Hz, 1H, H-6b), 4.02 (ddd, *J* = 10.0, 4.0, 2.0 Hz, 1H, H-5), 3.95 (ddd, *J* = 10.5, 6.5, 3.5 Hz, 1H, H-4), 3.82 (s, 6H, CH₃OCO), 3.44 (d, *J* = 3.5 Hz, 1H, OH); **¹³C-NMR**: (125 MHz; CDCl₃) δ_C 156.4 (C, CH₃OCO), 156.1 (C, CH₃OCO), 146.3(CH, C-1), 98.8 (CH, C-2), 76.2 (CH, C-5), 76.1 (CH, C-3), 66.9 (CH, C-4), 65.7(CH₂, C-6), 55.2 (CH₃, CH₃OCO), 55.2 (CH₃, CH₃OCO)

4,6-Di-*O*-(methoxycarbonyl)-2,3-dideoxy-D-erythro-hex-2-eno-pyranose (68)

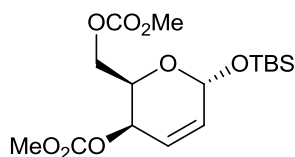


68

A solution of the tricarbonate **65** (2.15 g, 6.7 mmol) in H₂O was stirred at 80 °C for 30 minutes. The solution was then cooled to room temperature and concentrated to afford the α anomer **67** (1.77g, 6.7 mmol, quantitative yield) as a colourless oil.

R_f : 0.43 (50% EtoAc/ pet. Ether); **¹H-NMR**: (500 MHz, CDCl₃) δ_H **Major Anomer (α)**: 6.21 (dd, *J* = 10.0, 5.5 Hz 1H, H-3), 6.11 (dd, *J* = 10.3, 3.3 Hz 1H, H-3), 5.51 (br s, 1H, H-1), 4.89 (d, *J* = 10.0 Hz, 1H, H-4), 4.50 (dd, *J* = 12.0, 2.0 Hz, 1H, H-6a), 4.35 (dd, *J* = 12.0, 5.0Hz, 1H, H-6b), 4.25-4.22 (obs. m, 1H, H-5), 3.802 (s, 3H, CH₃OCO), 3.796 (s, 3H, CH₃OCO); **¹³C-NMR**: (125 MHz; CDCl₃) δ_C **Major Anomer (α)**: 155.6 (C, CH₃OCO), 155.03 (C, CH₃OCO), 128.7 (CH, C-3), 128.6 (CH, C-2), 88.8 (CH, C-1), 68.6 (CH, C-4), 66.5 (CH, C-5), 66.3 (CH₂, C-6), 55.21 (CH₃, CH₃OCO), 55.00 (CH₃, CH₃OCO);

4,6-Di-*O*-(methoxycarbonyl)-1-*O*-(*tert*-butyldimethylsilyl)-2,3-dideoxy-D-erythro-hex-2-eno-pyranoside (**48**)

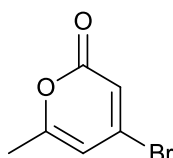


48

A solution of **68** (2.0 g, 7.5 mmol) in DCM (100 mL) and pyridine (0.75 mL, 8.3 mmol) was cooled to 0 °C. Silver nitrate (1.34 g, 8.3 mmol) was added and after all solid was dissolved TBSCl (1.13 g, 8.3 mmol) was added and the reaction was allowed to warm to room temperature and left to proceed overnight. The solution was filtered through CeliteTM, washed with DCM (50 mL) and concentrated to give the crude product and pyridine as the white semi-crystalline solid. Chromatography of the solid (10% EtOAc / pet. Ether) afforded the α anomer **48** (2.85 g, 7.5 mmol, quantitative yield) as a colourless oil.

R_f: 0.9 (30% EtOAc/ pet. Ether); **¹H-NMR**: (500 MHz, CDCl₃) δ _H **Major Anomer (α)**: 6.22 (d, J = 10.8 Hz, 1H, H-3), 6.11 (dt, J = 10.8, 2.4 Hz, 1H, H-2), 5.50 (d, J = 1.8 Hz, 1H, H-1), 5.16 (dd, J = 9.6, 0.6 Hz, 1H, H-4), 4.89 (dd, J = 4.5, 3.0 Hz, 1H, H-6_a), 4.50 (ddd, J = 9.6, 4.8, 3.0 Hz, 1H, H-5) 4.35 (d, J = 6.3 Hz, 1H, H-6_b), 3.81 (s, 3H, CH₃OCO), 3.78 (s, 3H, CH₃OCO), 0.91 (s, 9H, OSiC(CH₃)₃), 0.12 (s, 3H, OSiCH₃), 0.10 (s, 3H, OSiCH₃) **¹³C-NMR**: (125 MHz; CDCl₃) δ _C **Major Anomer (α)**: 155.7 (C, CH₃OCO), 155.08 (C, CH₃OCO), 130.7 (CH, C-2), 126.3 (CH, C-3), 89.0 (CH, C-1), 68.8 (CH, C-4), 66.41 (CH, C-5), 66.35 (CH₂, C-6), 55.14 (CH₃, CH₃OCO), 54.89 (CH₃, CH₃OCO), 25.6 (CH₃, OSiC(CH₃)₃), 17.95 (C, OSi(CH₃)₃), -4.5 (CH₃, OSiCH₃), -5.4 (CH₃, OSiCH₃)

4-Bromo-6-methyl-2*H*-pyran-2-one (**69**)



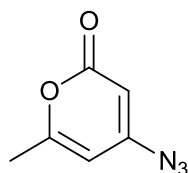
69

A solution of phosphorus tribromide (22.90 g, 84.6 mmol) in anhydrous diethyl ether (50 mL) was added dropwise to cooled and magnetically stirred *N,N*-dimethylformamide (70

mL). A solution of 4-hydroxy-6-methyl-2H-pyran-2-one (2.67 g, 21.2 mmol) in *N,N*-dimethylformamide (45 mL) was then added dropwise to the reaction vessel, the reaction was heated to 60 °C and left to react for 20 hrs. Water (200 mL) was poured into the reaction vessel and extracted with diethyl ether (4 × 50 mL). The organic phase was dried with anhydrous magnesium sulfate, filtered and concentrated to provide crude **69** as a brown solid (3.2 g, 17.0 mmol, 80%), which was then purified by sublimation affording **69** as a white solid (2.43 g, 12.7 mmol, 60%). Spectral data matched those which have been previously reported.⁵¹

¹H-NMR: (500 MHz, CDCl₃) δ_H 6.45 (s, 1H, H-2), 6.19 (s, 1H, H-4), 2.25 (s, 3H, H-6); **¹³C-NMR:** (125 MHz; CDCl₃) δ_C 162.2 (C, C-1), 160.8 (CH, C-2), 141.3 (C, C-5), 114.9 (CH, C-4), 108.6 (C, C-3), 19.9 (CH₃, C-6)

4-Azido-6-methyl-2H-pyran-2-one (**70**)

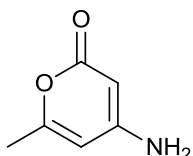


70

A mixture of **69** (2.85 g, 15.1 mmol), sodium azide (1.48 g, 22.7 mmol) and *N,N*-dimethylformamide (50 mL) was magnetically stirred at r.t. for 1 hr. the reaction mixture was poured into ice-water (50 mL), stirred for 10 min and extracted with diethyl ether (3 × 100 mL). The organic phase was washed with water (3 × 100 mL), dried with anhydrous magnesium sulfate, filtered, and concentrated to afford **70** as a white solid (1.93 g, 15.1 mmol, quantitative yield). Spectral data matched those which have been previously reported.⁵¹

¹H-NMR: (500 MHz, CDCl₃) δ_H 5.75 (s, 2H, H-2,3), 2.25 (s, 3H, H-6); **¹³C-NMR:** (125 MHz; CDCl₃) δ_C 164.3 (CH, C-2), 163.1 (C, C-1), 156.8 (C, C-5), 99.6 (CH, C-2), 97.3 (CH, C-4), 20.5 (CH₃, C-6)

4-Amino-6-methyl-2H-pyran-2-one (49)

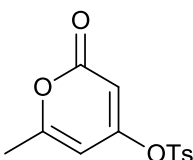


49

A magnetically stirred mixture of **70** (1.93g 15.1 mmol), 10 mol% Pd/C (0.19 g, 1.5 mmol) and ethanol (200 mL) was treated with hydrogen at atmospheric pressure and r.t.. The reaction was monitored by TLC and after 1 hr the reaction was filtered and concentrated to afford **49** as a white solid (1.90 g, 15.1 mmol, quantitative yield). Spectral data matched those which have been previously reported.⁵¹

¹H-NMR: (500 MHz, CDCl₃) δ_H 5.57 (s, 1H, H-2), 5.13 (s, 1H, H-4), 4.44 (broad s, 2H, NH₂) 2.18 (s, 3H, H-6); **¹³C-NMR:** (125 MHz; CDCl₃) δ_C 163.1 (CH, C-2), 161.5 (C, C-1), 159.8 (C, C-5), 99.0 (CH, C-4), 84.9 (C, C-3), 20.4 (CH₃, C-6)

6-Methyl-4-tosyloxy-2H-pyran-2-one (71)



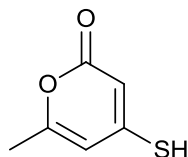
71

A mixture of 4-hydroxy-6-methyl-2H-pyran-2-one (1.04 g, 8.3 mmol) and *p*-toluenesulfonyl chloride (1.58 g, 8.3 mmol) in pyridine (20 mL) was left to react at r.t for 24 hr and then poured into cold 5M HCl, extraction with diethyl ether (4 × 20 mL), dried with anhydrous magnesium sulfate, filtered and concentrated to afford **71** as a white solid (2.35 g, 7.5 mmol, 90%). Spectral data matched those which have been previously reported.⁵²

¹H-NMR: (500 MHz, CDCl₃) δ_H 7.83 (d, J= 8.1 Hz, 2H, -O₂SC₆H₄CH₃), 7.39 (d, J= 8.4 Hz, 2H, -O₂SC₆H₄CH₃), 6.01 (s, 1H, H-2), 5.80 (s, 1H, H-4), 2.48 (s, 3H, -O₂SC₆H₄CH₃), 2.24 (s, 3H, H-6); **¹³C-NMR:** (125 MHz; CDCl₃) δ_C 164.4 (C, C-1), 162.1 (CH, C-2), 145.8 (C, C-3),

131.8 (C, -O₂SC₆H₄CH₃), 130.4 (C, -O₂SC₆H₄CH₃), 128.6 (C, -O₂SC₆H₄CH₃), 100.94 (CH, C-4), 100.88 (C, -O₂SC₆H₄CH₃), 22.0 (C, -O₂SC₆H₄CH₃), 20.4 (CH₃, C-6)

4-Mercapto-6-methyl-2H-pyran-2-one (53)

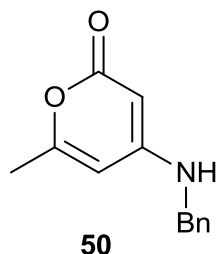


53

To a magnetically stirred solution of NaSH (0.74 g, 1.3 mmol) in dry ethanol (50 mL), a solution of 4-bromo-6-methyl-2Hpyran-2-one (0.25 g, 1.3 mmol) in dry ethanol was added dropwise at room temperature under argon atmosphere for 30 minutes. The reaction mixture was left for a further 2 hours, and then concentrated under reduced pressure at room temperature. The residue was acidified with conc HCL (20 mL). The aqueous layer was extracted with chloroform (4 × 25 mL), the chloroform was then washed with water (2 × 20 mL) and dried with anhydrous magnesium sulfate. Attempt to evaporate the chloroform led to complete decomposition of compound **53**. So this chloroform solution was directly used for subsequent reactions.⁵²

¹H-NMR: (500 MHz, CDCl₃) δ_H 6.45 (s, 1H, H-2), 6.19 (s, 1H, H-4), 2.24 (s, 3H, H-6); **¹³C-NMR:** (125 MHz; CDCl₃) δ_C 162.0 (C, C-1), 160.6 (CH, C-2), 141.1 (C, C-5), 114.7 (CH, C-4), 108.4 (C, C-3), 20.0 (CH₃, C-6)

4-N-Benzylamino-6-methyl-2H-pyran-2-one (50)



50

A solution of 4-bromo-6-methyl pyrone (**69**) (0.20 g, 1.0 mmol) and *N*-benzylamine (0.15 mL 1.0 mmol) in 80 mL of absolute ethanol was heated at reflux for 24 hours. After cooling to room temperature the reaction mixture was concentrated under reduced pressure. The crude **50** was filtered through silica gel, and eluted with 50% acetone in pet. ether. The

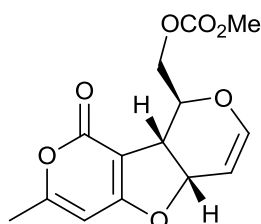
resulting filtrate was concentrated under reduced pressure, and the resulting solid recrystallised from ethyl acetate to give **40** as tan crystals (0.21 g, 1.0 mmol). Spectral data matched those which have been previously reported.⁶⁶

¹H-NMR: (500 MHz, CDCl₃) δ_H; 7.38 (t, J = 6.1 Hz, 2H, -CH₂CCH₂CH₂CH), 6.36 (t, J = 9.3 Hz, 2H, -CH₂CCH₂CH₂CH), 7.29 (d, J = 6.6 Hz, -CH₂CCH₂CH₂CH), 5.53 (s, 1H, H-2), 5.07 (s, 1H, H-4), 4.74 (broad s, 1H, NH), 4.30 (s, 2H, -CH₂CCH₂CH₂CH), 2.16 (s, 3H, H-6) **¹³C-NMR:** (125 MHz; CDCl₃) δ_C 165.3 (C, C-1), 161.3 (CH, C-2), 158.1 (C, C-3), 136.7 (C, -CH₂CCH₂CH₂CH), 129.0 (CH, -CH₂CCH₂CH₂CH), 127.9 (CH, -CH₂CCH₂CH₂CH), 127.5 (CH, -CH₂CCH₂CH₂CH), 99.2 (CH, C-4), 81.1 (C, C-5), 46.8 (CH₂, -CH₂CCH₂CH₂CH), 19.9 (CH₃, C-6)

4.3. Palladium-Catalyzed Allylic Alkylation Cascade General Procedures

A reaction vessel was charged with the bis-nucleophile (1.0 equiv) and Pd⁽⁰⁾ catalyst (15 mol%), evacuated and back-filled with argon. Toluene (ca. 0.05 M, degassed by freeze/pump/thaw method and backfilled with argon) was added to the reaction vessel, followed base if needed and then by the bis-electrophile substrate, (1.0 eq.). The reaction was stirred overnight at room temperature before being concentrated in vacuo and purified by flash column chromatography.

Methyl (((1*S*,4*aS*,9*bS*)-7-Methyl-9-oxo-1,4*a*,9,9*b*-tetrahydrofuro[3,2-*c*:4,5-*c'*]-dipyran-1-yl)methyl) carbonate (**47**)

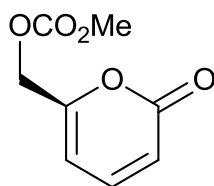


47

The reaction was performed with 4-hydroxy-6-methyl-2H-pyran-2-one (**31**) (33 mg, 0.26 mmol), the glucosyl bis-electrophile (**48**) (100 mg, 0.26 mmol), TEA (6 μ L, 0.04 mmol), Pd₂(dba)₃ (18 mg, 0.019 mmol, 15 mol%), and Xantphos (23 mg, 0.04 mmol) according to the general method. The crude product was purified by flash column chromatography (40% EtoAc / pet. ether) to give **47** as a yellow oil (76 mg, 0.23 mmol, 87%). Spectral data matched those which have been previously reported.

¹H-NMR: (500 MHz, CDCl₃) δ_{H} 6.81 (d, *J* = 6.2 Hz, 1H), 5.96 (s, 1H), 5.30 (dd, *J* = 77.2, 7.5 Hz, 1H), 5.08 (ddd, *J* = 7.4, 4.8, 1.4 Hz, 1H), 4.75 (dd, *J* = 12.4, 2.0 Hz, 1H), 4.43 (dd, *J* = 13.2, 6.6 Hz, 1H), 3.80 (s, 3H), 3.64 (ddd, *J* = 11.2, 6.6, 1.9 Hz, 1H), 3.24 (dd, *J* = 11.2, 7.5 Hz, 1H), 2.28 (s, 3H) **¹³C-NMR:** (125 MHz; CDCl₃) δ_{C} 172.6, 161.7, 161.9, 155.4, 149.5, 99.59, 97.9, 95.9, 79.4, 74.6, 67.7, 54.9, 37.1, 20.6

Methyl-2-hydroxymethyl-2H-pyran-6-one carbonate (73)

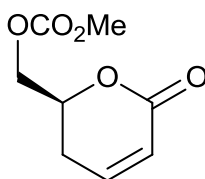


73

4-Amino-6-methyl-2H-pyran-2-one (**49**) (33 mg, 0.26 mmol) and NaH (8 mg, 0.26 mmol) were added premixed for 1 hour in toluene. The resulting mixture was then added to a round bottom flask containing the glucosyl bis-electrophile (**48**) (100 mg, 0.26 mmol), TEA (6 μ L, 0.04 mmol), Pd₂(dba)₃ (18 mg, 0.019 mmol, 15 mol%), and Xantphos (22 mg, 0.038 mmol). The reaction was stirred overnight at room temperature before being concentrated in vacuo and the crude product was purified by flash column chromatography (40% EtOAc / pet. ether) to give **73** as a yellow oil (0.03 g, 0.16 mmol, 63%). Spectral data matched those which have been previously reported.⁴³

R_f: 0.2 (40% EtOAc/ pet ether); **¹H-NMR**: (500 MHz, CDCl₃) δ _H 7.33 (dd, *J*=11.0, 7.8 Hz, 1H, H-2), 6.28 (complex m, 2H, H-3, 4), 4.94 (s, 1H, H-6), 3.80 (s, 3H, CH₃OCO); **¹³C-NMR**: (125 MHz; CDCl₃) δ _C 161.5 (C, C-1), 158.6 (C, C-5), 155.5 (C, CH₃OCO), 143.2 (CH, C-2), 116.3 (CH, C-3) 103.3 (CH, C-4) 65.0 (CH₂, C-6), 55.8 (CH₃, CH₃OCO)

Methyl ((6-oxo-3,6-dihydro-2H-pyran-2-yl)methyl) carbonate (77)



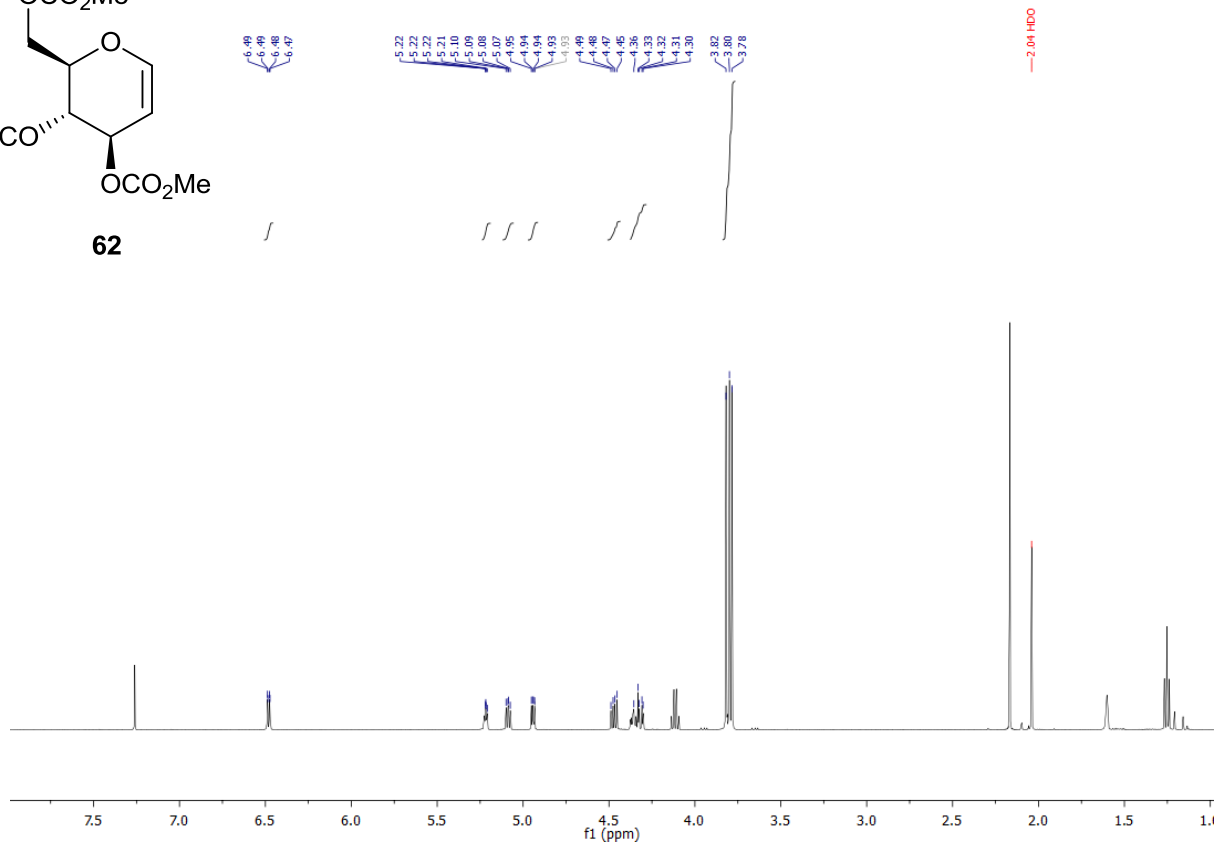
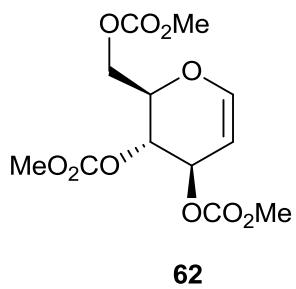
77

The reaction was performed with 4-mercapto-6-methyl-2H-pyran-2-one (**53**) (36 mg, 0.26 mmol), the glucosyl bis-electrophile (**48**) (100 mg, 0.26 mmol), TEA (6 μ L, 0.04 mmol), Pd₂(dba)₃ (18 mg, 0.019 mmol, 15 mol%), and Xantphos (22 mg, 0.038 mmol). The reaction was stirred overnight at room temperature before being concentrated in vacuo and the crude product was purified by flash column chromatography (40% EtOAc / pet. ether) to give **77** as a yellow oil (0.035 g, 0.18 mmol, 74%).

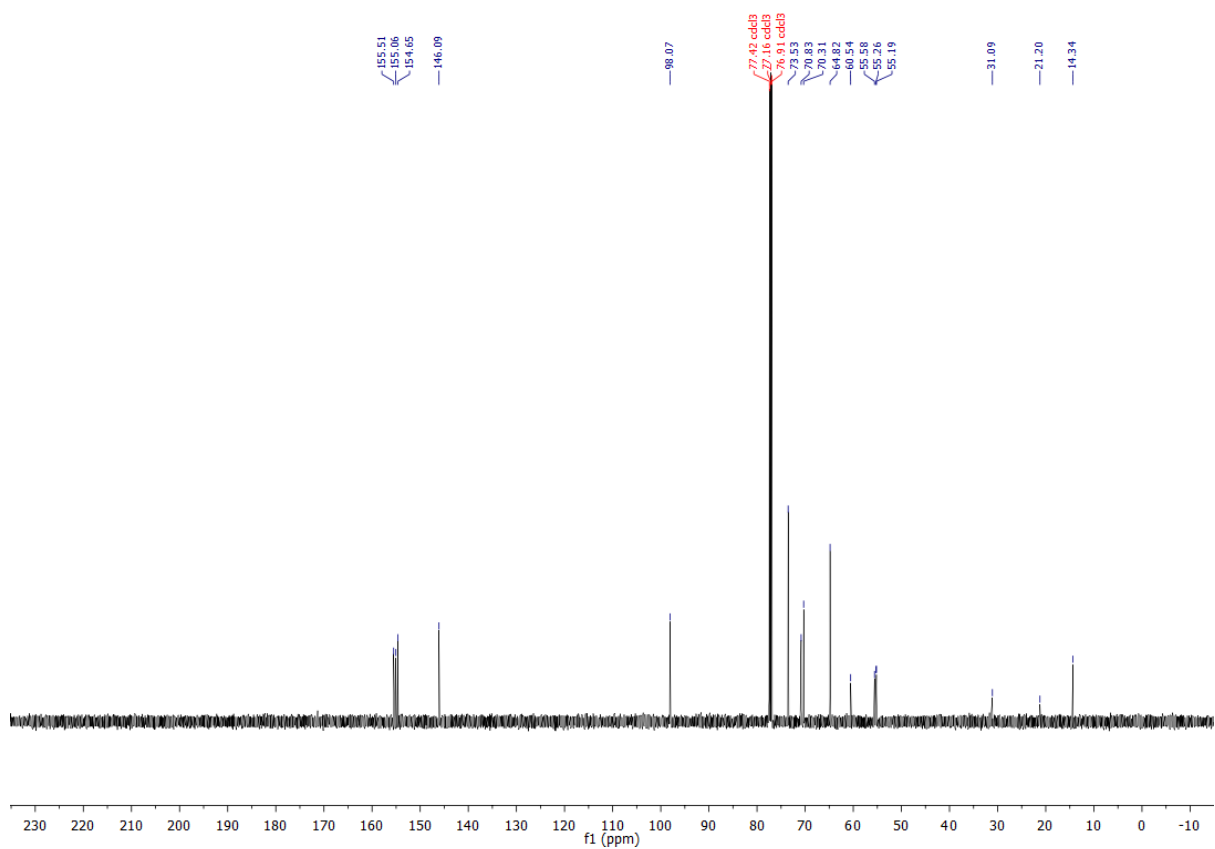
R_f : 0.22 (40% EtOAc/ pet ether): **¹H-NMR:** (500 MHz, CDCl₃) δ_H 6.91 (ddd, J = 9.9, 5.9, 2.6 Hz, 1H, H-3), 6.06 (ddd, J = 9.8, 2.7, 1.1 Hz, 1H, H-2), 4.71 (App dq, 1H, H-5), 4.36 (d, J = 4.8 Hz, 2H, H-5), 3.81 (s, 3H, CH₃OCO), 2.53, 2.43 (dd, 2H, H-4); **¹³C-NMR:** (125 MHz; CDCl₃) δ_C 163.1 (C, C-1), 155.5 (C, CH₃OCO), 144.3 (CH, C-3), 121.5 (CH, C-2), 74.9 (CH, C-5), 67.9 (CH₂, C-6), 55.3 (CH₃, CH₃OCO), 25.7 (CH₂, C-4)

5. Appendix

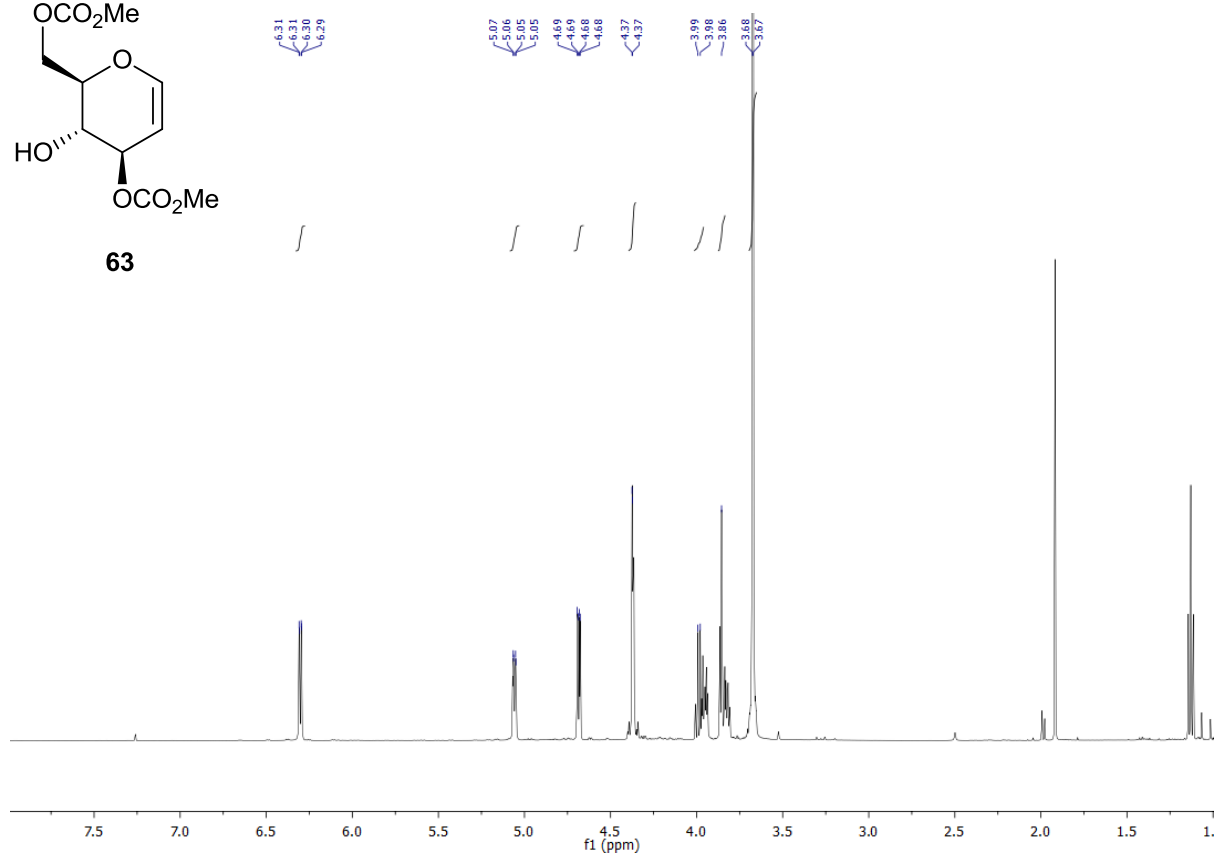
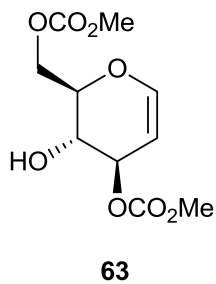
Spectra of New and Selected Compounds



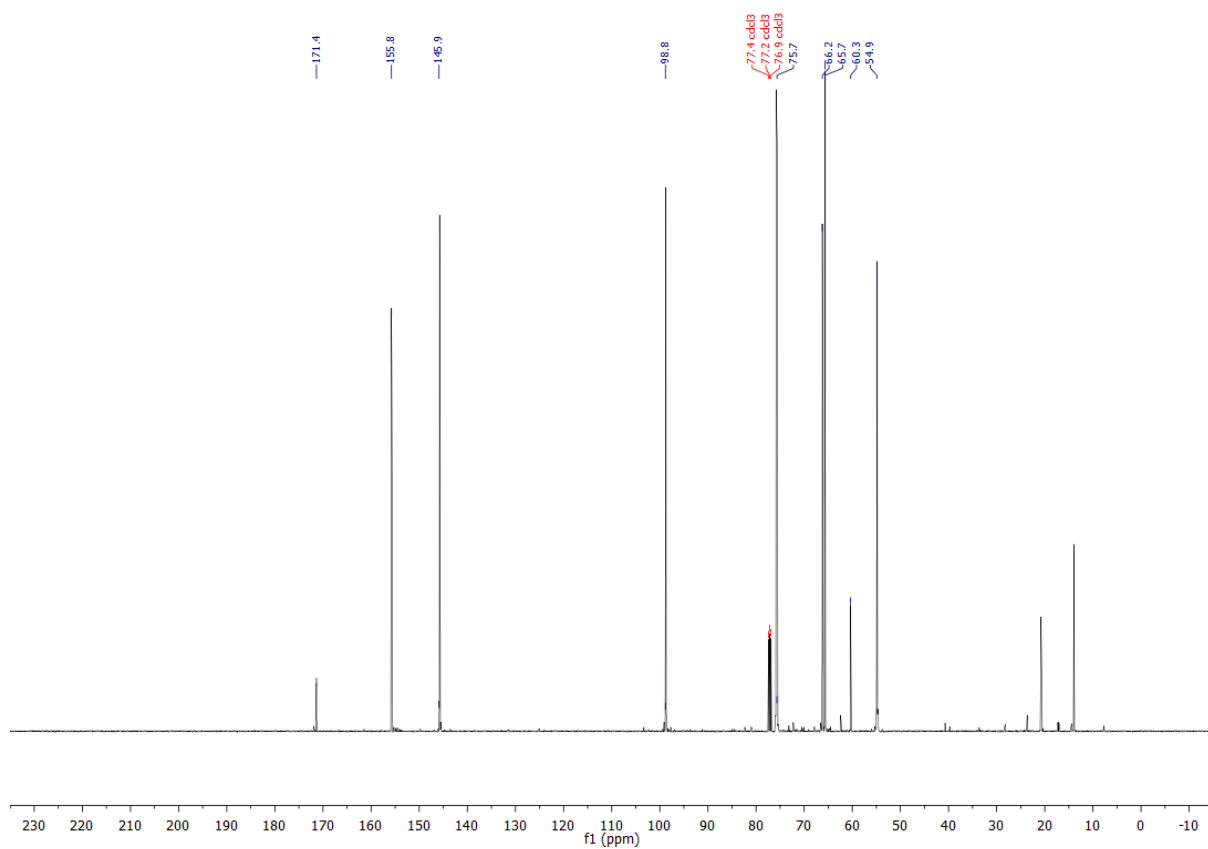
¹H NMR spectrum of **62** (500 MHz, CDCl₃)



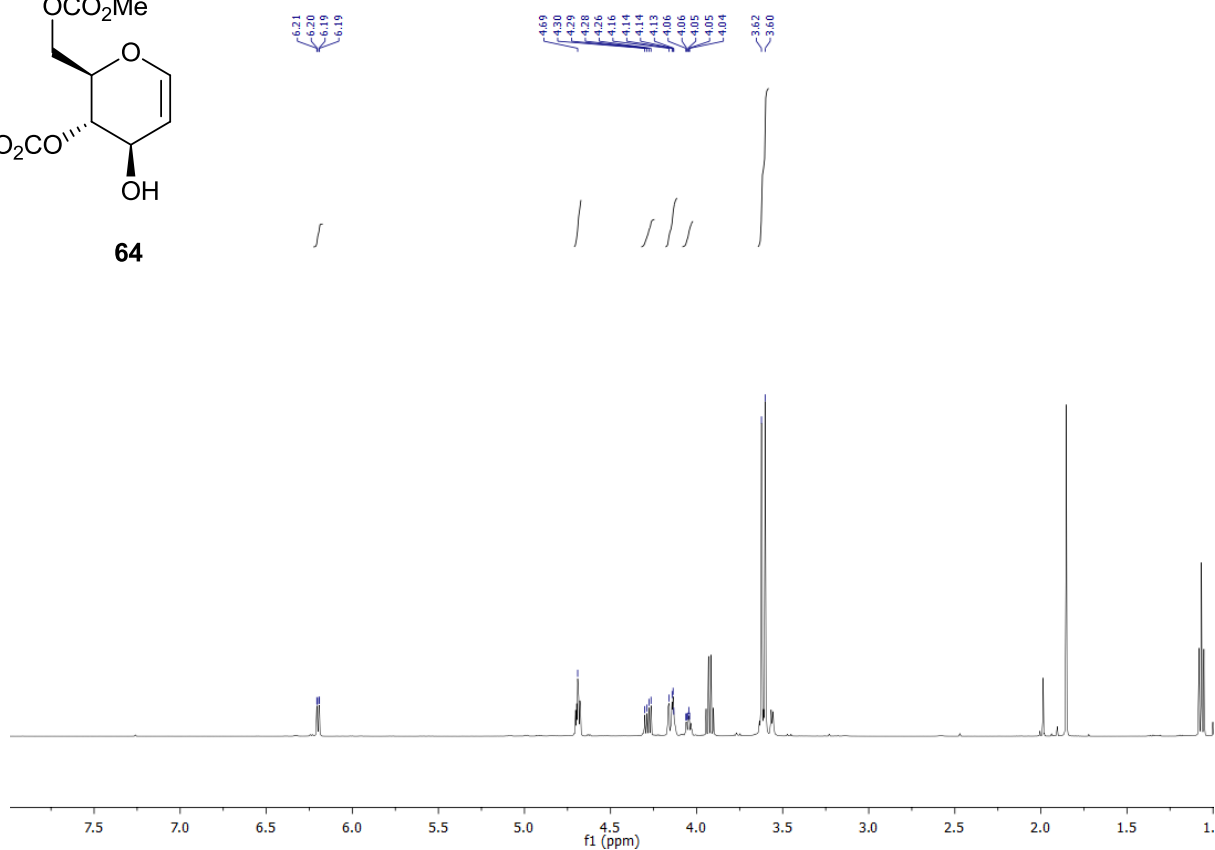
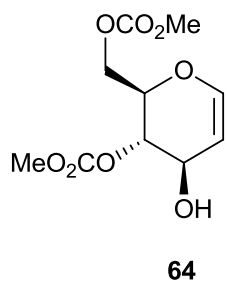
¹³C NMR spectrum of **62** (500 MHz, CDCl₃)



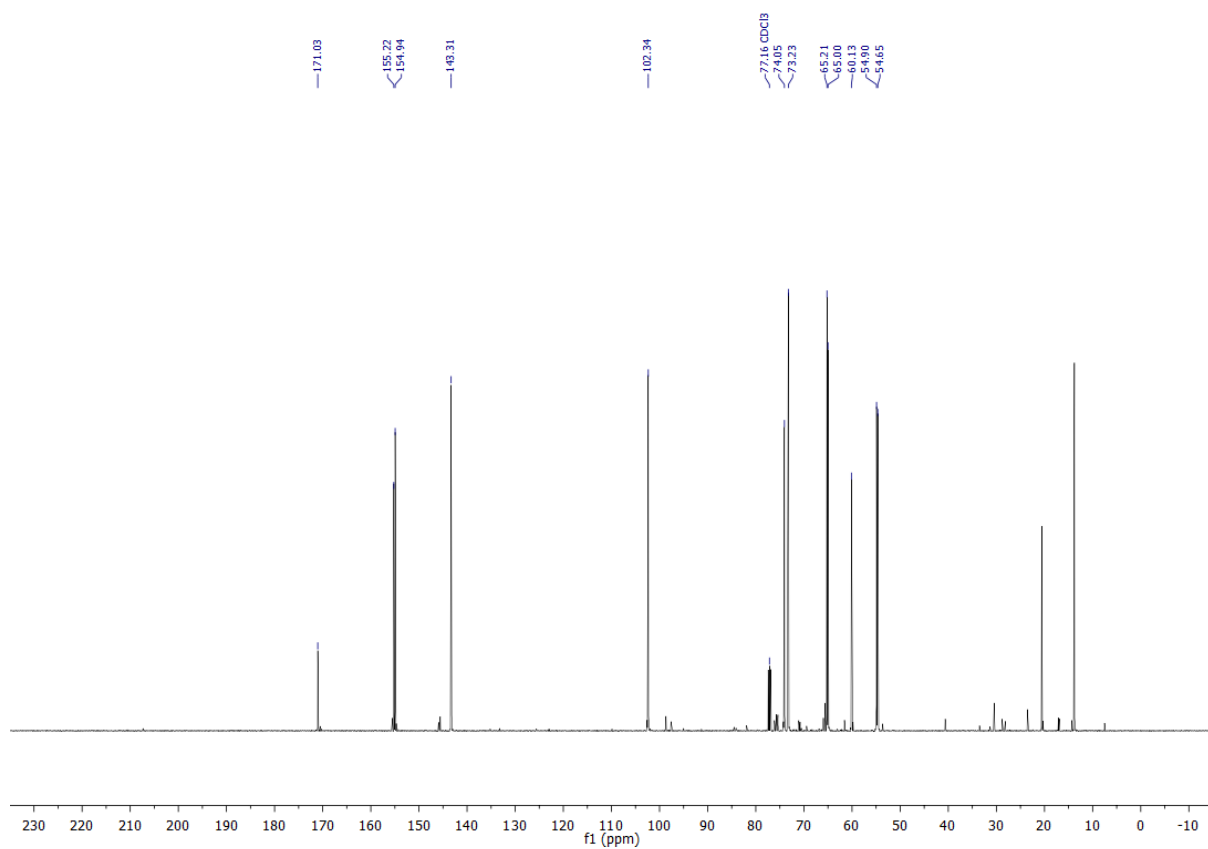
¹H NMR spectrum of **63** (500 MHz, CDCl₃)



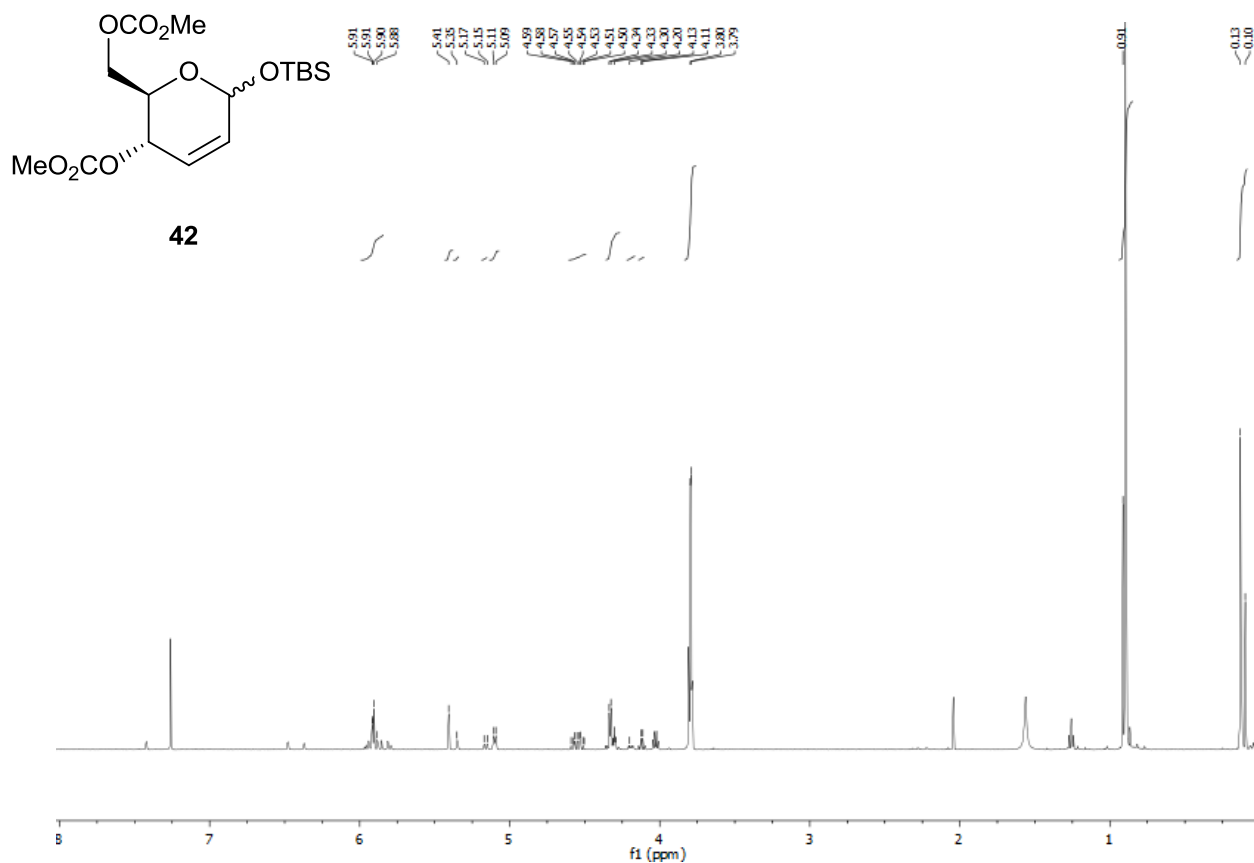
¹³C NMR spectrum of **63** (500 MHz, CDCl₃)



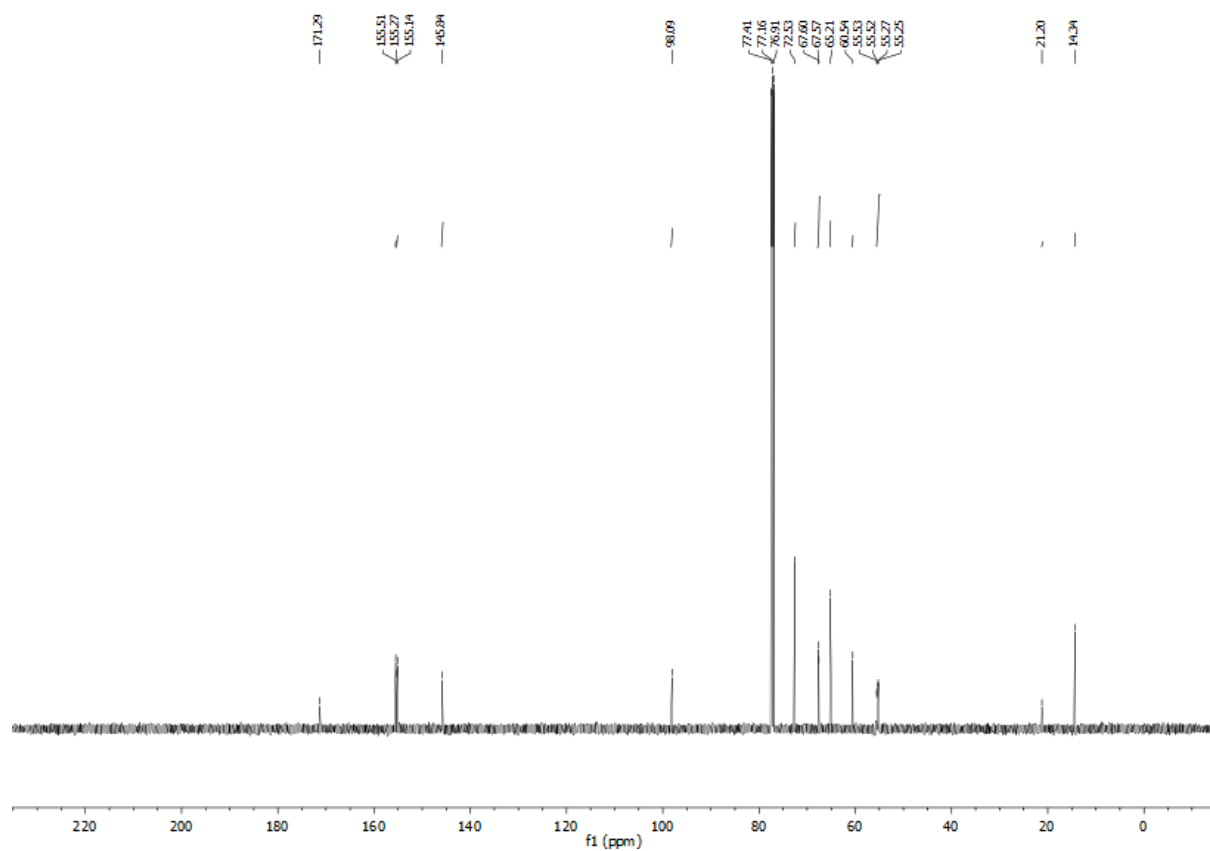
¹H NMR spectrum of **64** (500 MHz, CDCl₃)



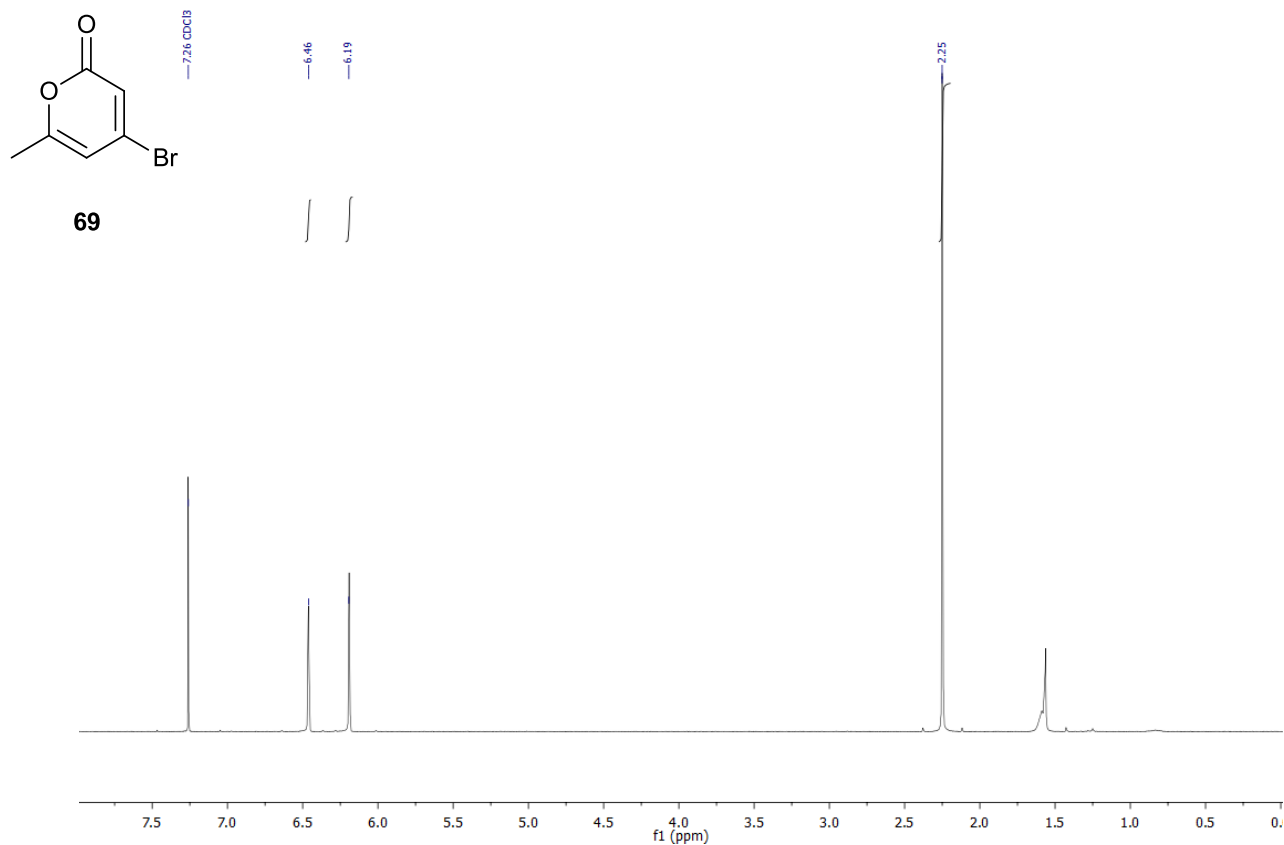
¹³C NMR spectrum of **64** (500 MHz, CDCl₃)



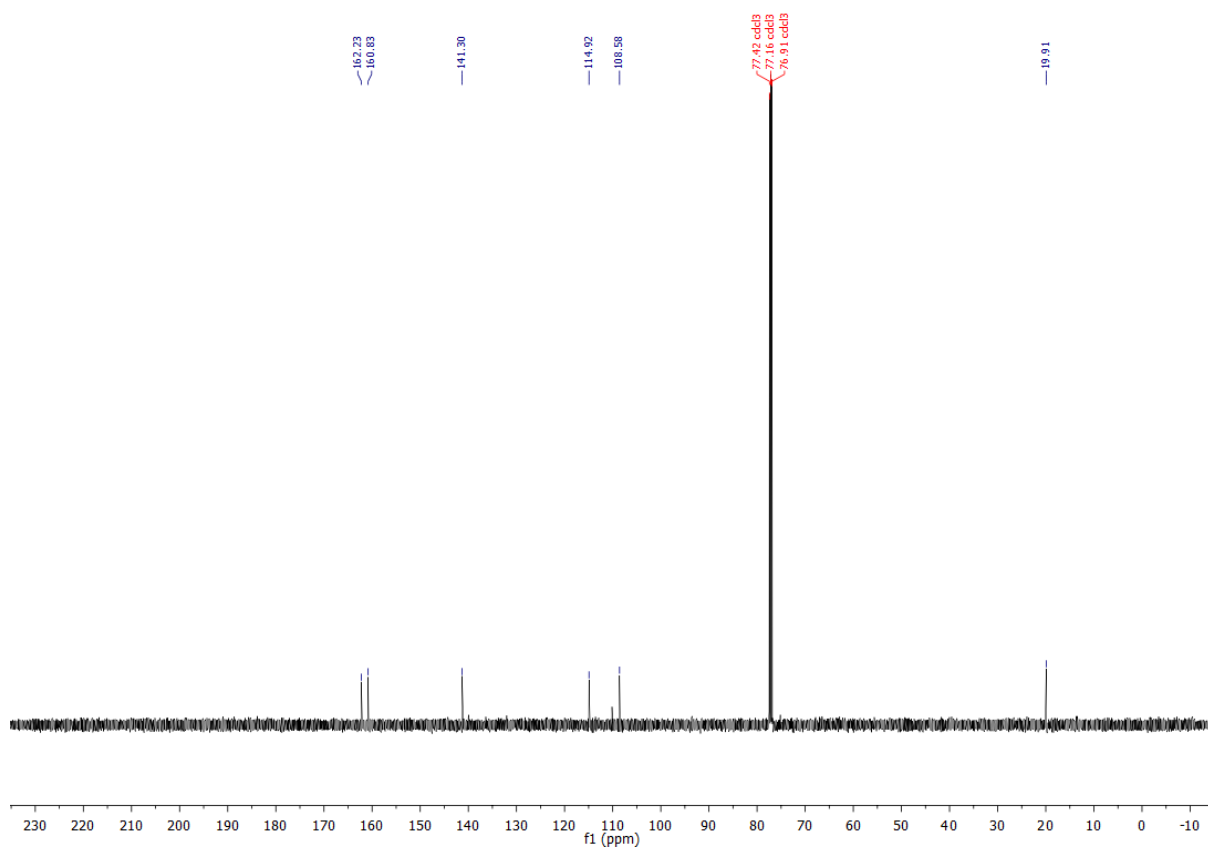
¹H NMR spectrum of **42** (500 MHz, CDCl₃)



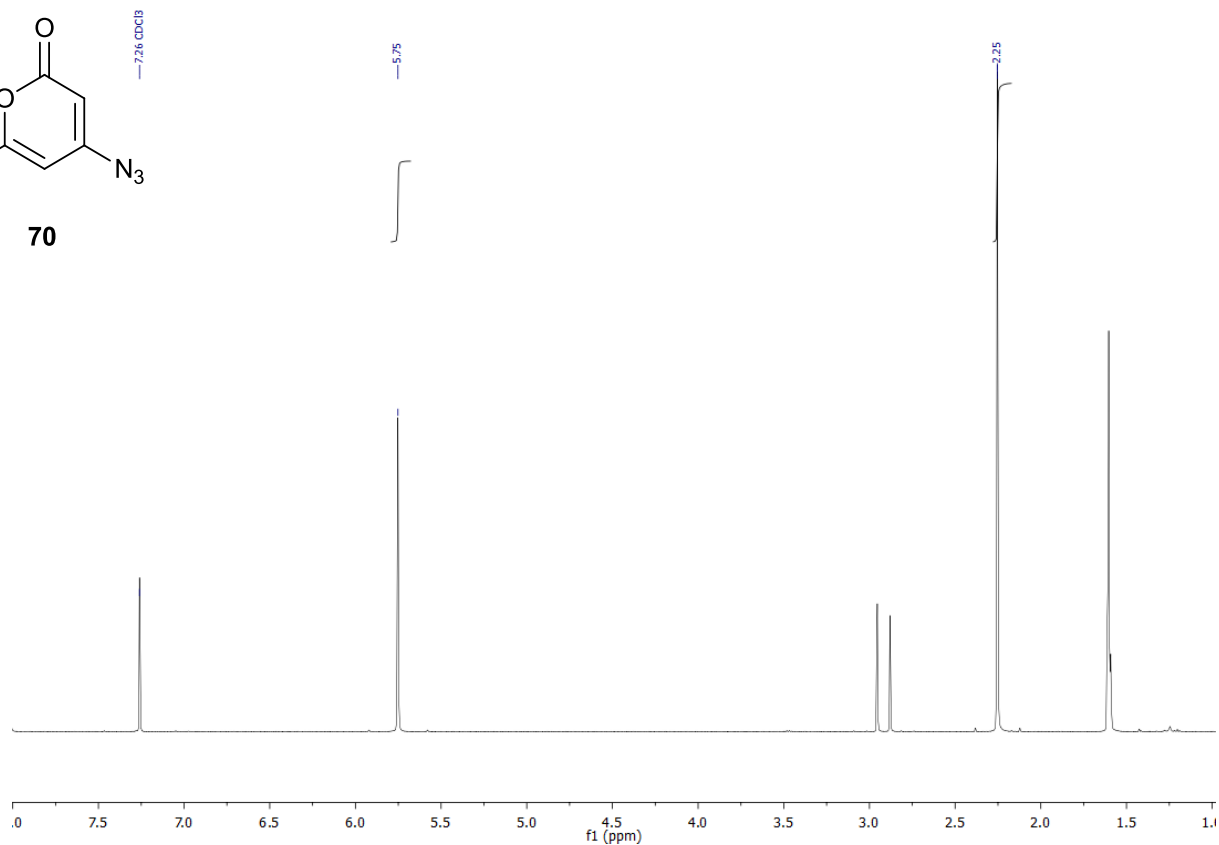
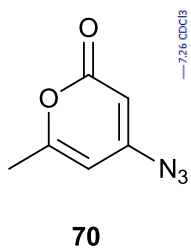
¹³C NMR spectrum of **42** (500 MHz, CDCl₃)



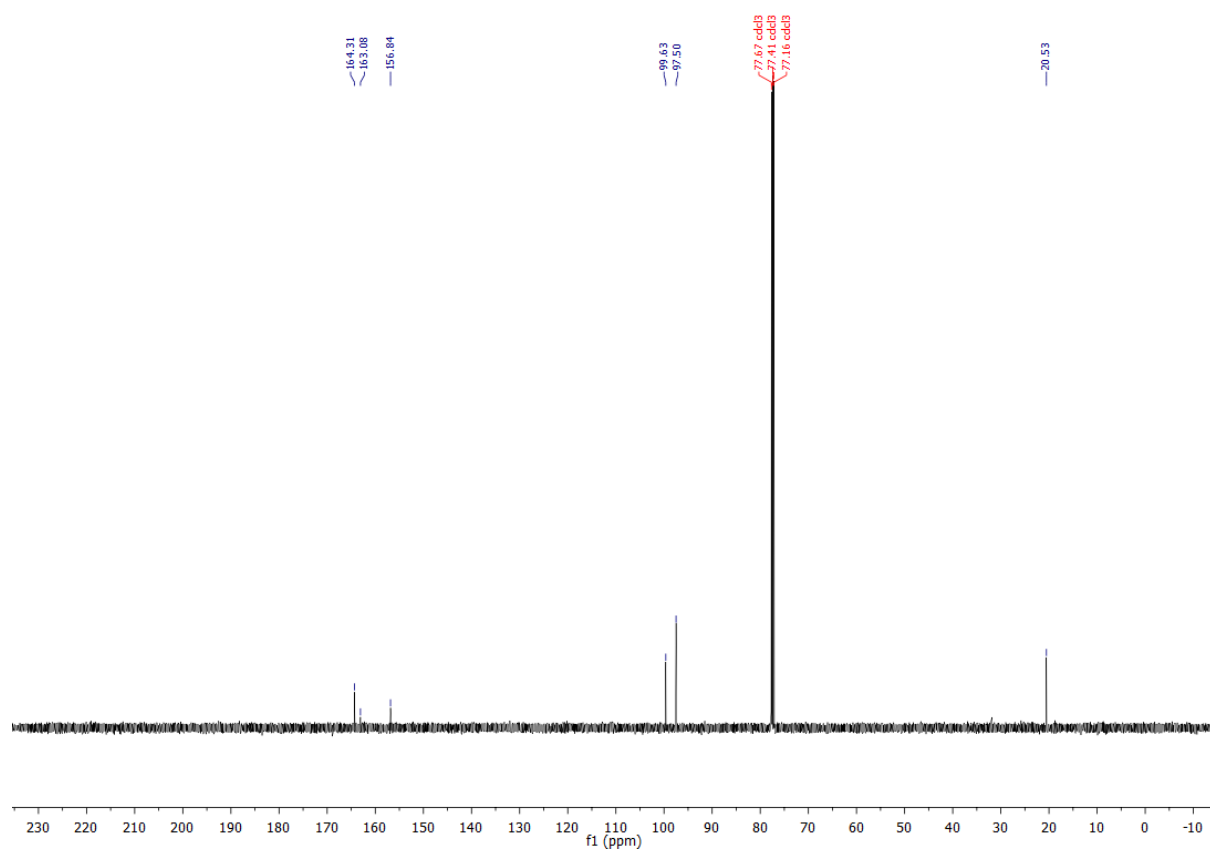
¹H NMR spectrum of **69** (500 MHz, CDCl₃)



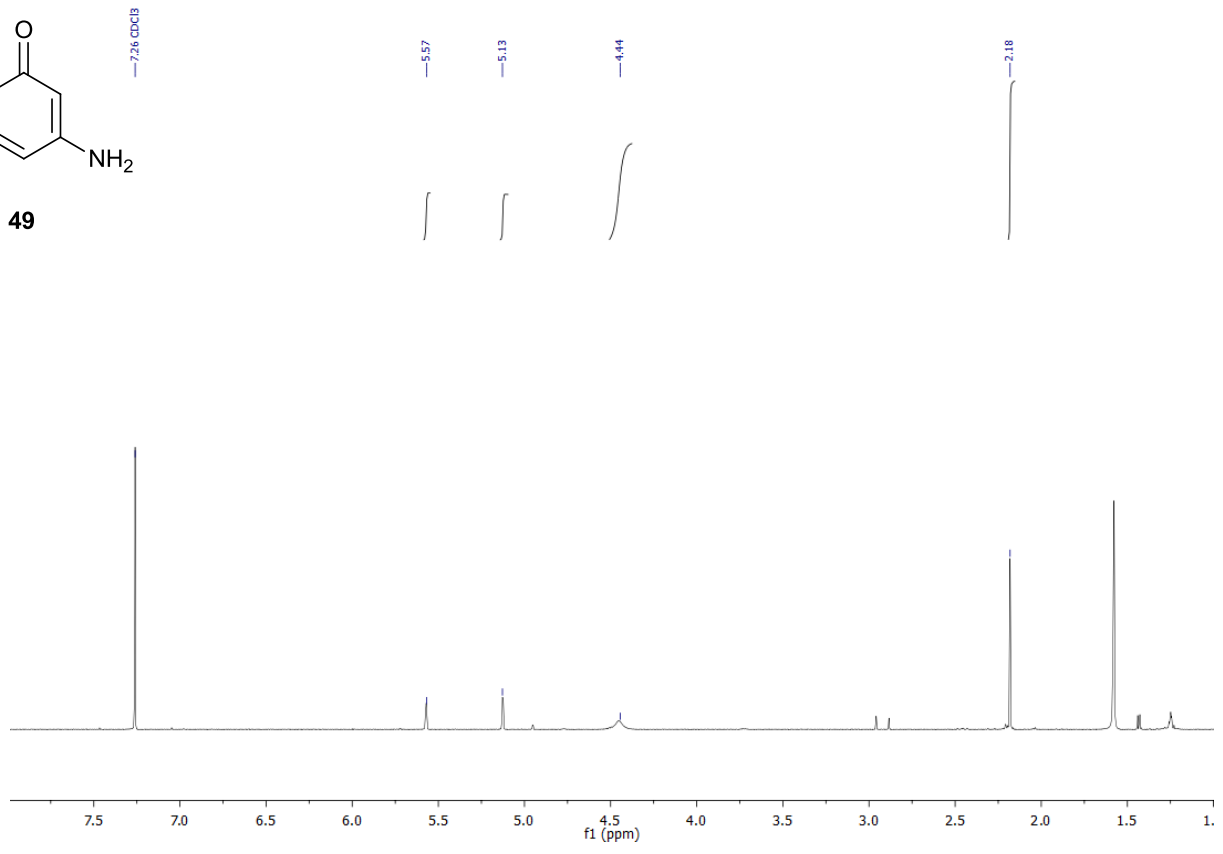
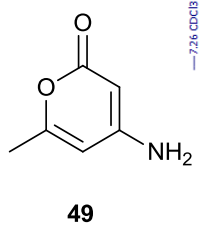
¹³C NMR spectrum of **69** (500 MHz, CDCl₃)



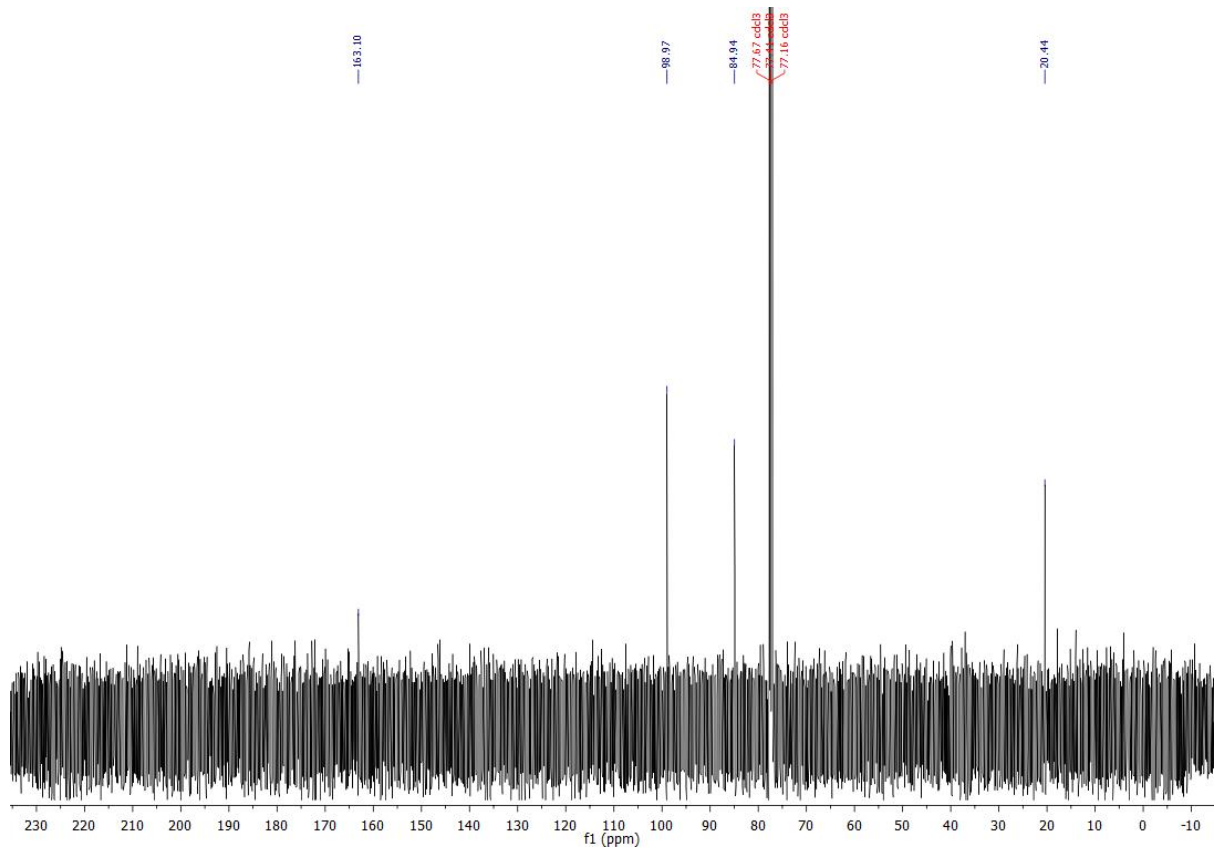
¹H NMR spectrum of **70** (500 MHz, CDCl₃)



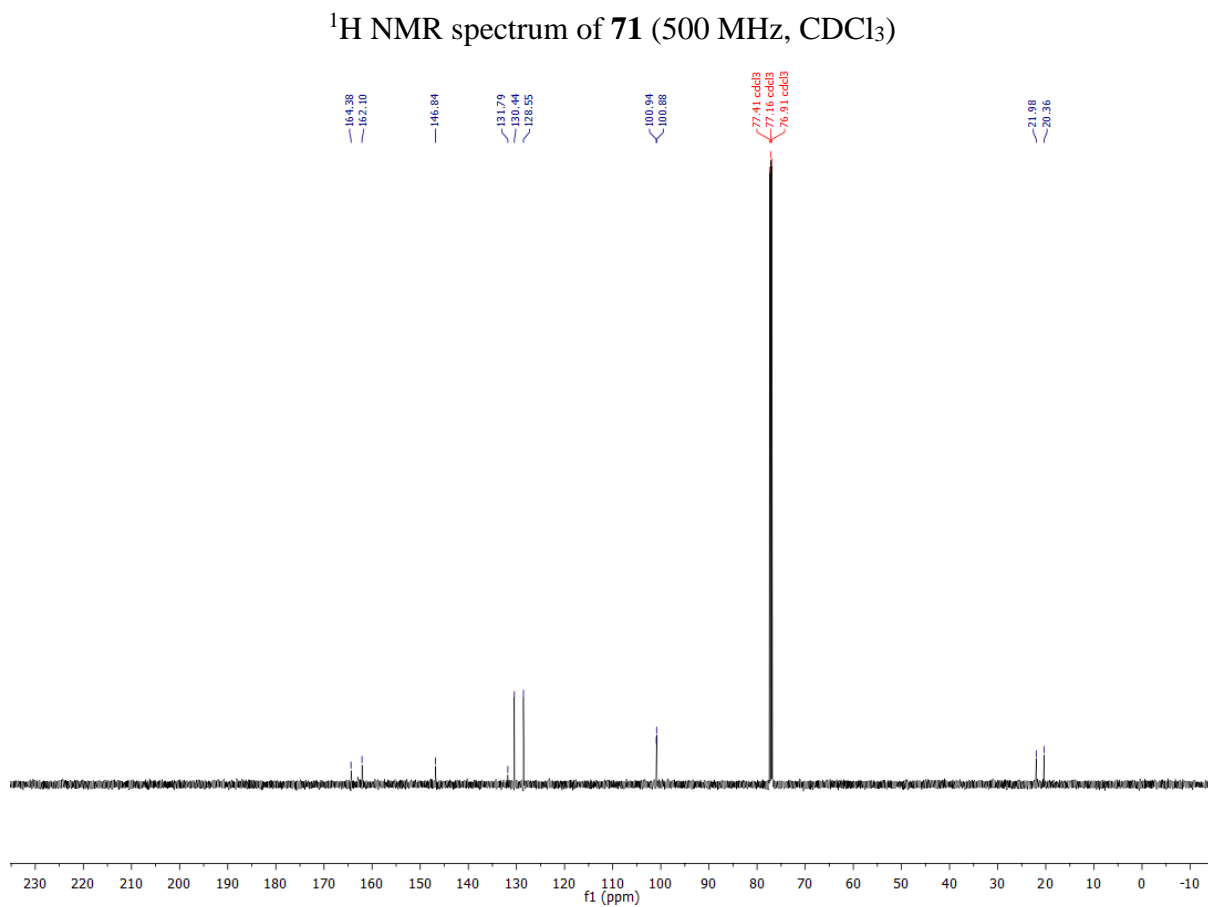
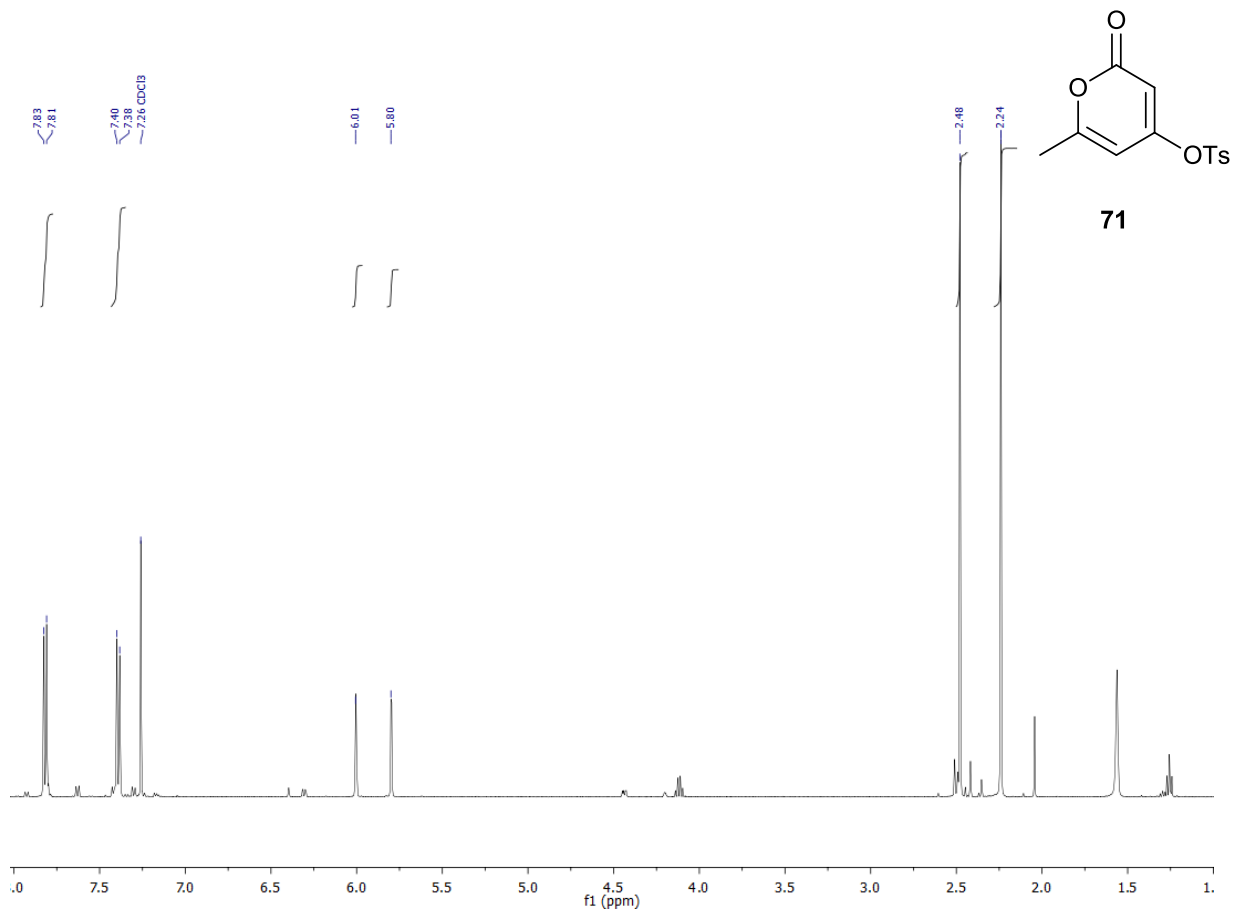
¹³C NMR spectrum of **70** (500 MHz, CDCl₃)

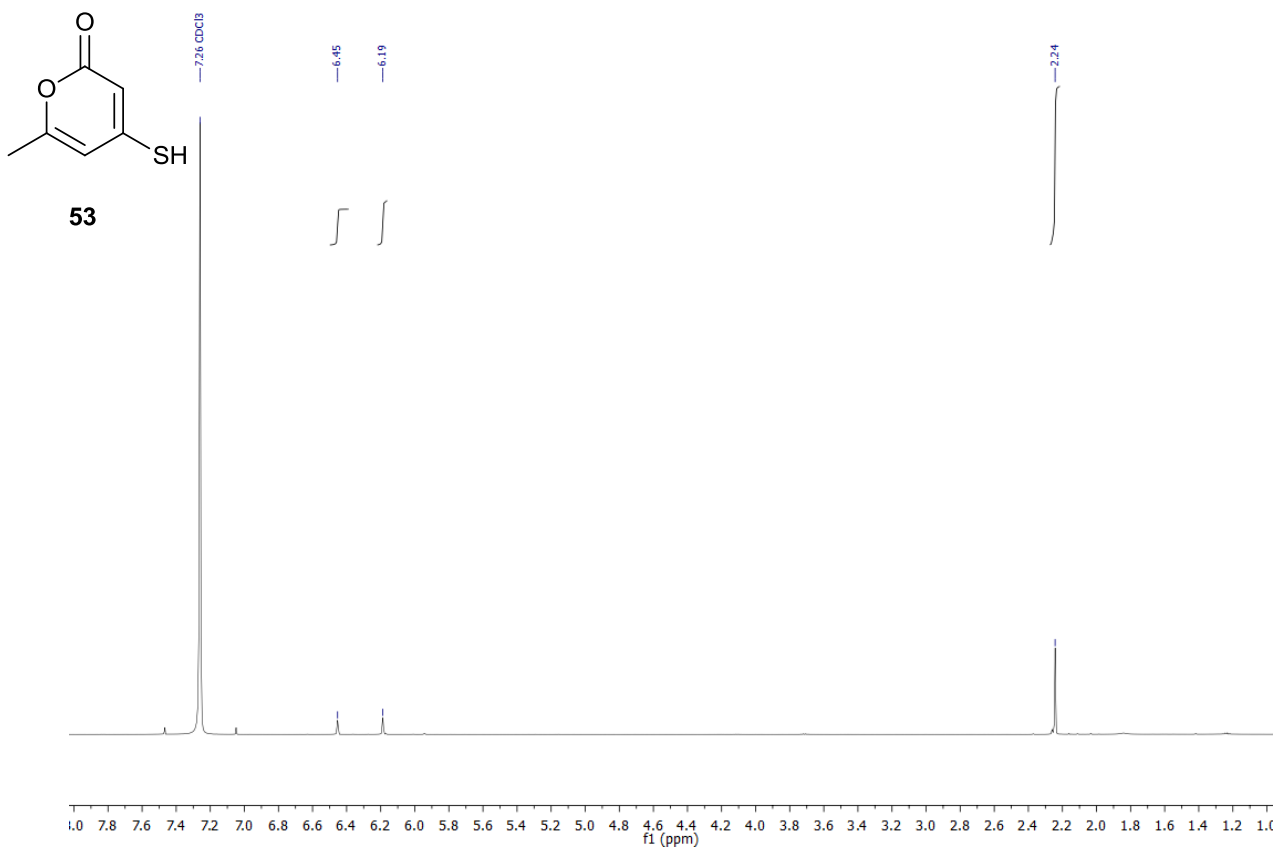


¹H NMR spectrum of **49** (500 MHz, CDCl₃)

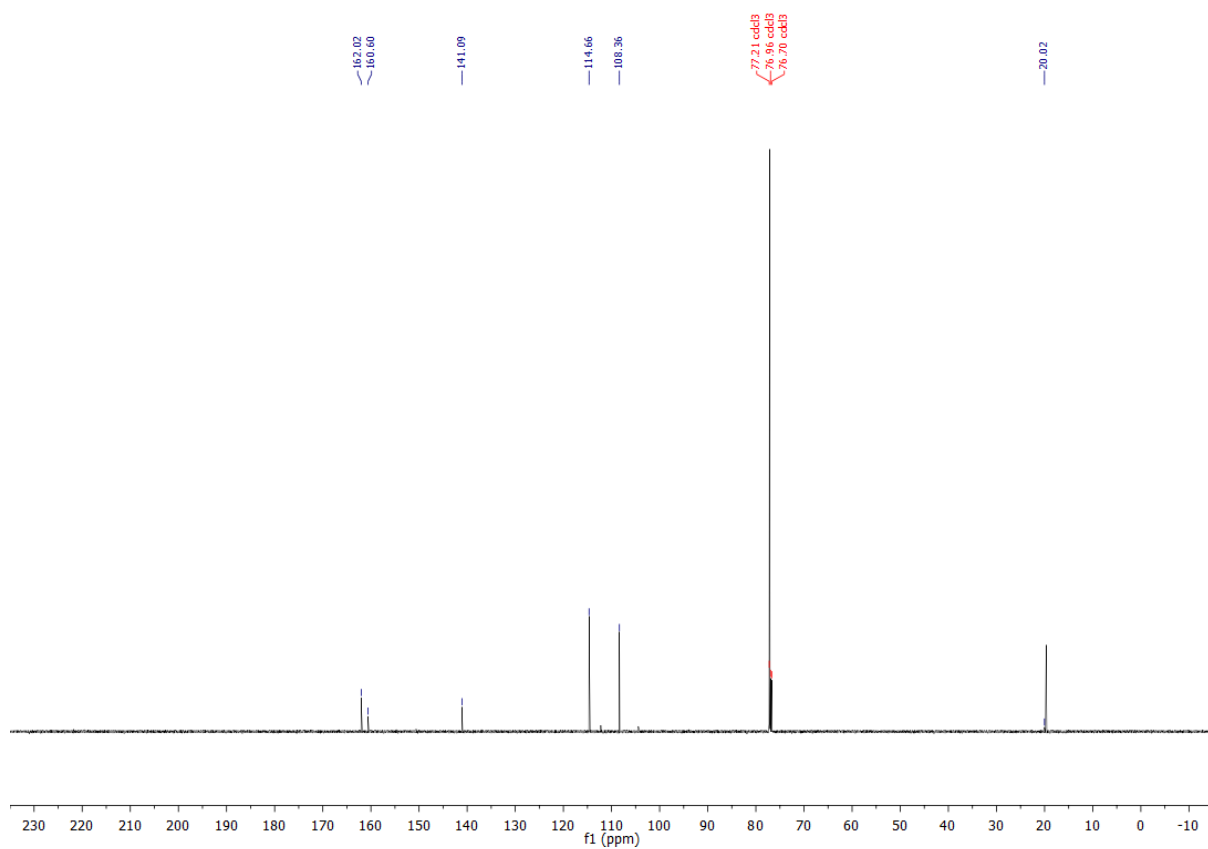


¹³C NMR spectrum of **49** (500 MHz, CDCl₃)

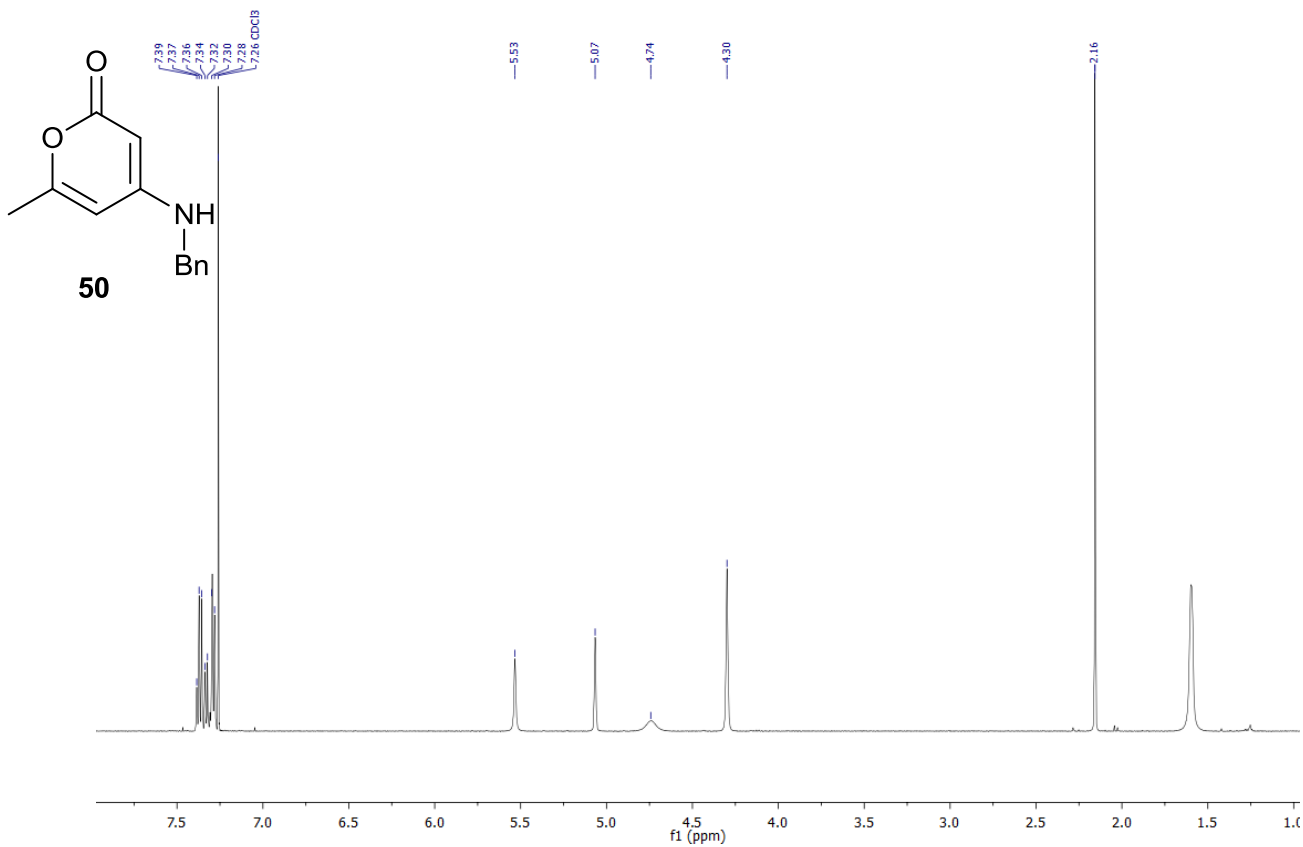




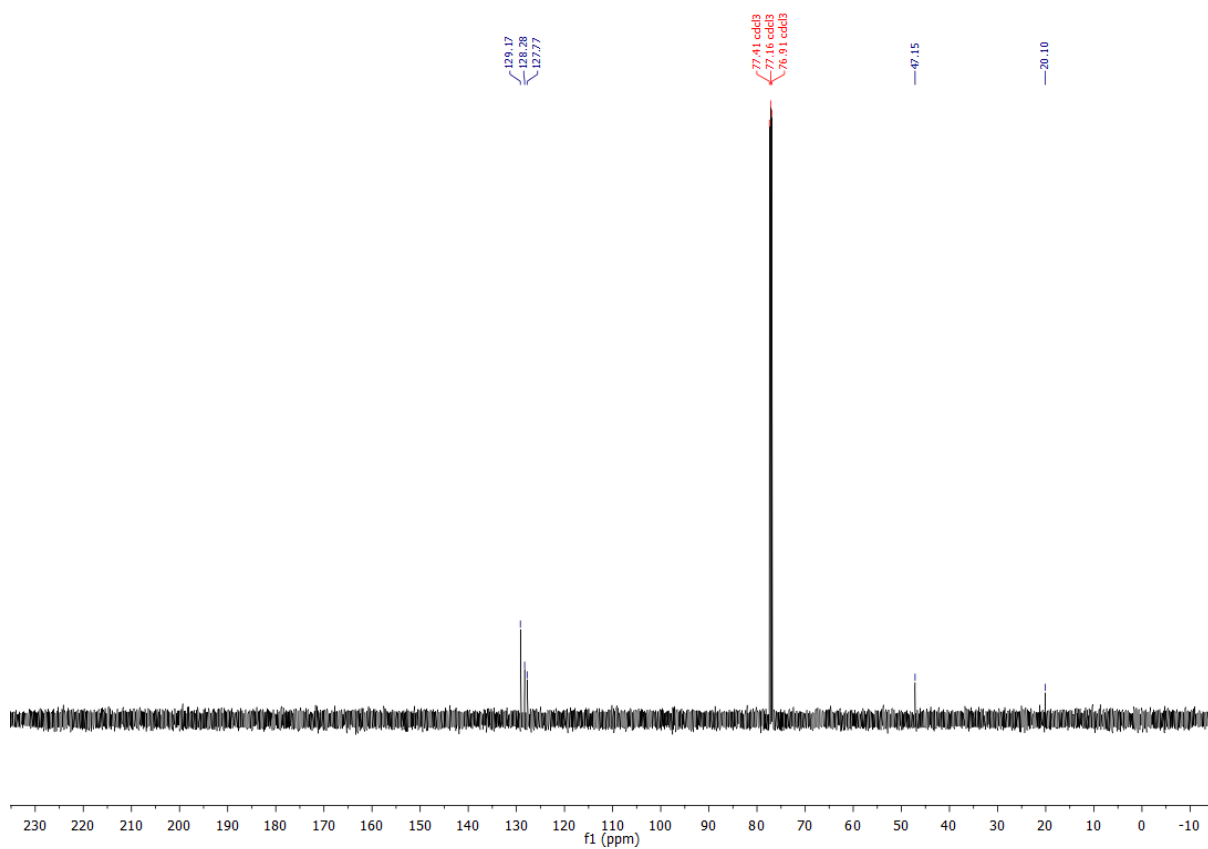
¹H NMR spectrum of **53** (500 MHz, CDCl₃)



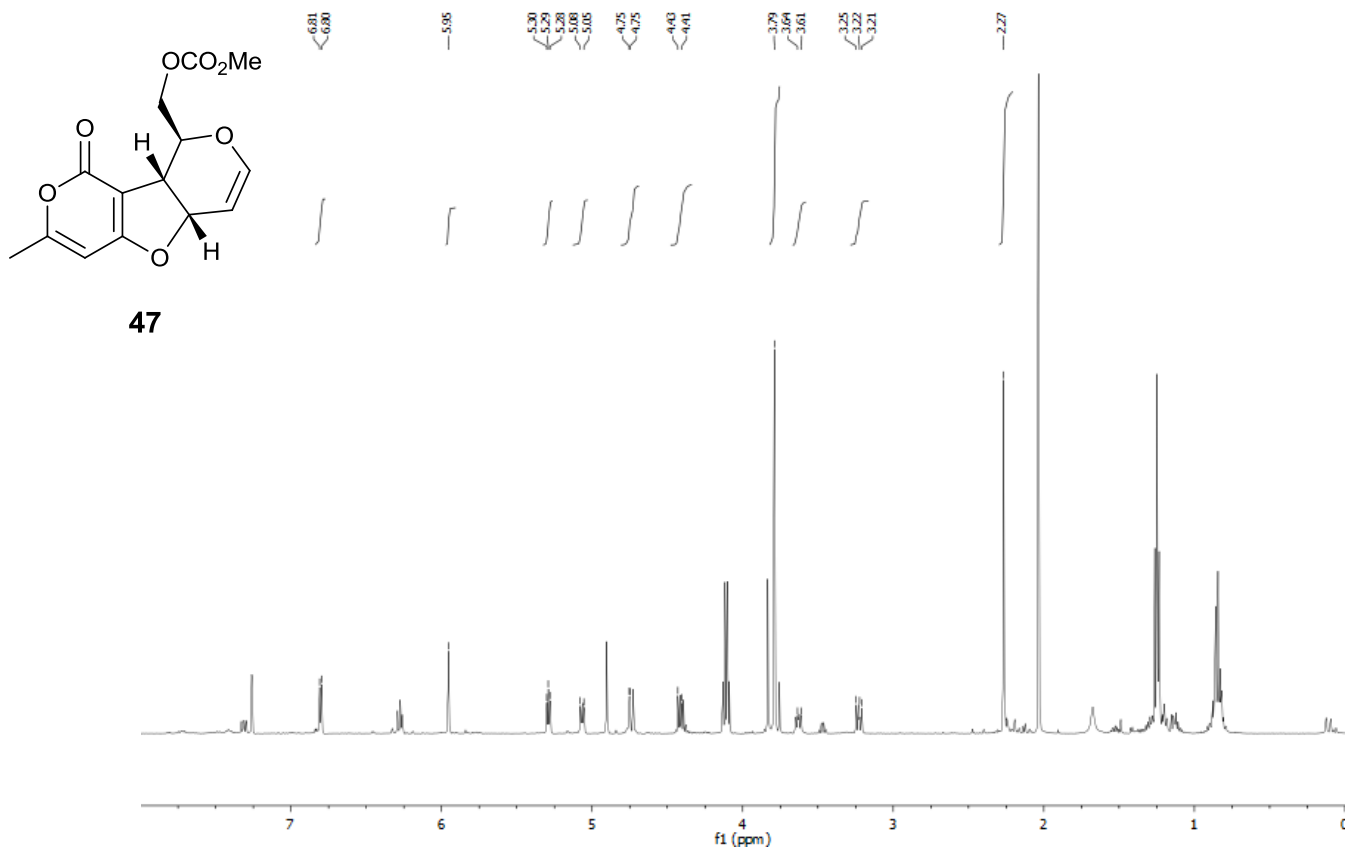
¹³C NMR spectrum of **53** (500 MHz, CDCl₃)



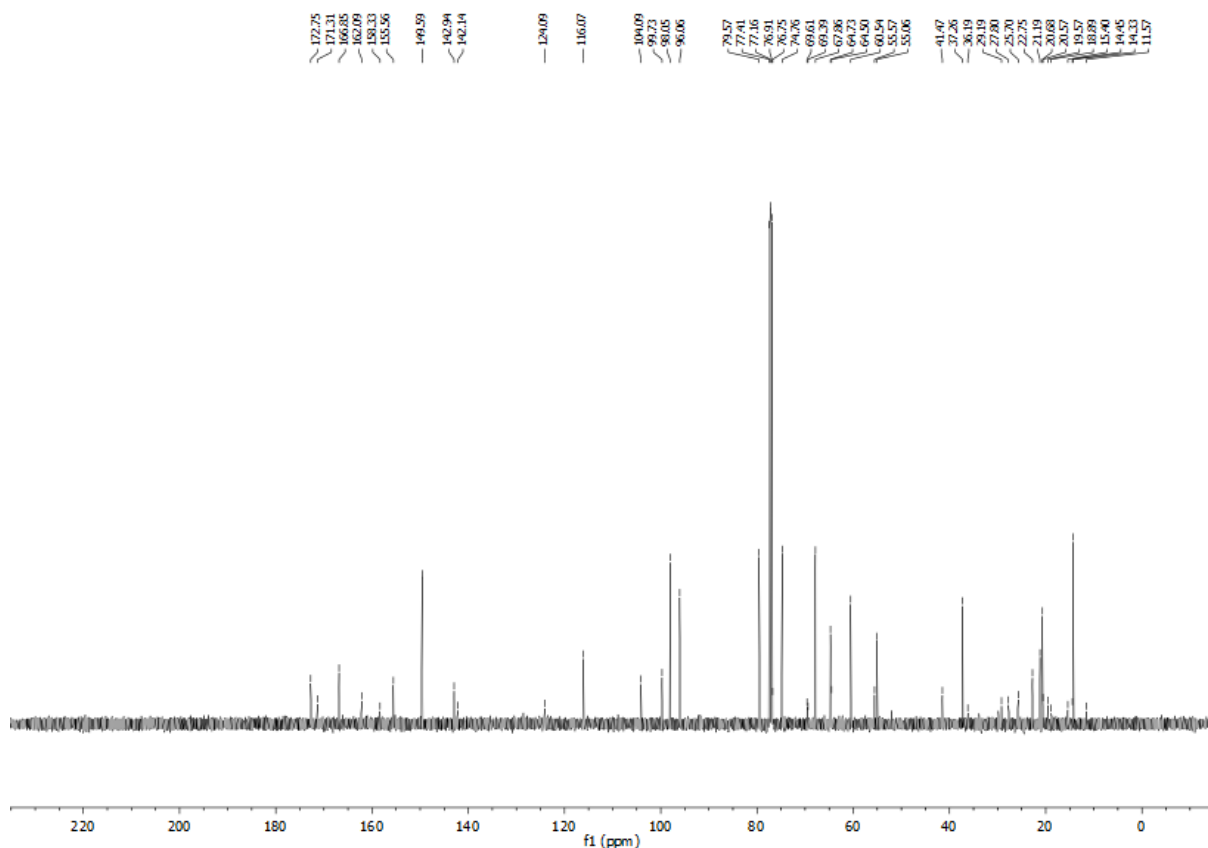
¹H NMR spectrum of **50** (500 MHz, CDCl₃)



¹³C NMR spectrum of **50** (500 MHz, CDCl₃)



¹H NMR spectrum of **47** (500 MHz, CDCl₃)



¹³C NMR spectrum of **47** (500 MHz, CDCl₃)

6. References

1. D. J. Newman and G. M. Cragg, *J. Nat. Prod.*, 2016, **79**, 629.
2. G. M. Cragg and D. J. Newman, *Biochem. Biophys. Acta.*, 2013, **1830**, 3670.
3. E. A. Crane and K. Gademann, *Angew. Chem. Int. Ed.*, 2016, **55**, 3882.
4. K. C. Nicolaou and T. Montagnon, *Molecules That Changed the World*, Wiley-VCH, Weinheim, 2008.
5. K. A. Lyseng-Williamson and C. Fenton, *Drugs*, 2005, **65**, 2513.
6. H. A. Kirst and G. D. Sides, *Antimicrob Agents Chemother*, 1989, **33**, 1419.
7. J. T. Spence and J. H. George, *Org. Lett.*, 2011, **13**, 5318.
8. S. K. Kim, D. E. Gross, D. G. Cho, V. M. Lynch and J. L. Sessler, *J. Org. Chem.*, 2011, **76**, 1005.
9. G. Hölfe, N. Bedorf, H. Steinmetz, D. Schomburg, K. Gerth and H. Reichenbach, *Angew. Chem. Int. Ed.*, 1996, **35**, 1567.
10. E. M. Balog and R. H. Fitts, *J. Appl. Physiol. (1985)*, 1996, **81**, 679.
11. S. Danishefsky, *Nat. Prod. Rep.*, 2010, **27**, 1114.
12. A. Rivkin, T. C. Chou and S. J. Danishefsky, *Angew. Chem. Int. Ed.*, 2005, **44**, 2838.
13. A. Stein, *Clinical Journal of Oncology Nursing*, 2010, **14**, 65.
14. H. M. L. Davies and E. J. Sorensen, *Chem. Soc. Rev.*, 2009, **38**, 2981.
15. B. M. Trost, *Acc. Chem. Res.*, 2002, **35**, 695.
16. H. C. Barrett and G. Buechi, *J. Am. Chem. Soc.*, 1967, **89**, 5665.
17. A. G. Myers, M. E. Fraley and N. J. Tom, *J. Am. Chem. Soc.*, 1994, **116**, 11556.
18. A. G. Myers, M. E. Fraley, N. J. Tom, S. B. Cohen and D. J. Madar, *Chemistry & Biology*, 1995, **2**, 33.
19. P. A. Wender and C. K. Zercher, *J. Am. Chem. Soc.*, 1991, **113**, 2311.
20. K. Majumdar and B. Sinha, *Synthesis*, 2013, **45**, 1271.
21. E. Negishi and A. de Meijere, *Handbook of Organopalladium Chemistry for Organic Synthesis*, Wiley, 2003.
22. P. E. Slade and H. B. Jonassen, *J. Am. Chem. Soc.*, 1957, **79**, 1277.
23. J. Tsuji, H. Takahashi and M. Morikawa, *Tetrahedron. Lett.*, 1965, **6**, 4387.
24. J. Tsuji, *Pure. Appl. Chem.*, 1982, **54**, 197.
25. B. M. Trost, *Acc. Chem Res*, 1980, **13**, 385.
26. B. M. Trost, *Tetrahedron*, 1977, **33**, 2615.
27. B. M. Trost and D. L. Van Vranken, *Chem. Rev.*, 1996, **96**, 395.
28. H. Matsushita and E. Negishi, *J. Am. Chem. Soc.*, 1982, 160.
29. M. E. Hoke, M. R. Brescia, S. Bogaczyk, P. DeShong, B. W. King and M. T. Crimmins, *J. Org. Chem.*, 2002, **67**, 327.
30. B. M. Trost, *J. Org. Chem.*, 2004, **69**, 5813.
31. B. M. Trost and P. E. Strege, *J. Am. Chem. Soc.*, 1977, **99**, 1649.
32. A. Y. Hong and B. M. Stoltz, *Eur. J. Org. Chem.*, 2013, **2013**, 2745.
33. K. C. Nicolaou, T. Montagnon and S. A. Snyder, *Chem. Comm.*, 2003, **39**, 551.
34. N. J. Green and M. S. Sherburn, *Aust. J. Chem.*, 2013, **66**, 267.
35. L. F. Tietze, G. Brasche and K. M. Gericke, *Domino Reactions in Organic Synthesis*, WILEY-VCH Verlag GmbH & Co. KGaA, 2006.
36. C. Grondal, M. Jeanty and D. Enders, *Nat. Chem.*, 2010, **2**, 167.
37. T. Newhouse, P. S. Baran and R. W. Hoffmann, *Chem. Soc. Rev.*, 2009, **38**, 3010.
38. K. C. Nicolaou, D. J. Edmonds and P. G. Bulger, *Angew. Chem. Int. Ed*, 2006, **45**, 7134.
39. R. Robinson, *J. Chem. Soc., Trans.*, 1917, **111**, 762.

40. X. Liao, S. Huang, H. Zhou, D. Parrish and J. M. Cook, *Org. Lett.*, 2007, **9**, 1469.
41. M. J. Bartlett, Ph.D. thesis, Victoria University of Wellington, 2013.
42. M. J. Bartlett, C. A. Turner and J. E. Harvey, *Org Lett*, 2013, **15**, 2430.
43. C. A. Turner, Master's Thesis, Victoria University of Wellington, 2013.
44. S. Tat., Honours, Victoria University of Wellington, 2013.
45. M. R. Brescia, Y. C. Shimshock and P. DeShong, *J. Org. Chem.*, 1997, **62**, 1257.
46. J. J. Field, A. J. Singh, A. Kanakkanthara, T. Halafihi, P. T. Northcote and J. H. Miller, *J. Med. Chem.*, 2009, **52**, 7328.
47. R. Hoetelmans, PK-PD relationships for antiretroviral drugs, <https://www.fda.gov/ohrms/dockets/ac/00/slides/3621s1d/tsld036.htm>, (accessed 22/05/17, 2017).
48. C. A. Tolman, *Chem. Rev.*, 1977, **77**, 313.
49. E. Galardon, S. Ramdeehul, J. M. Brown, A. Cowley, K. K. Hii and A. Jutand, *Angew. Chem.Int. Ed.*, 2002, **41**, 1760.
50. A. C. Hillier, G. A. Grasa, M. S. Viciu, H. M. Lee, C. L. Yang and S. P. Nolan, *J. Organomet. Chem.*, 2002, **653**, 69.
51. M. Cervera, M. Moreno-mañas and R. Pleixats, *Tetrahedron*, 1990, **46**, 7885.
52. K. C. Majumdar and S. Muhuri, *Synthesis-Stuttgart*, 2006, **16**, 2725.
53. P. G. Gildner and T. J. Colacot, *Organometallics*, 2015, **34**, 5497.
54. S. S. Zaleskiy and V. P. Ananikov, *Organometallics*, 2012, **31**, 2302.
55. C. Amatore and A. Jutand, *Coordination Chem. Rev.*, 1998, **178**, 511.
56. H. Clavier and S. P. Nolan, *Chem. Comm.*, 2010, **46**, 841.
57. C. A. Tolman, *Chem. Rev.*, 1977, **77**, 313.
58. A. M. Johns, M. Utsunomiya, C. D. Incarvito and J. F. Hartwig, *J Am Chem Soc*, 2006, **128**, 1828.
59. G. Pacchioni and P. S. Bagus, *Inorganic Chemistry*, 1992, **31**, 4391.
60. R. A. Widenhoefer, H. A. Zhong and S. L. Buchwald, *Organometallics*, 1996, **15**, 2745.
61. M. J. Burns, T. O. Ronson, R. J. Taylor and I. J. Fairlamb, *J. Org. Chem.*, 2014, **10**, 1159.
62. J. M. Dickinson, *Natural Product Reports*, 1993, **10**, 71.
63. A. P. Kozikowski and J. Lee, *J. Org. Chem.*, 1990, **55**, 863.
64. P. Blom, B. Ruttens, S. Van Hoof, I. Hubrecht, J. Van der Eycken, B. Sas, J. Van hemel and J. Vandekerckhove, *J. Org. Chem.*, 2005, **70**, 10109.
65. J. Zhao, S. Wei, X. Ma and H. Shao, *Carbohydr. Res.*, 2010, **345**, 168.
66. M. J. McLaughlin, R. P. Hsung, K. P. Cole, J. M. Hahn and J. Wang, *Org. Lett.*, 2002, **4**, 2017.